NATIONAL TRANSPORTATION SAFETY BOARD

Office of Research and Engineering
Washington, D.C. 20594

October 11, 2016

Aircraft Performance Radar & Cockpit Visibility Study

by John O'Callaghan

Location:	San Diego, California
Date:	August 16, 2015
Time:	11:03 Pacific Daylight Time (PDT) / 18:03 Coordinated Universal Time (UTC)
Aircraft:	Cessna 172M, registration N1285U
	North American Rockwell NA265-60SC Sabreliner, registration N442RM
NTSB#:	WPR15MA243A (C172)
	WPR15MA243B (Sabreliner)

CONTENTS

FIGURES

NATIONAL TRANSPORTATION SAFETY BOARD

Office of Research and Engineering
Washington, D.C. 20594

October 11, 2016

Aircraft Performance Radar & Cockpit Visibility Study

by John O'Callaghan

A. ACCIDENT

Location: San Diego, California
Date: August 16, 2015
Time: 11:03 Pacific Daylight Time (PDT) / 18:03 Coordinated Universal Time (UTC)
Aircraft: Cessna 172M, registration N1285U
North American Rockwell NA265-60SC Sabreliner, registration N442RM
NTSB#: WPR15MA243A (C172)
WPR15MA243B (Sabreliner)

B. GROUP

Not Applicable

C. SUMMARY

On August 16, 2015, about 11:03 PDT[1], a Cessna 172M, N1285U, and an experimental North American Rockwell NA265-60SC Sabreliner, N442RM (call sign EAGLE1[2]), collided in midair about 1 mile northeast of Brown Field Municipal Airport (KSDM), San Diego, California. The pilot (and sole occupant) of N1285U and the two pilots and two mission specialists aboard EAGLE1 died; both airplanes were destroyed. N1285U was registered to a private individual and operated by Plus One Flyers under the provisions of 14 Code of Federal Regulations (CFR) Part 91 as a personal flight. EAGLE1 was registered to and operated by BAE Systems Technology Solutions & Services, Inc. (BAE), for the US Department of Defense as a public aircraft in support of the US Navy. No flight plan was filed for N1285U, which originated from Montgomery-Gibbs Executive Airport, San Diego, California (KMYF). A mission flight plan was filed for EAGLE1, which originated from KSDM about 08:30 and was returning to KSDM. Visual meteorological conditions prevailed at the time of the accident.

This *Aircraft Performance Radar & Cockpit Visibility Study* presents the results of using North Island Naval Air Station (NZY) and San Diego Miramar (NKX) Airport Surveillance Radar (ASR) data, Cockpit Voice Recorder (CVR) information from the Sabreliner, and the wreckage locations of the airplanes to calculate the position and orientation of each airplane in the minutes preceding the collision. This information is then used to estimate the approximate location of each airplane in the other airplane's field of view (the "visibility study"), and to estimate the Cockpit Display of Traffic

[1] All times in this *Study* are in PDT based on a 24-hour clock, unless otherwise noted.
[2] For clarity and consistency with other investigative documents (including the transcript of the Air Traffic Control (ATC) communications (Reference 1), in this *Study* the accident airplanes will be referred to by their ATC call signs (N1285U for the Cessna 172 and EAGLE1 for the Sabreliner).

Information (CDTI) data that could have been presented to the pilots had the airplanes been equipped to provide this information. As described further in Section D-V, CDTI uses the Federal Aviation Administration (FAA) Automatic Dependent Surveillance – Broadcast (ADS-B) system to drive a traffic situation display in the cockpits of appropriately-equipped aircraft.

The sections that follow present the radar data and other information used in this *Study*, and describe the methods used to calculate aircraft speeds, orientation (pitch, yaw and roll angles), CDTI information, and cockpit visibility from this data. The results of these calculations are presented in the Figures and Tables described throughout the *Study*.

The accident occurred in the traffic pattern at KSDM, while the airplanes were under the control of the KSDM Air Traffic Control Tower (ATCT). Several other aircraft were also under ATCT control at the time. In order to better understand the circumstances of the accident, including the larger air-traffic picture and the ATCT staff workload in the minutes preceding the collision, this *Study* also presents the movements of the other aircraft communicating with the KSDM ATCT in the minutes preceding the collision. These movements were determined based on NZY ASR data, supplemented with simulations of the aircrafts' movements when the aircraft were below radar coverage. These simulations are based on the known intentions of the aircraft (e.g., landing on a particular runway, or taxiing to particular points on the airport) as determined from recorded ATCT communications.

Per the NTSB factual report (Reference 2), on the morning of the accident, the KSDM ATCT had all control positions (local and ground control) in the tower combined to the local control position. The position was staffed by a qualified local controller (LC)/controller-in-charge who was conducting on-the-job training with a developmental controller (LC trainee) on the local control position. At the time that EAGLE1 contacted the KSDM ATCT inbound for landing, the LC trainee was transmitting control instructions for all operations; however, the qualified LC was monitoring the LC trainee's actions and was responsible for all activity at that position. At 10:59:33 (about 3.5 minutes before the collision), the qualified LC terminated the LC trainee's training and took over control of communications.

The location of the aircraft in the pattern and on the ground at KSDM at the times of significant events leading up to the collision (such as communications between the accident airplanes and the ATCT, and comments on the EAGLE1 CVR concerning other traffic in the pattern) are annotated in several of the Figures presented in this *Study*, as discussed below.

D. DETAILS OF THE INVESTIGATION

I. The accident airplanes

The North American Rockwell NA265-60SC Sabreliner

The North American Rockwell NA265-60SC Sabreliner is a low-wing, five seat airplane powered by two Pratt and Whitney JT12A-8 turbojet engines, each rated at 3,000 lbs of thrust. The accident airplane was manufactured in 1974 and was operating with an experimental airworthiness certificate because it had been modified with an external test pod attached to the lower side of the airplane aft of the nose landing gear. The airplane had a maximum gross weight of 22,900 lbs.

Figure 1 shows diagrams of the NA265-60SC, taken from Reference 3. A pre-accident photograph of N442RM (EAGLE1) is shown in Figure 2. Table 1 provides some dimensions of the airplane, as well as the estimated weight at the time of the accident (15,701 lb.), as provided by BAE.

Item	**Value**
Reference dimensions (from References 3 & 5):	
Wing area	392 ft.^{2} (estimated from Figure 1)
Wing span	50.51 ft. (see Figure 1)
Mass properties for EAGLE1 on accident flight:	*(as provided by BAE)*
Basic empty weight	13,774 lb.
Pilots, operators & equipment	855 lb.
Zero fuel weight	14,629 lb.
Estimated fuel load at landing	1,072 lb.
Gross weight at time of accident	**15,701 lb.**

Table 1. Relevant geometry and mass properties for EAGLE1.

The Type Certificate (TC) for the North American Rockwell NA265-60SC is now held by Sabreliner Corporation. However, Sabreliner Corporation was unable to provide the NTSB with detailed information about the airplane's aerodynamic characteristics, such as the lift coefficient (C_L) as a function of angle of attack (α), needed to estimate the airplane's Euler angles (pitch roll, and heading) throughout the flight (the Euler angles are needed to evaluate the visibility of N1285U from EAGLE1's cockpit). Consequently, the required aerodynamic characteristics were determined by analyzing airplane performance data recorded during N442RM's flight the day before the accident (on August 15, 2015). This data was recorded on a laptop computer carried on the airplane, downloaded from the laptop after the August 15 flight by BAE, and subsequently made available to the NTSB. The laptop computer was also recording data during the accident flight, but was destroyed in the accident, and so no recorded data for the accident flight is available. The analysis of the August 15 data is described in Section D-III.

The geometry of an exemplar Sabreliner[3] that was made available to the NTSB by the Flight Research, Inc. in Mojave, CA was measured with a laser scanner in support of the cockpit visibility study described in Section D-IV and Appendix A.

The Cessna 172M

The C172 is a single-engine, four-seat high-wing airplane with a conventional tail. Figure 3 is a pre-accident photograph of the accident airplane (N1285U), and Figure 4 shows a 3-view image of the C172, taken from Reference 4. Table 2 provides some dimensions of the airplane, as well as relevant mass properties for N1285U on the accident flight. The mass properties at takeoff are based on information provided by the flight school that operated the airplane. A flight time of 1.75 hr. is assumed based on N1285U departing KMYF between 09:15-09:20, per the flight school. The rate of fuel consumption is based on Reference 4.

[3] The scanned airplane was a Sabreliner model NA265-60, while the accident Sabreliner was a model NA265-60SC. However, the cockpit and window geometries of both models are identical.

Item	Value
Reference dimensions (from References 4 & 5):	
Wing area	175.5 ft.^{2} (from Reference 5)
Wing span	36 ft. (see Figure 4)
Mass properties for N1285U:	
Empty weight	1443 lb.
Pilot weight	232 lb.
Baggage weight (assumed)	15 pounds
Fuel weight (takeoff)	228 pounds (38 gallons @ 6 lb./gal.)
Gross weight at takeoff	1,918 lb.
Fuel consumed (estimated)	116 lb. (1.75 hr. x 11 gal./hr.) x (6 lb./gal.)
Gross weight at time of accident	**1,802 lb.**

Table 2. Relevant geometry and mass properties for N1285U.

Aerodynamic information for the C172 (such as the lift coefficient (C_L) as a function of angle of attack (α)) was provided to the NTSB by Textron Aviation (Textron). This information is used along with the gross weight and wing area shown in Table 2 in the analysis of the radar data for N1285U to estimate the pitch and roll angles throughout the flight (see Section D-II).

The geometry of an exemplar C172 owned by an NTSB employee was measured with a laser scanner in support of the cockpit visibility study described in Section D-IV and Appendix A.

II. Radar data

Description of ARSR and ASR radar data

In general, two types of radar are used to provide position and track information, both for aircraft cruising at high altitudes between airport terminal airspaces, and those operating at low altitude and speeds within terminal airspaces.

Air Route Surveillance Radars (ARSRs) are long range (250 nmi) radars used to track aircraft cruising between terminal airspaces. ARSR antennas rotate at 5 to 6 RPM, resulting in a radar return every 10 to 12 seconds. Airport Surveillance Radars (ASRs) are short range (60 nmi) radars used to provide air traffic control services in terminal areas. ASR antennas rotate at about 13 RPM, resulting in a radar return about every 4.6 seconds. The ASRs at NZY and NKX received returns from both airplanes involved in this accident. In addition, data recorded by the Symphony® OpsVue™ system operated by Harris Corporation, which fuses information from multiple radar sites and aircraft Automatic Dependent Surveillance – Broadcast (ADS-B) position reports, was obtained for both airplanes.

Primary and secondary radar returns

A radar detects the position of an object by broadcasting an electronic signal that is reflected by the object and returned to the radar antenna. These reflected signals are called *primary returns.*

Knowing the speed of the radar signal and the time interval between when the signal was broadcast and when it was returned, the distance, or range, from the radar antenna to the reflecting object can be determined. Knowing the direction the radar antenna was pointing when the signal was broadcast, the direction (or bearing, or azimuth) from the radar to the object can be determined. Range and azimuth from the radar to the object define the object's position. In general, primary returns are not used to measure the altitude of sensed objects, though some ARSRs do have height estimation capability. ASRs do not have height estimation capabilities.

The strength or quality of the return signal from the object depends on many factors, including the range to the object, the object's size and shape, and atmospheric conditions. In addition, any object in the path of the radar beam can potentially return a signal, and a reflected signal contains no information about the identity of the object that reflected it. These difficulties make distinguishing individual aircraft from each other and other objects (e.g., flocks of birds) based on primary returns alone unreliable and uncertain.

To improve the consistency and reliability of radar returns, aircraft are equipped with transponders that sense beacon interrogator signals broadcast from radar sites, and in turn broadcast a response signal. Thus, even if the radar site is unable to sense a weak reflected signal (primary return), it can sense the response signal broadcast by the transponder and be able to determine the aircraft position. The response signal can also contain additional information, such as the identifying "beacon code" for the aircraft, and the aircraft's pressure altitude (also called "Mode C" altitude). Transponder signals received by the radar site are called *secondary returns*.

N1285U was flying according to Visual Flight Rules (VFR, as opposed to Instrument Flight Rules, or IFR), broadcasting a "1200" transponder beacon code. EAGLE1 was assigned and broadcasting a transponder beacon code of 4644 and entered the pattern under visual flight rules.

Recorded radar data

Recorded data from the NZY and NKX ASRs was obtained from the U.S. Navy and FAA, respectively, and includes the following parameters:

- UTC time of the radar return, in hours, minutes, and seconds. PDT = UTC – 7 hours.
- Transponder beacon code associated with the return (secondary returns only)
- Transponder reported altitude in hundreds of feet associated with the return (secondary returns only). The transponder reports pressure altitude. The altitude recorded in the file can include both pressure altitude, and pressure altitude adjusted for altimeter setting (altitude above mean sea level (MSL)), or may include just one or the other. The FAA file only contains valid data for the pressure altitude.[4] The resolution of this data is ± 50 ft.
- Slant Range from the radar antenna to the return, in nmi. The accuracy of this data is ±1/16 nmi or about ± 380 ft.
- Azimuth relative to magnetic north from the radar antenna to the return. The KCHS ASR azimuth is reported in Azimuth Change Pulses (ACPs). ACP values range from 0 to 4096, where 0 = 0° magnetic and 4096 = 360° magnetic. Thus, the azimuth to the target in degrees would be:

[4] The altimeter setting for the time and location of the accident was 29.87 "Hg, resulting in a pressure altitude about 46 ft. higher than MSL altitude. Because the altitude corrections are rounded to the nearest 100 ft., in this case the reported pressure and MSL altitudes would be identical.

(Azimuth in degrees) = (360/4096) x (Azimuth in ACPs) = (0.08789) x (Azimuth in ACPs)

The accuracy of azimuth data is ± 2 ACP or ± 0.176º.

- The latitude and longitude of the radar return, as computed by the radar's processing algorithms from its raw range and azimuth measurements.

While the data file contains the latitude and longitude coordinates of each return, it is useful to compute latitude and longitude from the range and azimuth data itself, for two reasons:

- As a consistency check on the latitude and longitude recorded in the file; and
- To compute "uncertainty boxes" associated with each return, resulting from the uncertainty in the raw range and azimuth measurements (see discussion below).

To determine the latitude and longitude of radar returns from the range and azimuth data recorded by the radar, the geographic location of the radar antenna and the magnetic variation assumed in its azimuth data must be known. The nominal[5] coordinates and magnetic variation of the NZY ASR antenna are:

32° 42' 13.6" N latitude
117° 12' 59.16" W longitude
elevation 47 feet
magnetic variation 0° E (azimuth reported relative to true north)

The nominal coordinates and magnetic variation of the NKX ASR antenna are:

32° 52' 59.82" N latitude
117° 08' 37.93" W longitude
elevation 540 feet
magnetic variation 14° E

The nominal data for the NKX ASR resulted in good agreement between the recorded latitude and longitude coordinates for each radar return, and the computed coordinates based on the recorded range and azimuth. The NKX ASR data also aligned the track for N1285U reasonably well with the KSDM runways on which it operated (i.e., a go-around on runway 26R and a touch-and-go on runway 26L). However, while the nominal data for the NZY ASR resulted in good agreement between the recorded and computed latitude and longitude coordinates for that radar, the resulting tracks for N1285U were not in good alignment with the KSDM runways, but were offset about 1/8 nmi to the south of the runways and the NKX tracks. An examination of recent (March 2016) *Google Earth* imagery revealed that the NZY antenna appears to have been moved about 275 ft. southwest from an earlier site. The current coordinates of the NZY antenna were observed to be:

32° 42' 11.21" N latitude
117° 13' 00.72" W longitude
elevation 47 feet (assumed)

[5] The nominal data for the NZY and NKX ASRs are taken from radar databases maintained by the U.S. Navy and the FAA, respectively.

Using these antenna coordinates, a magnetic variation of 0.80° W resulted in tracks for N1285U that were better aligned with the KSDM runways and the NKX tracks. Consequently, the updated NZY ASR coordinates are used in this *Study*. Nonetheless, as described further below, the updated NZY radar tracks for N1285U require further adjustment or "shifting" to best align them with the runways, the NKX tracks, and the location of the collision.

Harris Corporation Symphony® OpsVue™ data

As noted above, data recorded by the Symphony® OpsVue™ system operated by Harris Corporation was obtained for both airplanes. OpsVue fuses information from multiple radar sites and aircraft ADS-B position reports into a single database accessible to OpsVue customers (this data is hereafter referred to as the "OpsVue" data).[6]

While the OpsVue data conveniently fuses the returns from multiple radar sites and ADS-B reports into a single track for each aircraft,[7] it is not possible to identify which specific radar sites contributed to the track for each aircraft, or to associate an uncertainty box (depicting the range and azimuth uncertainties in the raw radar data) with the returns.[8] Furthermore, the OpsVue data apparently also includes "coast" returns, which are projections or extrapolations of an aircraft's track based on prior radar returns, rather than on actual radar returns, when returns from a tracked aircraft cease unexpectedly. "Coast" returns are apparent in the recorded tracks of the accident airplanes, as discussed further below.

For these reasons, the usefulness of the OpsVue data is limited. Nonetheless, the OpsVue data was obtained so as to observe how the system fused and placed the radar returns for EAGLE1 and N1285U relative to the KSDM runways, and for comparison with the tracks determined from the NZY and NKX range and azimuth data. The OpsVue data is presented below, along with the NZY and NKX returns. Determining how the OpsVue data fuses returns from multiple radar sites into a single track, or projects a track in "coast" mode, is beyond the scope of this *Study.*

Presentation of the radar data

To calculate performance parameters from the radar data (such as groundspeed, track angle, pitch and roll angles, etc.), it is convenient to express the position of the airplane in rectangular Cartesian coordinates. The Cartesian coordinate system used in this *Study* is centered on the KSDM runway 26R threshold, and its axes extend east, north, and up from the center of the Earth. The data from the NZY and NKX ASRs and OpsVue are converted into this coordinate system using the WGS84 ellipsoid model of the Earth.

Figures 5a and 5b present this information for EAGLE1 and N1285U near the KSDM runways, plotted in terms of nautical miles north and east of the 26R runway threshold, and at two different

[6] For more information about OpsVue, see https://www.harris.com/solution/opsvue and http://www.symphonycdm.com/Pages/sites/default/files/products/pdf/OpsVueBrochure.pdf.

[7] Neither EAGLE1 nor N1285U were ADS-B equipped, so no ADS-B position reports from these airplanes were recorded.

[8] OpsVue only includes radar sites used by the FAA to surveil the National Airspace System (NAS). NZY is not used by the FAA, and so returns from NZY are not included in the OpsVue data. However, NKX and other, long-range FAA radar sites would be included in the OpsVue data.

scales.[9] For clarity, the NKX returns are omitted from Figure 5a. Figure 6 is similar to Figure 5, but presents the data over a Google Earth image of the area.

Figures 5 and 6 also present the adjustments made to the radar tracks in order to enforce certain constraints in the airplanes' trajectories, and to reduce the "noise" in the performance calculations resulting from position uncertainty in the radar data (see "Estimates of airplane performance based on radar data," below). The constraints used to adjust the airplane radar tracks are as follows:

- The requirement that the N1285U track reflect a touch-and-go on runway 26L;
- The requirement for a collision (airplanes at the same place and altitude at the same time);
- The time of the collision as determined from the EAGLE1 CVR (11:03:10.2);
- The wreckage locations of the airplanes;
- The convergence angle of the airplanes as evidenced by scrape marks on EAGLE1's right wing.

These constraints are discussed further below. The final trajectories of EAGLE1 and N1285U used for the airplane performance and cockpit visibility calculations presented in this *Study* are denoted by the "computed trajectory" lines for these airplanes in Figures 5 and 6.

The content of radio communications between the airplanes and the KSDM ATCT, and of selected content on the EAGLE1 CVR, are also annotated in Figures 5 and 6, at the locations along the airplane tracks where they occurred. The annotations are depicted as boxes labeled A-S; the events associated with each label (along with the corresponding time and airplane positions) are described in Table 3. The CVR information presented in Table 3 is taken from Reference 6.

The trajectories of the other aircraft in the pattern at KSDM in the four minutes preceding the collision are depicted in Figure 7. For clarity, this Figure is broken into two time periods: 10:59:04 to 11:01:30 (Figure 7a), and 11:01:30 to 11:03:11 (Figure 7b). As noted above, these trajectories are based on the NZY ASR returns for each aircraft, supplemented by simulations of the aircrafts' movements based on ATCT communications when the aircraft are below radar coverage (i.e., below about 700 ft. MSL or 175 ft. above the runways).[10]

The operations of all the aircraft communicating with the KSDM ATCT and under ATCT control from the time that N1285U first contacted the ATCT requesting touch-and-goes (at 10:49:44) to the collision (at 11:03:10.2) is summarized in Table 4. This information is also presented graphically in Figure 8.

---

[9] Several Figures in this *Study* have an "a" and a "b" version, which present the same information but at different scales, or with different background images. When the *Study* refers to a Figure with two or more versions without specifying the version, all versions are meant to be included in the reference.

[10] The simulations were performed by manually flying representative aircraft through their (corrected) radar targets in *Microsoft Flight Simulator X* (FSX), and then completing each aircraft's maneuver (e.g., a landing and taxi to parking) based on the KSDM ATCT clearances and instructions. The radar returns were corrected so as to make each aircraft's trajectory consistent with the location and geometry of the runway on which it was operating. FSX can display graphical objects (representing radar targets) at user-defined positions in space, as well as record a user's simulated flight. The recorded flights for each aircraft were subsequently "spliced" into the aircraft's recorded radar data, and are presented in Figures 7 and 13.

Symbol	Time HH:MM:SS PDT	Time before collision MM:SS	Event Events in *italics* are ATC communications; others are EAGLE1 CVR events	Altitude, ft. MSL		Groundspeed, kt.		Separation, nmi	Closure rate, kt.
				EAGLE1	N1285U	EAGLE1	N1285U		
A	10:59:04.00	04:06.2	*[EAGLE1] brown tower eagle1 9 west inbound bravo full stop*	2505	1045	235	73	Not computed	
B	10:59:20.20	03:50.0	[CAM] [sound of high pitch whine for about 20 seconds (about 4500 Hz), similar to flap in motion]	2462	842	208	67		
C	10:59:50.00	03:20.2	*[TWR] eagle1 maintain at or above 2000 right traffic runway 26R*	2424	559	202	63		
D	11:00:13.00	02:57.2	[CAM] [sound of high pitch whine for about 2 seconds (about 4500 Hz), similar to flap in motion]	2332	643	186	67	5.13	249
E	11:00:29.00	02:41.2	[HOT-2] got one on short final.	2257	779	181	73	4.05	250
F	11:00:46.40	02:23.8	[CAM] [sound of high pitched whine (about 5,000 Hz) for about 10 seconds; start of whine contained the sound of clunk followed about 5 seconds later by another clunk, similar to landing gear extension]	2189	1019	170	68	2.90	228
G	11:01:15.50	01:54.7	[HOT-2] got one on the runway.	2100	1415	156	65	1.24	171
H	11:01:24.60	01:45.6	[HOT-1] I got twelve o'clock on a climb out.	2100	1591	145	70	0.84	141
I	11:01:43.10	01:27.1	[HOT-2] (must be) the jump plane.	2070	1701	142	91	0.46	17
J	11:01:49.00	01:21.2	[HOT-3] see him right there?	2037	1701	135	96	0.46	-7
K	11:02:14.00	00:56.2	[CAM] [sound of high pitch whine for about 2 seconds (about 4500 Hz), similar to flap in motion]	2109	1646	145	110	0.65	-30
L	11:02:14.00	00:56.2	*[EAGLE1] eagle 1 is right downwind abeam traffic to the left and right in sight*	2109	1646	145	110	0.65	-30
M	11:02:32.00	00:38.2	*[TWR] cessna 6ZP make a right 360 right 360 rejoin the downwind*	2073	1510	143	104	0.80	-22
N	11:02:32.40	00:37.8	[HOT-1] you still got the guy on the right side?	2070	1509	142	104	0.81	-21
O	11:02:42.00	00:28.2	*[TWR] eagle1 turn base 26R clear to land*	1962	1462	131	100	0.82	9
P	11:02:59.30	00:10.9	[HOT-1] I see the shadow but I don't see him.	1593	1392	143	103	0.49	142
Q	11:03:04.00	00:06.2	*[TWR] N85U tower*	1489	1374	139	101	0.29	161
R	11:03:08.00	00:02.2	*[TWR] are you still on downwind sir right downwind*	1400	1359	137	98	0.11	171
S	11:03:10.20	00:00.0	Collision (end of EAGLE1 CVR recording)	1351	1351	135	98	0.00	171

Table 3. Summary of significant ATC communication and EAGLE1 CVR events. NOTE: a version of this table is also presented in Figures 5a and 6a; in the Figures, the CVR content is paraphrased for brevity. The full CVR content text is shown on this page.

Time HH:MM:SS PDT	Operation	# aircraft under KSDM ATCT ground control	# aircraft under KSDM ATCT local control	Total # aircraft under KSDM ATCT control
10:49:44	N1285U calls for touch-n-goes; N6ZP pattern work 26R; N5058U inbound landing; N8360R pattern work 26L	0	4	4
10:51:52	N81962 calls for landing	0	5	5
10:52:43	N5058U lands and taxis to parking	0	4	4
10:53:48	XALVV calls for landing	0	5	5
10:55:10	N5058U calls for taxi for takeoff	1	5	6
10:55:57	N18WZ calls for landing	1	6	7
10:57:01	XALVV lands, holds between runways	2	5	7
10:58:02	N81962 lands & stops at alpha	3	4	7
10:58:48	N5161U calls for landing	3	5	8
10:59:04	EAGLE1 calls for landing	3	6	9
10:59:36	N81962 taxis to ramp	2	6	8
11:00:31	N5058U cleared for takeoff	1	7	8
11:01:02	N5442P calls over Tijuana for landing	1	8	9
11:01:20	XALVV taxis to customs	0	8	8
11:01:23	N18WZ lands and exits at bravo	1	7	8
11:01:42	N18WZ taxis to customs	0	7	7
11:02:51	N5161U lands and taxis to parking	0	6	6
11:03:10	Collision	0	4	4

Table 4. Summary of KSDM ATCT aircraft operations, 10:49:44 – 11:03:10.

Radar data uncertainty and estimates of airplane performance based on radar data

The boxes surrounding the NZY and NKX ASR returns in Figures 5 and 6 represent the (nominal) uncertainty in the radar return location; the sensed location is at the center of the box, but uncertainties in range and azimuth could place the actual location anywhere within the box. Note that the uncertainty boxes only depict potential point-to-point, random errors in the radar range and azimuth data, and do not account for "bias" errors in the radar data that may shift the entire radar track away from the true track. The offset of the N1285U track from the KSDM runway 26L centerline during the airplane's touch-and-go on that runway is evidence of some bias error in the radar data. Additional evidence of bias errors are the offsets between the NZY and NKX tracks of the same aircraft, shown in Figures 5b and 6b.

Random point-to-point uncertainty or error in airplane position and altitude leads to unrealistic noisiness in aircraft performance parameters, such as speed and track angle, calculated using the "raw" (i.e., uncorrected) radar data.[11] To reduce the noisiness and obtain a better estimate of airplane performance, in this *Study* the NZY radar data is smoothed using a running-average algorithm. There are other smoothing techniques that can result in a reasonable fit of the raw radar data (i.e., that keep each radar return within its uncertainty box), and each of these will produce slightly different performance calculation results. Figures 5 and 6 show the smoothed track used in this *Study* to compute the airplane performance parameters (the track for EAGLE1 is also based on a simulation of the airplane's turn from downwind to base so as to match the EAGLE1 radar data at the start of the turn and the collision location and geometry at the end of the turn, as described in Section D-III). The smoothed N1285U track has also been shifted so as to align the touch-and-go of the airplane with the KSDM runway 26L centerline, and to force a collision with EAGLE1 at the correct time and location. The final track used as the basis for the N1285U performance calculations and the cockpit visibility study is the line labeled "N1285U computed trajectory" in Figures 5 and 6. The final EAGLE1 track used for the cockpit visibility study is the line labeled "EAGLE1 computed trajectory" and is described further in Section D-III.

The radar data for EAGLE1 during its downwind-to-base turn is relatively sparse, and so cannot be used by itself to compute performance information for the airplane during this critical time.[12] Instead, during this time the performance parameters for EAGLE1, including altitude, speed, and Euler angles (pitch, roll, and heading), are based on the simulation of the airplane's motion during the turn. However, the radar data for N1285U is continuous (with an NZY ASR return about every 4.8 seconds) up to the collision, and so is used to compute all the performance information for that airplane, including the Euler angles required for the cockpit visibility study.

If the position (latitude, longitude, and altitude) of an airplane is known as a function of time, then its orientation (i.e., the Euler angles) can also be estimated as long as the following are true:

- The motion of the air mass relative to the Earth, i.e., the wind, is known;
- The lift coefficient of the airplane as a function of angle of attack is known;
- The gross weight of the airplane is known;
- The sideslip angle and lateral acceleration are negligible (i.e., coordinated flight).

[11] A constant bias error in the radar track does not contribute to noise in speed and other performance calculations.

[12] Note the large gap in the NZY and NKX ASR returns for EAGLE1 between points "O" and "P" in Figures 5 and 6. The OpsVue points that appear in this gap may be "coast" data rather than real radar returns, and are not necessarily reliable. Nonetheless, they match simulation track for EAGLE1 relatively well.

The winds aloft in the vicinity of KSDM for the performance calculations were provided by an NTSB meteorologist, and are based on the North American Mesoscale (NAM) weather model sounding for KSDM at 18:00 UTC (11:00 PDT) on August 16, 2015. The wind speed and direction, and static air temperature, are plotted as a function of altitude in Figure 9.

The KSDM Meteorological Aerodrome Reports (METARs) surrounding the time of the accident are shown in Table 5:

Parameter \ Report	KSDM METAR 09:53 PDT	KSDM METAR 10:53 PDT	KSDM METAR 11:53 PDT
Sky condition	clear	clear	clear
Visibility	10 statute miles	10 statute miles	10 statute miles
Winds	calm	310° @ 6 kt.	280° @ 10 kt.
Temperature / Dew Point	32°C / 13°C	33°C / 19°C	28°C / 19°C
Altimeter setting	29.87 “Hg	29.87 “Hg	29.88 “Hg

Table 5. Weather observations at KSDM surrounding the time of the accident.

As noted above, aerodynamic data for the C172 was provided by Textron Aviation. A gross weight of 1802 lb. (see Table 2) is assumed in the N1285U performance calculations. Per Reference 7, the flap actuator found in the N1285U wreckage indicated a flap deflection of 10° at the time of impact. For this *Study*, it is assumed that the flaps were set from 0° to 10° at 11:02:26, when the airplane was between the thresholds of runways 26L and 26R and descending on the downwind leg (the flap setting affects the pitch angle of the airplane at a given weight and airspeed).

The position coordinates of an airplane as a function of time define its velocity and acceleration components. In coordinated flight, these components lie almost entirely in the plane defined by the airplane’s longitudinal and vertical axes. Furthermore, any change in the *direction* of the velocity vector is produced by a change in the lift vector, either by increasing the magnitude of the lift (as in a pull-up), or by changing the direction of the lift (as in a banked turn). The lift vector also acts entirely in the aircraft’s longitudinal-vertical plane, and is a function of the angle between the aircraft longitudinal axis and the velocity vector (the angle of attack, α). These facts allow the equations of motion to be simplified to the point that a solution for the airplane orientation can be found given the additional information about wind and the airplane lift curve (i.e., C_L vs. α).

The results of the EAGLE1 and N1285U radar-based performance calculations are presented along with the EAGLE1 performance parameters estimated by simulation during its base turn in Section D-III. The limited accuracy of the radar-based performance calculations should be considered when drawing conclusions based on these calculations. This caveat must also be borne in mind when considering the results of the cockpit visibility calculations described in Section D-IV, which depend on the pitch, roll, and heading angles computed from the radar data.

III. EAGLE1 simulation data and estimated collision geometry

Introduction

As noted above, the radar data for EAGLE1 during its downwind-to-base turn is relatively sparse, and so is not suitable by itself for deriving performance information during this dynamic maneuver. Furthermore, it is difficult to find a satisfactory trajectory for the turn simply by interpolation between the last radar returns on downwind and the collision location (indicated approximately by the location of the N1285U wreckage). EAGLE1's trajectory must satisfy the constraints listed on p. 8, as well as be consistent with the performance and operational procedures (such as typical pattern speeds) of the airplane.

For this ***Study,*** a satisfactory solution for EAGLE1's trajectory during the downwind-to-base turn was found by combining an interpolation of the radar data and collision location with a 3-degree-of-freedom (DOF) simulation of the airplane's motion. In this approach, the interpolated trajectory was supplied to the simulation as a "target" trajectory, while a mathematical control algorithm (or "math pilot") manipulated the simulated airplane pitch and roll angles and thrust in an attempt to follow the target trajectory. The math-pilot derived roll angle was then adjusted by trial-and-error to obtain a trajectory for EAGLE1 that satisfied the requirement of a collision near the N1285U wreckage, at the time at which the EAGLE1 CVR recording stopped, and at a collision angle with N1285U that was consistent with the scrape mark found on EAGLE1's lower right wing.

Modeling the NA265-60SC Sabreliner

As stated earlier, Sabreliner Corporation was unable to define the lift curve (C_L as a function α) of the NA265-60SC, which is needed to model the airplane in the simulation. Consequently, for this ***Study*** the lift curve was determined by analyzing airplane performance data recorded during N442RM's flight the day before the accident. The recorded data included GPS position data and inertial parameters such as accelerations, groundspeed, and track angle, and the Euler angles (heading, pitch, and roll). Pneumatic parameters (such as airspeed) and air temperature were not recorded; consequently, a NAM model of the winds and temperature aloft over KSDM on August 15 was used to estimate airspeed and dynamic pressure from the recorded inertial speeds.

The airplane stability-axis lift, drag, and side force coefficients (C_L, C_D, and C_Y, respectively) are equivalent to the body-axis force coefficients C_x, C_y, and C_z transformed from the body-axis system to the stability-axis system by a rotation about the body y-axis through the angle of attack α (see Figure 10):

$$\begin{Bmatrix} -C_D \\ C_Y \\ -C_L \end{Bmatrix} = \begin{Bmatrix} C_x \\ C_y \\ C_z \end{Bmatrix}_s = \begin{bmatrix} \cos\alpha & 0 & \sin\alpha \\ 0 & 1 & 0 \\ -\sin\alpha & 0 & \cos\alpha \end{bmatrix} \begin{Bmatrix} C_x \\ C_y \\ C_z \end{Bmatrix}_b \quad [1]$$

Where the subscripts s and b denote the stability-axis and body-axis systems, respectively. In Equation [1], C_L, C_D, and C_Y include the effects of both aerodynamic and thrust forces acting on the airplane; to isolate the aerodynamic coefficients, the effect of the thrust forces need to be subtracted from the total coefficients. Since in this ***Study*** we are interested in the total forces acting on the airplane, and the conditions used to compute these forces are similar to those in which the

results will be applied (i.e., the airplane on approach into KSDM), it is not necessary to break out the aerodynamic and thrust contributions to the total forces.

The total body-axis force coefficients are given by

$$C_i = \frac{F_i}{qS} = \frac{n_i W}{qS} \quad [2]$$

Where the subscript i denotes each of the airplane body axes, i.e., the longitudinal (x), lateral (y), and vertical (z) axes. W is the gross weight, S is the wing area, and q is the dynamic pressure:

$$q = \left(\frac{1}{2}\right)\rho {V_T}^2 \quad [3]$$

Where ρ is the air density, and V_T is the true airspeed. ρ can be computed from the static air pressure and temperature (known at a given GPS altitude from the NAM model sounding). V_T can be computed from the recorded groundspeed and ground track and the NAM winds:

$$\vec{V}_T = \vec{V}_G - \vec{V}_W \quad [4]$$

Where $\vec{V}_T$ is the true airspeed vector, $\vec{V}_G$ is the groundspeed vector, and $\vec{V}_W$ is the wind vector.

For small roll and sideslip angles, α is given by

$$\alpha \cong \theta - \gamma \quad [5]$$

Where θ is the recorded pitch angle, and γ is the flight path angle, computed from

$$\gamma = \sin^{-1}\left(\frac{\dot{h}}{V_T}\right) \quad [6]$$

Where $\dot{h}$ is the rate of climb (computed from the recorded altitude).

The lift curve computed using Equations [1]-[6] and the data from N442RM's August 15 approach into KSDM is presented in Figure 11. Note that there are two distinct segments to the lift curve; based on the position of the airplane relative to the landing runway and the recorded groundspeed, these segments likely correspond to the airplane's flaps 20° and flaps 30° configurations. Straight lines through the segments indicate the flaps 20° and flaps 30° lift curves assumed in the simulation. In the simulation, the flaps were set at 20° and ramped to 30° at 11:02:14 based on the sound of flap motion on the CVR at that time (see Table 3), and evidence in the EAGLE1 wreckage that the flaps were at 30° at impact.[13] Additional sounds of flap motion were recorded at 10:59:20.2 and 11:00:13, suggesting deflections from 0° to 10° and 10° to 20°, respectively; consequently, the use of flaps 20° in the simulation prior to 11:00:13 likely underestimates the pitch angle during that time. However, at 11:00:13 EAGLE1 was over 5.5 miles from the runway 26R threshold, and so the visibility angles from the cockpit (which are dependent in part on the pitch angle) prior to this time are of less interest, and the error in pitch associated with using 20° flaps is tolerated.

[13] Per an email from the NTSB Investigator In Charge to the NTSB Aircraft Performance Specialist, dated 11/17/2015.

Estimated collision time, location, and geometry

The EAGLE1 track derived from the simulation, merged with EAGLE1's radar track, and used for the cockpit visibility study is the line labeled "EAGLE1 computed trajectory" in Figures 5 and 6. This track is consistent with the (adjusted) NZY and NKX ASR returns, and with the constraints listed on p. 8. The time of the collision is assumed to coincide with the end of the EAGLE1 CVR recording, at 11:03:10.2; consequently, N1285U and EAGLE1 must have been close to the N1285U wreckage location at this time (given N1285U's lesser speed and weight (momentum), it likely fell nearer to the impact location than EAGLE1). Furthermore, Reference 2 states that

> Detailed examination of the wreckage from both airplanes was conducted at a secure facility several days after the accident. The right wing of Eagle1 was positioned with the N1285U wreckage, and investigators conducted an examination for contact evidence between the airplanes. The Eagle1 right wing had impact marks consistent with the impact of N1285U's engine. Specifically, the spacing of the impact marks on the inboard lower surface of the Eagle1 right wing were consistent with the spacing of the N1285U engine crankcase upper studs, flanges, and engine lifting eye. The angle of the marks relative to the Eagle1's longitudinal axis was about 30˚ and indicates that this was the convergence angle between the airplanes. The damage on the N1285U crankcase upper studs, flanges, and engine lifting eye was consistent with impact from its left side and with the computed convergence angle.
>
> In addition, the conformity of the Cessna fuselage, wing strut, and wing spar damage to the Eagle1 wing shape indicates that the Eagle1 right wing impacted the left side of the Cessna. The evidence is consistent with the longitudinal axes of the two airplanes being approximately perpendicular to one another at the time of impact, with Eagle1 approaching the Cessna from the left, and with the Eagle1 right wing below the Cessna left wing.

The groundspeeds and track angles of N1285U and EAGLE1 corresponding to the computed tracks shown in Figures 5 and 6 indicate that at the time of the collision, the *relative velocity* of N1285U with respect to EAGLE1 was 171 kt. along a heading of 55° (these and other details about the tracks are discussed further below). Since EAGLE1 was tracking about 201° at the time of collision (per the simulation), N1285U would have been moving at an angle of 201° - 55° = 146° relative to EAGLE1's centerline. The smaller angle between the centerline and a line drawn 146° to the centerline is 180° - 146° = 34°, which corresponds relatively well with the 30° scrape observed on EAGLE1's lower right wing. The approach of EAGLE1 from N1285U's left side cited in Reference 2 is also consistent with the collision geometry illustrated in Figures 5 and 6.

The computed EAGLE1 and N1285U trajectories plotted in Figures 5 and 6 result in the following time and coordinates for the collision:

Time of collision = 11:03:10.2 PDT NZY ASR time
East coordinate = 1.07 nmi east of KSDM runway 26R threshold
North coordinate = 0.49 nmi north of KSDM runway 26R threshold
Altitude = 1350 ft. MSL

The north and east positions of EAGLE1 and N1285U are presented as a function of time in Figure 12. This Figure presents the NZY and NKX ASR raw radar returns, OpsVue data, and "computed trajectory" lines for each airplane. The labels for the events listed in Table 3 are shown near the top of the bottom plot in Figure 12, at the time coordinate at which they occurred. This annotation scheme also appears on many subsequent plots of data vs. time.

The altitudes of EAGLE1, N1285U, and other aircraft in the KSDM traffic pattern are presented as a function of time in Figure 13. The NZY and NKX ASR Mode C returns and OpsVue altitude data

for EAGLE1 and N1285U are presented, along with the associated 50 ft. Mode C uncertainty bands. The altitude lines corresponding to the computed trajectories for EAGLE1 and N1285U are also shown. Note that the computed trajectories are consistent with the Mode C uncertainty bands, with a few exceptions. For example, where the NZY and NKX Mode C returns are very close in time but differ by 100 ft. in altitude, the best estimate of altitude is likely exactly halfway between the recorded altitudes, but in some cases the computed trajectories shown in Figure 13 differ from these "halfway points" by a few feet, and hence lie outside the uncertainty band of one of the ASRs. However, the error or uncertainty introduced into the performance and visibility calculations by this difference is small compared to the overall uncertainty associated with radar-based data, the winds aloft model, the aerodynamic characteristics of the airplanes, and the pilot eye locations (the effects of uncertainty in pilot eye location are discussed in Section D-IV).

Figure 13 also provides evidence of "coasting" in the EAGLE1 OpsVue data. Note that there is a gap in the NZY and NKX EAGLE1 returns between 11:02:42 and 11:03:01, but that OpsVue data for EAGLE1 appears in this interval, and follows the decreasing altitude trend apparent in the data prior to the gap. The last OpsVue data point in this interval is at 11:03:00, at an altitude of 1906 ft.; however, a return for EAGLE1 from NZY was received at 11:03:01, indicating an altitude of 1500 ft. Since EAGLE1 clearly did not descend 400 ft. in one second, the OpsVue data in the gap is likely the result of coasting. Further evidence of coasting is the OpsVue point for EAGLE1 at 11:03:14 and 1200 ft., 3 seconds after the time of the collision per the end of the EAGLE1 CVR recording.

Figure 14 shows the true airspeed, calibrated airspeed, groundspeed, and rate of climb calculated from the computed trajectories for EAGLE1 and N1285U. Figure 14 indicates that at the time of the collision, EAGLE1's groundspeed was about 135 knots, and N1285U's groundspeed was about 98 knots. EAGLE1 was descending at about 1330 ft./min., and N1285U was descending at about 220 ft./min.

Figure 15 shows the separation distance between the two airplanes and the closure rate (information from this Figure is also included in Table 3). The Figure indicates that the closure rate was about 170 knots at the time of the collision.

Figure 16 presents the pitch, roll, heading, and ground track angles calculated from the smoothed radar data for N1285U, and by the 3-DOF simulation for EAGLE1. EAGLE1's track angle at the time of the collision was about 201°, and N1285U's track angle was about 107°. Therefore, the collision angle (the smallest angle between the longitudinal axes of the aircraft at the time of impact)[14] is about 86° (180° - [201°- 107°]), with EAGLE1 descending into N1285U from the left, and N1285U "climbing" (relatively) into EAGLE1 from the right.

Figure 17 presents the estimates of the airplane configuration (flap and gear settings) for EAGLE1 and N1285U as a function of time. The flap positions are discussed above, and the EAGLE1 gear extension is based on the "sound similar to landing gear extension" recorded on the CVR at 11:00:46.4 (see Table 3).

The yaw, pitch and roll angles plotted in Figure 16 are used along with the computed airplane trajectories shown in Figures 5 and 6 in the cockpit visibility study presented in Section D-IV.

[14] The collision angle is not be confused with the angle the velocity vector of N1285U *relative to EAGLE1* made with the centerline of EAGLE1 (the scrape angle), as discussed above. The relative velocity depends on the airplanes' groundspeeds, as well as their track angles; the collision angle as defined here only depends on the track angles.

IV. Cockpit visibility study

Azimuth and elevation angles of "target" aircraft relative to "viewer" aircraft

Once the position and orientation of each airplane has been determined, their positions in the body axis system of the other airplane can be calculated. These relative positions then determine where the "target" aircraft will appear in the field of view of the pilot of the "viewer" aircraft.

For this S*tudy*, the relative positions of the two aircraft (and the visibility of each from the other) were calculated at 1-second intervals up to the collision, beginning at 11:00:06, as N1285U was climbing after completing its touch-and-go on runway 26L, and 7 seconds before the EAGLE1 flaps were likely set to 20° (consequently, the pitch angle error associated with using 20° of flaps in the simulation prior to 11:00:13 is largely irrelevant for the visibility study).

The "visibility angles" from the "viewer" airplane to the "target" airplane correspond to the angular coordinates of the line of sight between the airplanes, measured in a coordinate system fixed to the viewer airplane (the viewer's "body axis" system), and consist of the azimuth angle and elevation angle (see Figure 18). The azimuth angle is the angle between the x-axis and the projection of the line of sight onto the x-y plane. The elevation angle is the angle between the line of sight itself, and its projection onto the x-y plane. At 0° elevation, 0° azimuth is straight ahead, and positive azimuth angles are to the right. 90° azimuth would be out the right window parallel to the y axis of the airplane. At 0° azimuth, 0° elevation is straight ahead, and positive elevation angles are up. 90° elevation would be straight up parallel to the z axis. The azimuth and elevation angles depend on both the position (east, north, and altitude coordinates) of the viewer and target airplanes, and the orientation (yaw, pitch, and bank angles) of the viewer. The azimuth and elevation angles of points on the target away from its center of gravity (CG) also depend on the orientation of the target.

The position and Euler angles of EAGLE1 and N1285U are based on smoothed radar data and the constraints listed on p. 8, and so are sensitive to how the radar data is smoothed and the possibility of multiple, slightly differing trajectories that all result in solutions within the uncertainty bounds of the data. Consequently, there is also some uncertainty in the Euler angles associated with any particular trajectory.

Azimuth and elevation angles of airplane structures from laser scans

The target airplane will be visible from the viewer airplane unless a non-transparent part of the viewer's structure lies in the line of sight between the two airplanes. To determine if this is the case, the azimuth and elevation coordinates of the boundaries of the viewer's transparent structures (windows) must be known, as well as the coordinates of the viewer's structure visible from the cockpit (such as the wings and wing struts). If the line of sight passes through a non-transparent structure (such as the instrument panel, a window post, or a wing), then the target airplane will be obscured from the viewer.

For this *Study*, the azimuth and elevation angles of the window boundaries and wings of EAGLE1 and N1285U were determined from the interior and exterior dimensions of exemplar airplanes, as measured using a FARO laser scanner.[15] The laser scanner produces a "point cloud" generated by the reflection of laser light off of objects in the laser's path, as the scanner sweeps through 360° of

[15] Specifically, the FARO "Focus 3D" scanner; see http://www.faro.com/en-us/products/3d-surveying/faro-focus3d/overview.

azimuth and approximately 150° of elevation. The 3-dimensional coordinates of each point in the cloud are known, and the coordinates of points from multiple scans (resulting from placing the scanner in different positions) are "merged" by the scanner software[16] into a common coordinate system. By placing the scanner in a sufficient number of locations so that the scanner can "see" every part of the airplane, the complete exterior and interior geometry of the airplane can be defined.

In this *Study*, the scanner was placed in several locations to scan the exterior of the airplanes, and in the pilot seats to scan the interior of the airplanes.[17] The scanner software was then used to identify the points defining the outline of the cockpit windows (from the interior scans) and exterior structures visible from the cockpit (from the exterior scans). The coordinates were transformed into the airplane's body axis system and, ultimately, into azimuth and elevations angles from the pilot's eye position. The transformation method is described in Appendix A.

The azimuth and elevation angles of the viewer airplane's windows and other structures are very sensitive to the pilot's eye location in the cockpit. If the pilot moves his head forward or aft, or from a position centered over his seat to one close to a window surface, the view out the window (and the azimuth and elevation angles of all the airplane's structures) change substantially. This potential variability in the pilot's eye position, and the consequent variability in the location of the window edges and airplane structures in the pilot's field of view, is by far the greatest source of uncertainty as to whether the target aircraft is obscured or not at a given time.

To evaluate the effect of varying eye position on the visibility of the target airplane, the azimuth and elevation angles of the cockpit windows and other airplane structures were computed for a matrix of eye positions displaced from the nominal eye positions, as described below. The "nominal" eye positions were estimated by scanning a person seated in the exemplar aircraft, in the usual flying position (seated upright with the head centered over the seat).

In addition to the calculation of the visibility angles, this *Study* presents recreations of possible views from the pilots' seats (including simulation-based depictions of the outside world) constructed assuming the nominal eye positions as defined above.

Results: azimuth and elevation angle calculations

The azimuth and elevation angles from the "viewer" airplanes to the "target" airplanes are shown as a function of time in Figure 19. In the top plot, EAGLE1 is the "viewer" and N1285U is the "target," and in the bottom plot, N1285U is the "viewer" and EAGLE1 is the "target."

Plots of the "target" airplane elevation angle vs. azimuth angle are shown in Figure 20a, along with the azimuth and elevation coordinates of the "viewer" airplane cockpit windows and other structures, as computed for the nominal pilot eye position. Figure 20b presents photographs of the cockpits that help identify the cockpit structures depicted in gray in Figure 20a. EAGLE1 is the "viewer" in the top plot of Figure 20a, and N1285U is the "viewer" in the bottom plot. The multicolored line in these plots indicates the coordinates of the "target" aircraft, which change with time. The times corresponding to selected coordinates are indicated by the event labels, and by

[16] FARO SCENE software: see http://faro-3d-software.com/.
[17] Two scans each from the pilot and co-pilot seats of the airplanes were performed: one with the other seat empty, and one with the other seat occupied (to measure the obstruction to vision presented by the occupant).

the changing colors of the line itself, per the color legend in the bottom plot of Figure 20a. If the multicolored line passes through a shaded area of the plot, the "target" airplane is obscured from view by the "viewer" airplane structure.

The azimuth and elevation angles of the sun are also of interest, because sun glare can affect a pilot's ability to see other aircraft. The azimuth (relative to true north) and altitude angles of the sun at 11:03:00 PDT on August 16, 2015 at the accident site were 120.86° and 58.76°, respectively.[18] To compute the location (azimuth and elevation angles) of the sun in the EAGLE1 and N1286U pilots' fields of view, the coordinates of the sun in earth coordinates were computed (using the sun angles and an assumed very large distance to the sun), and then transformed into the airplane body axis coordinates using the Euler angles shown in Figure 16. The azimuth and elevation angles of the sun were then computed from its body axis coordinates.

The results of these calculations are shown in Figure 21, and indicate that at the time of the collision the sun would have been located above both airplanes' windows and behind the airplanes' structures, and so sun glare likely did not affect the pilots' abilities to see the target airplanes.

To simplify the discussion of the visibility from the cockpit of each airplane, in this *Study* EAGLE1's 10 cockpit windows (5 on each side of the airplane) are labeled L1 through L5 for the left windows, and R1 through R5 for the right windows, as shown in Figure 22a. N1285U's windows are the windshield, left window, and right window. The latter two are part of the airplane's doors; see Figure 22b.

As noted above, the azimuth and elevation angles of the window and cockpit structures are sensitive to the position of the pilot's eyes in the cockpit. To determine how these angles change as the pilot's eye position changes (e.g., by leaning in different directions, or by a seat height adjustment), plots similar to Figure 20a were generated for the 27 different eye positions shown in Table 6. The positions are expressed as displacements from the nominal eye position along the three airplane body axes ($\{\Delta x_b, \Delta y_b, \Delta z_b\}$[19]).

The results of the calculations are presented in Figure 23 for EAGLE1, and in Figure 24 for N1285U. The times associated with the trajectory of the "target" airplane in these figures is depicted by the color of the trajectory line, starting with green at 11:00:00, and progressing to red at 11:03:15. A color legend for these lines is shown in Figures 20a and 21.

As shown in Figures 23 and 24, variations in the pilot's eye position from the nominal position affects the times at which the target airplane may have become obscured by the viewer airplane's structure. For example, Figure 23 shows that if EAGLE1's co-pilot's eyes were 1.5" above the nominal position, at 11:02:52 N1285U would have become and remained obscured behind the window support structure between the R1, R2, R4 and R5 windows up until the collision. With the pilot's eyes at the nominal position, N1285U would have become obscured at 11:02:49, but then would have re-appeared in the R2 window at 11:02:56 before becoming obscured again behind the post between the R1 and R2 windows at 11:03:06 (4 seconds before the collision).

[18] This sun position was determined using the http://www.susdesign.com/sunangle/ website.
[19] The body axis system is illustrated in Figure 10.

Case name	Δx_b from nominal, in. (+ forward, - aft)	Δy_b from nominal, in. (+ right, - left)	Δz_b from nominal, in. (+ down, - up)
CCD	0	0	+1.5
FCD	+3	0	+1.5
ACD	-3	0	+1.5
FLD	+3	-3	+1.5
CLD	0	-3	+1.5
ALD	-3	-3	+1.5
FRD	+3	+3	+1.5
CRD	0	+3	+1.5
ARD	-3	+3	+1.5
CCC (nominal)	0	0	0
FCC	+3	0	0
ACC	-3	0	0
FLC	+3	-3	0
CLC	0	-3	0
ALC	-3	-3	0
FRC	+3	+3	0
CRC	0	+3	0
ARC	-3	+3	0
CCU	0	0	-1.5
FCU	+3	0	-1.5
ACU	-3	0	-1.5
FLU	+3	-3	-1.5
CLU	0	-3	-1.5
ALU	-3	-3	-1.5
FRU	+3	+3	-1.5
CRU	0	+3	-1.5
ARU	-3	+3	-1.5

Table 6. Matrix of eye positions for cockpit structure azimuth and elevation angle calculations.

The EAGLE1 nominal eye position is based on a 73" tall pilot,[20] and EAGLE1's co-pilot was 71" tall.[21] Consequently, the co-pilot's eye position may have been a little lower, but not likely higher, than the nominal position. At an eye position 1.5" below the nominal position, N1285U would become obscured at 11:02:51, reappeared at 11:02:55, and become obscured again at 11:03:06.

Similarly, if N1285U's pilot's eyes were 3" forward of the nominal position, then EAGLE1 would have appeared from behind the post separating the left window and windshield at about 11:02:51 (19 seconds before the collision), rather than remaining obscured behind this post as in the nominal case (the nominal position is based on a pilot 69" tall,[22] matching the height of the N1285U pilot[23]). If the pilot's eyes moved 3" to the right (towards the center of the cockpit), then EAGLE1 would have appeared from behind the post at 11:02:54 (16 seconds before the collision).

These results indicate that the visibility of one aircraft from the other is sensitive to the position of the pilots' eyes relative to the window structures. This observation underscores the fact that scanning for traffic visually can be more effective if pilots move their heads as well as redirect their eyes, since head movements may bring otherwise obscured aircraft into view.

[20] This is the height of the individual seated in the co-pilot's seat when the exemplar Sabreliner was laser-scanned.
[21] Per an email from the NTSB Investigator In Charge to the NTSB Aircraft Performance Specialist, dated 9/08/2016.
[22] This is the height of the individual seated in the pilot's seat when the exemplar Cessna 172 was laser-scanned.
[23] Per an email from the NTSB Investigator In Charge to the NTSB Aircraft Performance Specialist, dated 9/09/2016.

Simulated views from the EAGLE1 and N1285U cockpits

While Figures 19-24 depict where the "target" airplanes could have appeared in the "viewer" airplanes' windows, they do not provide a sense of the background against which the targets would appear, and against which the pilot of each airplane would have to see the target. To provide a rough approximation of these backgrounds and how the view from each cockpit evolved over time, the views were recreated in the *Microsoft Flight Simulator X* (*FSX*) simulation program, using airplane and sky graphics inherent in *FSX*, and terrain textures based on *Microsoft Visual Earth* satellite imagery.[24]

The cockpit structure of each airplane at the nominal pilot's eye point (based on the laser scans) was constructed in *FSX* as semi-transparent panels that "mask" the view from each cockpit (see Appendix B); the cockpit geometry built into the airplane models used in the simulation was not used. Airplane models were only used to represent the exterior "target" airplane geometry in the recreated views. The airplane models were chosen based on their color resemblance to the accident airplanes, and are freely provided by *FSX* enthusiasts.[25] The position (latitude, longitude, and altitude) and attitude (heading, pitch, and roll) of each airplane was recreated in *FSX* using the *FS Recorder* program developed by Matthias Neusinger,[26] based on the final estimated position and attitude data for each airplane described in Sections D-II and D-III.

FSX contains inherent options to customize the time, date, and weather depiction in the simulation. The time and date were set to those of the accident (11:03 PDT on August 16, 2015), which results in the correct placement of the sun in the sky. The weather option was set to "clear skies."

The view depicted by *FSX* depends on the "camera" settings. In this *Study*, the *FSX* camera is equivalent to the pilot's eyes: the view from the cockpit depends on the camera's position, orientation (where it's pointed), and its "field of view" (i.e., the range of azimuth and elevation angles that can be "seen" by the camera). The widest field of view available in *FSX* is 90° horizontally and about 62° vertically.[27] Consequently, if the camera is pointed straight ahead (0° azimuth), then only azimuth angles between -45° and +45° will be visible in that view. If objects of interest (e.g., the target airplane) are beyond this range, then to "see" them the camera will have to be rotated away from 0° azimuth toward the object. However, in this case, a portion of the view straight-ahead will be lost, which may be unsatisfactory for the purpose of giving the viewer a good sense of the airplane's direction of travel and general situation relative to the outside world.

To see objects beyond ±45° of azimuth while at the same time preserving a field of view of at least ±45° of azimuth about the direction of travel, the view from two co-located cameras can be joined side-by-side: the first camera pointed away from 0° azimuth to capture the object, and the second camera pointed in such a way that the boundaries of the fields of view of the cameras coincide at a particular azimuth angle. For example, if one camera is rotated to -75° azimuth, the left boundary of its field of view will be at -75° - 45° = -120°, and the right boundary will be at -75° + 45° = -30°. If the second camera is rotated to +15° azimuth, its left boundary will be at +15° - 45° = -30° (coinciding with the right boundary of the first camera), and its right boundary will be at +15° + 45°

[24] See https://www.bing.com/mapspreview.
[25] The Sabreliner model used is the "Rockwell T-39 Sabreliner Twin Package" by Fly Away Simulation; the white-and-yellow Cessna 172 model is included with the baseline *FSX* program.
[26] See http://www.fs-recorder.net/.
[27] These values are for an *FSX* window with an aspect ratio of 1.6, at "zoom" setting of 0.3.

= 60°. Setting the views from the cameras side-by-side, a continuous field of view from -120° to +60° is obtained.

However, discontinuities (kinks) in straight lines may appear at the boundary of these views when they are viewed side-by-side on a flat surface (such as a computer screen), because the viewer will be viewing both from the same angle, whereas the view on the left is intended to be viewed at an angle rotated 90° from that on the right. The discontinuities can be removed if each view is presented on a separate surface (monitor), and then the surfaces are joined at a 90° angle. However, this solution may be impractical (and is impossible for presenting screenshots of these views in a single document), and so the line discontinuities at the boundaries of the views may simply need to be tolerated, as they are in the present *Study*. In the views from N1285U, the slope of the horizon line is discontinuous at the boundary between the views, but there is no break in the horizon line itself. However, for EAGLE1, at certain times there is also a small break in the horizon line, in addition to a discontinuity in the slope. Based on experiments with *FSX*, this break appears to be dependent on the roll rate present at the time – the break appears at higher roll rates, but not at lower ones. This behavior is inherent to *FSX* and not completely understood, but does not materially affect the discussion of visibility in this *Study.*

As shown in Figure 20, N1285U appeared in EAGLE1's co-pilot's field of view between azimuth angles of +30° to +115°, and EAGLE1 appeared in the N1285U's pilot's field of view between azimuth angles of -115° and -50°. Consequently, for both airplanes two cameras are needed to depict both the approach of the target, and the view in the viewer's direction of travel. Based on these observations, the EAGLE1 cockpit view was recreated using two cameras pointed at -15° and +75°, respectively, and the N1285U cockpit view was recreated using two cameras pointed at -75° and +15°, respectively. The elevation angles for all cameras was 0°.

Screenshots of the EAGLE1 cockpit recreation are presented in Figures 25a-p, and screenshots of the N1285U cockpit recreation are presented in Figures 26a-p. The times of the screenshots correspond roughly to the events listed in Table 3, with some deletions and additions. For example, events corresponding to Cockpit Display of Traffic Information (CDTI) alerts issued to either airplane (had they been equipped with a CDTI) are added. Note that the locations of other aircraft are indicated by yellow N-number labels; the associated aircraft are located just beneath the middle of the labels, though they may be too small to be drawn in the image.

Images of what a CDTI could have displayed to the pilots are also included in Figures 25 and 26. These CDTI displays and alerts are described in more detail in Section D-V.

A measure of the size of the "target" airplane in the field of view of the "viewer" is the difference in azimuth and elevation angles between different points on the "target." For this *Study*, the azimuth and elevation angles of the nose, tail, center, and left and right wingtips of the targets were computed (the angles plotted in Figures 19-26 correspond to the center of the targets). The difference in azimuth and elevation angles between the nose and the tail of the targets are presented as a function of time in Figure 27 as the lines labeled "Δ azimuth, fuselage" and "Δ elevation, fuselage." The difference in angles between the left and right wingtips are presented as the lines labeled "Δ azimuth, wings" and "Δ elevation, wings." In these calculations, the nose, tail, and wingtips are assumed to lie in a plane, and so the airplanes in this representation have zero thickness. Hence, the information in Figure 27 does not represent the size of the *area* of the target presented to the viewer (which is what makes the target visible), but only the extent of a subset of

dimensions that contribute to the area. Nonetheless, Figure 27 does provide a measure of the target size, and of the very sudden increase in size (called the "blossom" effect) within a few seconds of the collision. Reference 8 indicates that on average, in ideal conditions people can see an object that spans at least 0.01° of the field of view, when looking directly at the object. However, the actual visual detection threshold depends on many factors, including viewer age, contrast, illumination, color, and the viewer's focus. Consequently, Figure 27 should not be used to determine a specific time at which the pilots "should" have been able to see the other airplane.

The dark gray shaded areas in Figure 27 indicate the times where the center of the target appears obscured by the viewer airplane's structure (with the viewer pilot's eyes at the nominal position), consistent with Figures 19-26. In these areas, the viewer pilot may not have been able to see the target airplane unless he moved his head from the nominal position (see Figures 23 and 24).

Figures 25 and 27 indicate that N1285U would have remained a relatively small object in EAGLE1's windows (spanning less than 0.5° of the field of view[28]) until about 7 seconds before the collision, and subsequently grown in size suddenly (the "blossom" effect). N1285U would have appeared slightly larger in the windows between about 11:01:40 and 11:02:00, when the airplanes approached within 0.5 nmi of each other on the downwind leg, before separating again prior to finally converging on EAGLE1's base leg (see Figures 5a, 15, and 27). It was during this period (at 11:01:49) that one of the crew members in the back of EAGLE1, recorded on CVR channel HOT3, asked "see him right there?" (see Table 3). It is not known to which aircraft HOT3 was referring. N6ZP was in front of EAGLE1 at the time and not likely visible to HOT3, but N1285U was only 0.5 nmi to the right of EAGLE1. More distant aircraft to the right of EAGLE 1 included N5058U, N8360R, and N5442P. Immediately following HOT3's question, the co-pilot stated "tally" (see Reference 6), though it is also not known to which aircraft the co-pilot was referring.

Figures 26 and 27 indicate that EAGLE1 would have been obscured from the N1285U pilot's view for most of N1285U's downwind leg, even during the period between 11:01:40 and 11:02:00 when the size of EAGLE1 in the field of view would have increased due to the proximity of the airplanes. The long period during which EAGLE1 was obscured from the N1285U pilot's "nominal" viewpoint underscores the importance of moving one's head (and occasionally lifting and dipping the wings) so as to see around structural obstacles when searching for traffic.

The circumstances of this accident also underscore the difficultly in seeing airborne traffic (the foundation of the "see and avoid" concept in visual meteorological conditions (VMC)), even when the cockpit visibility offers opportunities to do so, and the pilots are aware of and actively looking for traffic in the vicinity. On EAGLE1, there were at least 3 people searching for traffic (the pilot, co-pilot, and HOT3), and one of these may even have spotted and pointed out N1285U (if N1285U was in fact the object of HOT3's question at 11:01:49). Nonetheless, the airplanes still collided.

The CDTI images included in Figures 25 and 26 indicate that, had the airplanes been equipped with a CDTI, the system could have alerted the pilots to the presence of the other airplane, and presented precise bearing, range, and altitude information about each target, up to two minutes and 13 seconds prior to the collision. Such timely and information-rich traffic presentations would likely have helped the pilots to know where to look for the other airplane, and avoid a collision without the need for aggressive maneuvering (for example, EAGLE1 may have declined to turn base until the conflict with N1285U was resolved). The CDTI displays are discussed further below.

[28] 0.5° of the field of view is equivalent to the diameter of a penny viewed from about 7 ft. away.

V. Cockpit Display of Traffic Information (CDTI) Study

Introduction

According to a 2007 "Fact Sheet" published by the FAA,[29] the "Next Generation Air Transportation System" (NextGen) program "is a wide ranging transformation of the entire national air transportation system - not just certain pieces of it - to meet future demands and avoid gridlock in the sky and in the airports. It moves away from legacy ground based technologies [such as radar] to a new and more dynamic satellite based technology." A key component of NextGen is the surveillance of aircraft through the Global Positioning System (GPS) satellite constellation instead of by ground radar. This GPS-based surveillance is enabled through the "Automatic Dependent Surveillance – Broadcast" (ADS-B) system. As described in the FAA fact sheet,

> Automatic Dependent Surveillance Broadcast (ADS-B) is, quite simply, the future of air traffic control. As the backbone of the NextGen system, it uses GPS satellite signals to provide air traffic controllers and pilots with much more accurate information that will help keep aircraft safely separated in the sky and on runways. Aircraft transponders receive GPS signals and use them to determine the aircraft's precise position in the sky, which is combined with other data and broadcast out to other aircraft and air traffic control facilities. When properly equipped with ADS-B, both pilots and controllers will, for the first time, see the same real-time displays of air traffic, substantially improving safety.

After January 1, 2020, ADS-B Out equipment (that broadcasts the airplane's position to ATC and other aircraft) is required to be installed on all aircraft in the National Airspace System (NAS) operating above 10,000 ft. and within or above Class B and C airspace, with certain exceptions (see 14 CFR 91.225).

The ADS-B capabilities that enhance a pilot's awareness of airborne traffic in his vicinity are described in Advisory Circular (AC) 20-172B, "Airworthiness Approval for ADS-B In Systems and Applications." Per the AC,

> ADS-B In refers to an appropriately equipped aircraft's ability to receive and display other aircraft's ADS-B information and ground station broadcast information, such as TIS-B [Traffic Information Services – Broadcast] and ADS-R [Automatic Dependent Surveillance – Rebroadcast]. The information can be received by an appropriately equipped aircraft on either or both of two radio frequency (RF) links: 1090 ES [Extended Squitter] or 978 MHz UAT [Universal Access Transceiver]. The received information is processed by onboard avionics and presented to the flight crew on a display.

ADS-B In avionics enable a number of aircraft surveillance applications. The applications most relevant to this accident are the enhanced visual acquisition (EVAcq) and ADS-B Traffic Advisory System (ATAS) applications. AC 20-172B describes these applications as follows:

> The enhanced visual acquisition application (EVAcq) … displays ADS-B traffic on a plan view (bird's eye view) relative to own-ship. This application is designed to support only the display and alerting of ADS-B traffic, including ADS-R, TIS-B, and TCAS [Traffic Collision Avoidance System] derived traffic. … The traffic information assists the flight crew in visually acquiring traffic out the window while airborne. EVAcq does not relieve the pilot of see and avoid responsibilities under 14 CFR 91.113b. This application is expected to improve both safety and efficiency by providing the flight crew enhanced traffic awareness. …

[29] See: http://web.archive.org/web/20150403151639/http://www.faa.gov/news/fact_sheets/news_story.cfm?newsid=8145

> ADS-B Traffic Advisory System (ATAS) is an Automatic Dependent Surveillance-Broadcast (ADS-B) In application intended to reduce the number of mid-air collisions and near mid-air collisions involving general aviation aircraft. Previously known as Traffic Situation Awareness with Alerts (TSAA), the name ATAS has been used in this AC as well as TSO-C195b to be more consistent with existing traffic advisory systems. ATAS provides voice annunciations to flight crews to draw attention to alerted traffic and also adds visual cues to the underlying basic traffic situation awareness application (e.g., Enhanced Visual Acquisition [EVAcq] or Basic Airborne Situation Awareness [AIRB]) in installations where a Traffic Display is available. The ATAS application uses ADS-B information, and where available Automatic Dependent Surveillance-Rebroadcast (ADS-R) and Traffic Information Service-Broadcast (TIS-B) information to provide the flight crew with indications of nearby aircraft in support of their see-and-avoid responsibility. ATAS is the only ADS-B application with an aural-only implementation (via an annunciator panel). All other applications require a traffic display as defined by the CDTI [Cockpit Display of Traffic Information] requirements.

NTSB CDTI simulation description

The cockpit display that presents traffic information to the pilot in a plan or "birds eye" view as stated in the EVAcq and ATAS application descriptions is the Cockpit Display of Traffic Information, or CDTI. For this accident, simulated CDTI displays for both EAGLE1 and N1285U were created based on the TIS-B information[30] that would have been displayed to the pilots of each aircraft assuming that both aircraft were equipped with:

- ADS-B In capability
- Avionics capable of running the ATAS application
- A CDTI for displaying traffic information
- An audio system capable of annunciating the ATAS aural alerts

In addition, the simulation assumes that at least one ADS-B Out equipped aircraft was operating in the vicinity of the two accident aircraft, in order to trigger the broadcast of TIS-B information from a ground station (aircraft equipped only with ADS-B In cannot trigger the broadcast of this information; therefore, if no ADS-B Out equipped aircraft were in the vicinity,[31] the TIS-B information would not have been available for display on either airplane's CDTI).

AC 20-172B also describes the symbol requirements for the CDTI, which are more completely defined in RTCA document DO-317B, "Minimum Operational Performance Standards (MOPS) for Aircraft Surveillance Applications (ASA) System." These requirements specify that, among other things,

- The position of the ownship symbol should allow the display of traffic in all directions around the ownship, and indicate the direction of travel of the ownship (in the NTSB simulations, the ownship symbol is a white triangle with the direction of motion towards the top of the display (12 o'clock position)).

[30] This information was provided to the NTSB by the FAA, based on the FAA's recorded radar data for the event, and filtering algorithms that would have selected traffic targets for TIS-B uplinks within a moving 15 nmi radius and ±3500 ft "hockey puck" of the accident aircraft (the service volume associated with an ADS-B Out equipped aircraft co-located with the accident aircraft). Note that the TIS-B information is based on recorded radar data with an update rate of once every 4.5 seconds, and not on 1 sample-per-second, GPS-based, ADS-B Out data from the aircraft themselves. Further, no TIS-B data is available when these aircraft descend below radar coverage (i.e., below about 700 ft. MSL for aircraft in the KSDM traffic pattern). Consequently, the quality of TIS-B data is degraded compared to ADS-B or ADS-R data by the inherent position uncertainties, slower update rate, and reduced coverage area of the radar.

[31] Global Express N18WZ was in fact operating at KSDM at the time and was ADS-B Out equipped.

- Traffic symbols that are not proximate (i.e., not within 6 nmi and ±1200 ft. of the ownship) should be cyan-colored and open (not filled). In the NTSB simulations, these symbols are open cyan-colored arrowheads.
- Traffic symbols that are proximate should be cyan and filled. In the NTSB simulations, these symbols are filled cyan arrowheads.
- Traffic that generates an ATAS alert should be displayed with yellow symbols enclosed in a circle. In the NTSB simulation, these symbols are filled yellow arrowheads enclosed in a yellow circle.

DO-317B also specifies the aural annunciations that should accompany an ATAS traffic alert. The components of the annunciation include the alert "Traffic," followed by the relative traffic bearing expressed as a clock position (e.g., "two o'clock"), the relative altitude ("high," "low," or "same altitude"), the range to the target in nautical miles, and optionally, the vertical tendency[32] (e.g., "descending"). The example of a complete annunciation given in DO-317B is "Traffic, two o'clock, high, two miles, descending." The aural annunciation is provided both when a traffic target first generates an ATAS alert (by the algorithm predicting that the ownship will penetrate a "protected airspace zone" (PAZ) around the target), and again when the algorithm predicts that the ownship will penetrate a smaller, "collision airspace zone" (CAZ) around the target.[33] The NTSB simulations incorporate these elements of the aural annunciation of ATAS alerts.

It should be noted that while the simulation images presented in Figures 25-26 are representative of a CDTI that complies with the DO-317B MOPS, they do not duplicate the implementation or presentation of any particular operational display exactly. The actual images presented to a pilot depend on the range scale and background graphics selected by the pilot (which could reflect various implementations and combinations of moving maps, terrain elevation data, and weather information, rather than the simple black background presented in Figures 25-26). The two white lines in the NTSB CDTI simulations represent the KSDM runways. In addition, the aircraft N numbers shown in Figures 25-26 are included for clarity, but would not be presented in an actual display because none of the aircraft in the KSDM pattern (except for N18WZ) were ADS-B Out equipped (an actual display could include the N number for N18WZ).

NTSB CDTI simulation results: EAGLE1

The NTSB simulation of a CDTI display for EAGLE1 indicates that at 10:59:04, open cyan targets representing the local traffic at KSDM would have appeared at the 1 o'clock position, 8 nmi from EAGLE1, and traffic inbound for the San Diego area would have appeared at EAGLE1's 9 to 11 o'clock position, 8 nmi from EAGLE1 (see Figure 25a). N1285U would have been depicted 500 ft. below EAGLE1 east of the airport on a final approach leg. As EAGLE1 continued its east-bound track toward KSDM, N1285U would have disappeared from the display as it descended below radar coverage. At 10:59:48, as EAGLE1 approached within 7 nmi of the KSDM runway 26R threshold, Cessna N6ZP would have appeared over KSDM as an open arrowhead climbing from runway 26R. At 11:00:16, as N6ZP climbed to within 1200 ft. of EAGLE1's altitude, its CDTI symbol would have changed to a filled cyan-colored arrowhead. N6ZP would then have been depicted turning right and becoming established on the downwind leg for KSDM runway 26R at about 11:00:49. At 11:00:57, when EAGLE1 was about 3.5 nmi from the 26R threshold, N1285U

[32] The vertical tendency will only be annunciated when the computed rate of climb or descent is at least 500 ft./min.
[33] Per DO-317B, the size of the PAZ depends on the closure rate between the aircraft, increasing as the closure rate increases. The size of the CAZ is constant at a 500 ft. radius and a height of ±2000 ft.

would have reappeared on EAGLE1's CDTI display as a filled, cyan-colored arrowhead at EAGLE1's 1 o'clock position, about 2.5 nmi from and 1100 ft. below EAGLE1, climbing out from KSDM runway 26L. At 11:01:34, N6ZP would have been depicted turning left towards the northeast on a course that would eventually intercept EAGLE1's flight path (N6ZP crossed EAGLE1's extended flight path at about 11:01:45). At 11:01:38, N1285U's CDTI symbol would have changed to alert status (a filled, yellow-colored arrowhead, enclosed by a yellow circle), and EAGLE1 would have received an aural alert stating, "Traffic, 2 o'clock, low, less than 1 mile, climbing" (see Figure 25e). N1285U would have remained in this alert status (as a yellow, circled arrowhead) until 11:01:57, when it would have reverted to a filled cyan arrowhead.

When the EAGLE1 HOT3 CVR channel recorded someone asking "see him right there?" at 11:01:49, EAGLE1's CDTI display would have depicted N6ZP crossing EAGLE1's extended flight path, and N1285U at EAGLE1's 3 o'clock position, 0.7 nmi from and 300 ft. below EAGLE1 (see Figure 25g). When EAGLE1 reported "right downwind abeam traffic to the left and right in sight" at 11:02:14, both EAGLE1 and N1285U were approximately abeam the tower, and N1285U would have been depicted at EAGLE1's 4 o'clock position, 0.7 nmi from and 400 ft. below EAGLE1. N6ZP would have been depicted about 1.5 nmi in front of EAGLE1 at the 11 o'clock position, departing the KSDM area to the northeast (see Figure 25h).

At 11:02:32.4, just after EAGLE1 started rolling into the base turn, the pilot asked "you still got the guy on the right side?" Reference 6 indicates that the co-pilot responded, "yeah we good," and then the pilot stating "(good goin')."[34] It is not known which aircraft the pilot was referring to as "the guy on the right side," or which aircraft the co-pilot meant when he replied "we're good." Aircraft to the right of EAGLE1 at the time included Cessna N1285U, helicopter N8360R, and Piper N5442P. These aircraft would have been depicted on EAGLE1's CDTI display at the 4 o'clock, 3 o'clock, and 2 o'clock positions, respectively, with N8360R depicted as an open cyan arrowhead, and N1285U and N5442P depicted as filled cyan arrowheads (see Figure 25i).

At 11:02:59.3, during EAGLE1's base turn, the pilot stated "I see the shadow but I don't see him." The only aircraft close enough to EAGLE1 to cast a shadow visible by the pilot was N1285U, which at that time would have been depicted on EAGLE1's CDTI display at EAGLE1's 2 o'clock position, 1 nmi from and 500 ft. below EAGLE1 (see Figure 25l).

At 11:03:07, about 3 seconds before the collision, N1285U would have again changed to alert status (yellow, circled arrowhead), and EAGLE1 would have received a second aural alert stating, "Traffic, 1 o'clock, same altitude, zero miles" (see Figure 25n). This alert would likely have come too late for the pilots to avoid the accident.

NTSB CDTI simulation results: N1285U

The NTSB simulation of a CDTI display for N1285U indicates that at 11:01:01, as N1285U was climbing into radar coverage following its touch-and-go on runway 26L,[35] a filled cyan target corresponding to EAGLE1 would have appeared on N1285U's CDTI display at N1285U's 12 o'clock position, about 2 nmi from and 1000 ft. above N1285U. The display would also have depicted N6ZP on the downwind leg for runway 26R, at N1285U's 3 o'clock position, about 1 nmi from and 300 ft. above N1285U.

[34] Reference 6 notes that CVR transcript content in parentheses indicates a "questionable insertion."
[35] No CDTI images for N1285U are available prior to its climbing into radar coverage.

At 11:01:38, when EAGLE1 received an ATAS alert concerning N1285U, N1285U's CDTI would have depicted EAGLE1 at N1285U's 8 o'clock position, 0.6 nmi from and 400 ft. above N1285U (see Figure 26e). Interestingly, no parallel ATAS alert concerning EAGLE1 would have been issued to N1285U at this time. Hence, while at 11:01:38 the ATAS algorithms predicted that EAGLE1 would eventually penetrate N1285U's PAZ, they did not predict that N1285U would similarly penetrate EAGLE1's PAZ. This (counterintuitive) difference may be the result of variations in the EAGLE1 and N1285U predicted tracks stemming from the uncertainty in and relatively low sample rate of the radar data upon which the TIS-B information is based, and the effects of the smoothing and extrapolation functions used in the FAA tracker and DO-317B ATAS algorithms.

When the EAGLE1 CVR recorded HOT3 asking "see him right there?" at 11:01:49, N1285U's CDTI display would have depicted EAGLE1 at N1285U's 8 o'clock position, 0.5 nmi from and 400 ft. above[36] EAGLE1 (see Figure 26g). N6ZP would have been depicted at N1285U's 11 o'clock position, 1.5 nmi from and 200 ft. above N1285U, heading towards the northeast away from KSDM.

When EAGLE1 reported "right downwind abeam traffic to the left and right in sight" at 11:02:14, EAGLE1 would have been depicted on N1285U's CDTI display at N1285U's 9 o'clock position, 0.7 nmi from and 400 ft. above N1285U (see Figure 26h).

When the EAGLE1 pilot asked "you still got the guy on the right side?" at 11:02:32.4, EAGLE1 would have been depicted on N1285U's CDTI display at N1285U's 9 to 10 o'clock position, 0.8 nmi from and 600 ft. above N1285U (see Figure 26i).

At 11:02:48, N1285U would have received an ATAS alert associated with Piper N5442P, which was on a left base for landing on runway 26L. The depiction of N5442P on N1285U's CDTI display would have changed from a filled cyan arrowhead to filled yellow arrowhead enclosed by a yellow circle, accompanied by an aural alert stating "Traffic, 2 o'clock, low, less than one mile." At this time, EAGLE1 would have been depicted on N1285U's CDTI display at N1285U's 9 to 10 o'clock position, 0.8 nmi from and 500 ft. above N1285U (see Figure 26k). N5442P remained in alert status until 11:03:01.

At 11:02:59.3, when the EAGLE1 pilot stated "I see the shadow but I don't see him," EAGLE1 would have been depicted on N1285U's CDTI display at N1285U's 10 o'clock position, 0.7 nmi from and 500 ft. above N1285U, and turning from the downwind onto the base leg (see Figure 26l).

At 11:03:07, about 3 seconds before the collision, EAGLE1 would have changed to alert status (yellow, circled arrowhead), and N1285U would have received a second aural alert stating, "Traffic, 11 o'clock, same altitude, zero miles, descending" (see Figure 26n). This alert would likely have come too late for the pilots to avoid the accident.

[36] At 11:01:49, EAGLE1's CDTI would have shown N1285U 300 ft. (vs. 400 ft.) below EAGLE1. The difference in relative altitude between the EAGLE1 and N1285U CDTI displays is likely the result of the radar Mode C uncertainty and the effects of the smoothing and extrapolation functions used in the FAA tracker and DO-317B ATAS algorithms.

E. CONCLUSIONS

This *Aircraft Performance Radar & Cockpit Visibility Study* presents the results of using the NZY, NKX, OpsVue, and simulation data to calculate the position and orientation of each airplane in the minutes preceding the collision. This information is then used to estimate the approximate location of each airplane in the other airplane's windows during the same period, and to simulate the traffic information that could have been presented to the pilots, had the airplanes been equipped with CDTI displays.

The position, speed, track angle, separation distance, and closure rate of both airplanes are presented in Figures 5-7 and 12-15. These values of these quantities at significant times are also shown in Table 3. The azimuth and elevation angles of each airplane in the fields of view of the pilots are presented in Figures 19-24, and recreations of the out-the-window views from each airplane at significant times are presented in Figures 25 and 26. Figures 25 and 26 also present the traffic information that could have been presented on CDTI displays (had the airplanes been so equipped).

The information cited above, the ATC communications transcript (Reference 1), and the EAGLE1 CVR transcript (Reference 6) are consistent with the series of events leading up to the collision described below. As noted above, the visibility of one airplane from another is sensitive to the position of the pilot's eyes relative to the cockpit windows. This sensitivity is illustrated in Figures 23 and 24, which underscore the fact that looking for traffic can be more effective if pilots move their heads as well as redirect their eyes, since head movements may bring otherwise obscured aircraft into view. The descriptions of visibility that follow correspond to the pilots' eyes in their nominal positions, with the understanding that the views out the windows change if the pilots move their heads.

EAGLE1 contacted KSDM tower at 10:59:04 (4 minutes and 6 seconds before the collision, or 04:06), stating "brown tower eagle one nine west inbound bravo full stop." KSDM tower instructed EAGLE1 to "maintain at or above two thousand feet enter right traffic for runway two six right." At this time, N1285U was descending through 1000 ft. on a half-mile final for a touch-and-go on runway 26L.

At 11:00:06 (03:04), N1285U was climbing through 540 ft. over runway 26L after completing a touch-and-go. EAGLE1 was 6 nmi west and 1 nmi north of the KSDM runway 26R threshold, descending through 2380 ft.

At 11:00:29 (02:41), the CVR on EAGLE1 recorded the co-pilot commenting about an aircraft on short final, which must have been Global Express N18WZ. At this time, EAGLE1 was descending through 2260 ft., 1 nmi north and 4.9 nmi west of the runway 26R threshold. N1285U was climbing through 780 ft., along the extended centerline of runway 26L, and about 800 ft. past the departure end of that runway. N1285U would have been located in EAGLE1's R1 window at azimuth and elevation angles of about 13° and 6°, respectively, denoted here as viewing angles of (13°, 6°).[37] The other aircraft in the pattern would have been located in roughly the same area, except for Cessna N6ZP, which was north of the other aircraft and hence further to the left in the R1 window (see Figure 25b). At 11:00:29, EAGLE1 would have appeared in N1285U's windshield at (10°, 4°) (see Figure 26b). The aircraft were 4.1 nmi apart.

[37] For brevity, subsequent viewing angles will be referenced by the following notation: (azimuth, elevation).

At 11:00:55 (02:15), N1285U was climbing through 1150 ft. about 1200 ft. west of the departure end of runway 26R, and began a right turn to cross over the extended centerline of 26R so as to enter the right-hand traffic pattern for that runway. At this time, EAGLE1 was at 2190 ft., about 1 nmi north and 3.6 nmi west of the runway 26R threshold, about 2.4 nmi from N1285U, and would have been located in N1285U's windshield at about (14°, 6°), about in line with the top of the instrument panel. N1285U would have been located in EAGLE1's R1 window at (23°, -8°).

At 11:01:15.5 (01:54.7), the CVR on EAGLE1 recorded the co-pilot commenting about an aircraft on the runway, which again must have been N18WZ. Figure 25c indicates that at this time, N18WZ may have been obscured behind the post separating EAGLE1's R1 and R2 windows, if the co-pilot's eyes had been in the "nominal" position. Since the co-pilot saw and commented on N18WZ, however, this suggests that he may have been leaning closer to the window to scan for traffic, bringing N18WZ into view.

At 11:01:15.5, N1285U would have appeared in EAGLE1's R2 window at (36°, -12°), 1.2 nmi away. EAGLE1 would have appeared in the N1285U pilot's field of view near the forward edge of the post separating the left window from the windshield, at (-44°, -14°) (see Figure 26c).

At 11:01:24.6 (01:45.6), EAGLE1 was level at 2100 ft., about 1 nmi north and 2.4 nmi west of the runway 26R threshold, when the pilot commented about an airplane at 12 o'clock on climb-out. At this time, N6ZP was directly in front of EAGLE1, and Stationair N5058U had recently departed from runway 26L. At 11:01:24.6, N1285U was 0.8 nmi from EAGLE1, climbing through 1600 ft. and turning from crosswind to right downwind for runway 26R, 0.5 nmi north and 1.7 nmi west of the runway 26R threshold. N1285U would have appeared in EAGLE1's R2 window at (45°, -11°); N5058U would have appeared slightly below and to the left of N1285U (see Figure 25d). EAGLE1 would have been hidden from the N1285U pilot's view behind the window post between the left window and windshield (see Figure 26d).

When the EAGLE1 co-pilot commented "must be the jump plane" at 11:01:43.1, N6ZP would still have been located straight ahead, N1285U would have been located just to the left of the window post separating the EAGLE1 R2 and R3 windows, and Stationair N5058U would have been just to the right of this post (see Figure 25f). At this time, EAGLE1 would have appeared in the left window of N1285U, just below the wingtip (see Figure 26f). EAGLE 1 and N1285U were both on right downwind for runway 26R, with EAGLE1 about 0.5 nmi north of N1285U.

At 11:01:49.0 (01:21.2), the CVR on EAGLE1 recorded one of the crewmembers seated outside of the cockpit asking, "see him right there?" It is not known which airplane the crew member was referring to, though the proximity of N1285U to EAGLE1 at the time makes it a likely candidate. At this time, EAGLE1 was at about 2040 ft., 1.1 nmi north and 1.4 nmi west of the runway 26R threshold. N1285U was level at 1700 ft., 0.7 nmi north and 1.3 nmi west of the threshold. The airplanes were about 0.5 nmi apart, and N1285U would have appeared in EAGLE1's R3 window near the right edge of the post separating the R2 and R3 windows (see Figure 25g). EAGLE1 would have been obscured from the N1285U pilot's view by the left wing (see Figure 26g).

At 11:02:14.0 (00:56.2), EAGLE1 was at about 2110 ft., 1.3 nmi north and 0.4 nmi west of the runway 26R threshold, and reported "eagle one is right downwind abeam traffic to the left and right in sight." At this time, Cessna N6ZP would have appeared in EAGLE1's L1 window at (-34°, -6°),

and was the only aircraft to EAGLE1's left. Cessna N1285U would have appeared in EAGLE1's R3 window at (106°, 3°) (see Figure 25h). At 11:02:14.0, N1285U was descending through 1650 ft., about 0.7 nmi north and 0.5 nmi west of the runway 26R threshold. EAGLE1 would have remained obscured from the pilot's view by the left wing (see Figure 26h). Other airborne traffic to the right of EAGLE1 at this time included Piper N5442P, helicopter N8360R, and Stationair N5058U.

At 11:02:32.0 (00:38.2), KSDM ATCT mistakenly instructed Cessna 6ZP to make a right 360° turn, intending the instruction for Cessna N1285U. At about the same time, EAGLE1 started banking to the right, turning towards right base, and the EAGLE1 CVR recorded the pilot asking the co-pilot "you still got the guy on the right side?" N1285U was 0.8 nmi away, and would have appeared in EAGLE1's R3 window at (112°, -1°) (see Figure 25i). Also to EAGLE1s' right were helicopter N8360R, on short final for runway 26L, Piper N5442P, on a left base for runway 26L, and Stationair N5058U, which was climbing through 1500 ft. about 2.6 nmi to the west of the runway 26R threshold. EAGLE1 would have been obscured from the N1285U pilot's field of view by the left wing and strut (see Figure 26i).

At 11:02:42.0 (00:28.2), KSDM ATCT instructed EAGLE1 to "turn base 26 right clear to land." EAGLE1 was descending through 1960 ft. in a right bank, about 1.3 nmi north and 0.7 nmi east of the runway 26R threshold. N1285U was descending through 1460 ft., about 0.6 nmi north and 0.3 nmi east of the threshold, and would have appeared in EAGLE1's R3 window at (103°, 12°) (see Figure 25j). EAGLE1 would have appeared in the N1285U pilot's field of view near the edge or slightly behind the window post separating the left window from the windshield (see Figure 26j). The airplanes were still about 0.8 nmi away from each other.

At 11:02:59.3 (00:10.9), the EAGLE1 CVR recorded the pilot stating, "I see the shadow but I don't see him." The only aircraft that was close enough to EAGLE1 to cast a shadow visible to EAGLE1's pilot was N1285U, which was 0.5 nmi away, and would have appeared in the upper part of EAGLE1s' R2 window at (53°, 17°) (see Figure 25l, which also highlights the area where N1285U's shadow would have appeared). At this time, EAGLE1 may again have become obscured from the Cessna pilot's view by the post between the right window and the windshield (see Figure 26l).

At 11:03:04.0 (00:06.2), the KSDM ATCT controller called N1285U, apparently realizing that he may have instructed the wrong airplane to make the right 360° turn. At this time, EAGLE1 and N1285U were 0.3 nmi apart, with EAGLE1 descending through 1490 ft. and N1285U descending through 1370 ft. N1285U would have appeared near the top-left corner of EAGLE1's R2 window (see Figure 25m), and EAGLE1 may have remained obscured behind N1285U's left window post (see Figure 26m).

At 11:03:08.0 (00:02.2), with EAGLE1 and N1285U about 0.1 nmi apart, the controller asked N1285U, "are you still on downwind sir? Right downwind?" The collision occurred about two seconds later, likely as the controller finished speaking. At 11:03:08, the N1285U may have been obscured by the post between EAGLE1's R1 and R2 windows, and EAGLE1 may have been obscured by N1285U's left window post (see Figures 25o and 26o).

The appearance of the airplanes in the others' field of view at 11:03:09, 1.2 seconds before the collision, may have been as depicted in Figures 25p and 26p. The airplanes collided at 11:03:10.2,

at an altitude of about 1350 ft., and with a closure rate of about 170 kt., at a collision angle of about 86°.

Figures 26 and 27 indicate that EAGLE1 would have been obscured from the N1285U pilot's view for most of N1285U's downwind leg, even during the period between 11:01:40 and 11:02:00 when the size of EAGLE1 in the field of view would have increased due to the proximity of the airplanes. The long period during which EAGLE1 was obscured from the N1285U's "nominal" viewpoint underscores the importance of moving one's head (and occasionally lifting and dipping the wings) so as to see around structural obstacles when searching for traffic.

The circumstances of this accident also underscore the difficultly in seeing airborne traffic (the foundation of the "see and avoid" concept for aircraft self-separation in VMC), even when the cockpit visibility offers opportunities to do so, and the pilots are aware of and actively looking for traffic in the vicinity. On EAGLE1, there were at least 3 people searching for traffic (the pilot, co-pilot, and the speaker recorded on CVR channel HOT3), and HOT3 may even have spotted and pointed out N1285U (if N1285U was the object of HOT3's "see him right there?" question at 11:01:49). If in fact HOT3 pointed out N1285U to the pilots, then the EAGLE1 pilot may have been referring to N1285U when he asked the co-pilot, "you still got the guy on the right side?", just as EAGLE1 was rolling into the base turn. Though the co-pilot responded "yeah we good" (likely because he had *some* aircraft on his right in sight), the aircraft he was looking at may not have been N1285U, but possibly N5442P or N8360R. In any case, in spite of the EAGLE1 pilots' awareness of traffic in the vicinity and attempts to find all of the relevant traffic around them, the airplanes still collided.

The CDTI simulations discussed in detail in Section D-V indicate that, had the airplanes been equipped with a CDTI, the system could have alerted the pilots to the presence of the other airplane, and presented precise bearing, range, and altitude information about each target, up to two minutes and 13 seconds prior to the collision. While the solo N1285U pilot may have had limited opportunities to monitor a CDTI while flying in the pattern, one of the two pilots on EAGLE1 may have been able to use a CDTI to help search for traffic while the other pilot flew the airplane. Even though certain situations (like flying solo in a busy traffic pattern) may limit the time available to monitor a CDTI, in general, the timely and information-rich traffic picture offered by a CDTI can greatly improve a pilot's ability to detect traffic threats, and avoid a collision without the need for aggressive maneuvering.

_____

John O'Callaghan
National Resource Specialist - Aircraft Performance
Office of Research and Engineering

F. REFERENCES

1. Serco Inc., *Memo from San Diego Brown Federal Contract Tower to Aircraft Accident File SDM-FCT-0030, Subject: INFORMATION: Full Transcript, Aircraft Accident, N12285U / EAGLE 1, San Diego, CA, August 16, 2015,* dated March 8, 2016.

2. National Transportation Safety Board, *Factual Report: North American Rockwell NA265-60SC Sabreliner, N442RM, and Cessna 172M, N1285U, San Diego, California, August 16, 2015, NTSB Accident # WPR15MA243AB*. (Contact NTSB at pubinq@ntsb.gov).

3. Sabreliner Corporation, *Sabreliner Model NA 265-60SC Supplemental Maintenance Manual, document # SR-81-015*, dated July 24, 1987. Copyright © 1987 by Sabreliner Corporation.

4. Textron Aviation, *1976 Cessna Model 172M Skyhawk Pilot's Operating Handbook*, document D1057-13.

5. Textron Aviation, *Cessna Model 172M Basic Data*, report no. S-172M-0(73), dated April 3, 1972 (Textron proprietary document).

6. National Transportation Safety Board, Office of Research and Engineering, Vehicle Recorder Division, *Cockpit Voice Recorder Specialist's Factual Report, North American Sabreliner, Registration N442RM, San Diego, California, August 16, 2015, NTSB # WPR15MA243AB* (Washington, D.C., March 24, 2016). Available at http://dms.ntsb.gov/pubdms/search/document.cfm?docID=444246&docketID=59067&mkey=91793

7. Textron Aviation, *Air Safety Investigations Field Notes: 1976 Cessna Model 172M, Serial # 17266979, registration N1285U, San Diego, CA, 08-16-15, NTSB report # WPR15FA243, Textron Report # ASI-15-CA*, dated August 24, 2015.

8. Velasco e Cruz, A. *Historical Roots of 20/20 as a (Wrong) Standard Value of Normal Visual Acuity*, Optometry and Vision Science Journal, Vol. 67, No.8, p. 661, March 30, 1990. Copyright © American Academy of Optometry.

G. GLOSSARY

Acronyms

AC	Advisory Circular
ACP	Azimuth Change Pulses
ADS-B	Automatic Dependent Surveillance – Broadcast
ADS-R	Automatic Dependent Surveillance – Rebroadcast
ARSR	Air Route Surveillance Radar
ASA	Aircraft Surveillance Applications
ASR	Airport Surveillance Radar
ATAS	ADS-B Traffic Advisory System
ATC	Air Traffic Control
ATCT	Air Traffic Control Tower
BAE	BAE Systems Technology Solutions & Services, Inc.
CAZ	Collision Airspace Zone
CDTI	Cockpit Display of Traffic Information
CFR	Code of Federal Regulations
CVR	Cockpit Voice Recorder
CG	Center of Gravity
EAGLE1	Accident Sabreliner (N442RM) call sign
EVAcq	Enhanced visual acquisition
FAA	Federal Aviation Administration
FSX	Microsoft Flight Simulator X computer program
GPS	Global Positioning System
IFR	Instrument Flight Rules
IIC	Investigator In Charge
KMYF	Montgomery-Gibbs Executive Airport, San Diego, California
KSDM	Brown Field Municipal Airport, San Diego, California
LC	Local Controller
MAC	Mean Aerodynamic Chord
METAR	Meteorological Terminal Air Report
MOPS	Minimum Operational Performance Standards
MSL	Mean Sea Level
NAM	North American Mesoscale weather model sounding
NAS	National Airspace System
NextGen	Next Generation Air Transportation System
NKX	San Diego Miramar Airport Surveillance Radar
NTSB	National Transportation Safety Board
NZY	North Island Naval Air Station Airport Surveillance Radar
OpsVue	Symphony® OpsVue™ system operated by Harris Corporation
PAZ	Protected Airspace Zone
PDT	Pacific Daylight Time
RPM	Revolutions Per Minute
TC	Type Certificate
TIS-B	Traffic Information Services – Broadcast
TSAA	Traffic Situation Awareness with Alerts
UTC	Universal Coordinated Time
VMC	Visual Meteorological Conditions
VFR	Visual Flight Rules

English symbols

C_D	Drag coefficient
C_L	Lift coefficient
C_x	x-body axis force coefficient
C_Y	Side force coefficient
C_y	y-body axis force coefficient
C_z	z-body axis force coefficient
F_i	Force along i-body axis (i = x, y, or z)
h	Altitude
$\dot{h}$	Rate of climb
n_i	Load factor along i-body axis (i = x, y, or z)
q	Dynamic pressure
S	Wing area
$\vec{V}$	Airspeed vector
V_G	Groundspeed
$\vec{V}_G$	Groundspeed vector
V_T	True airspeed
$\vec{V}_T$	True airspeed vector
$\vec{V}_W$	Wind speed vector
W	Gross weight
x_b	Component along airplane x-body axis
y_b	Component along airplane y-body axis
z_b	Component along airplane z-body axis

Greek symbols

α	Angle of attack
β	Sideslip angle
γ	Flight path angle
Δ	Change in quantity following Δ
ρ	Air density
θ	Pitch angle
ϕ	Roll angle
ψ	Heading angle (true)
ψ_G	Ground track angle (true)

FIGURES

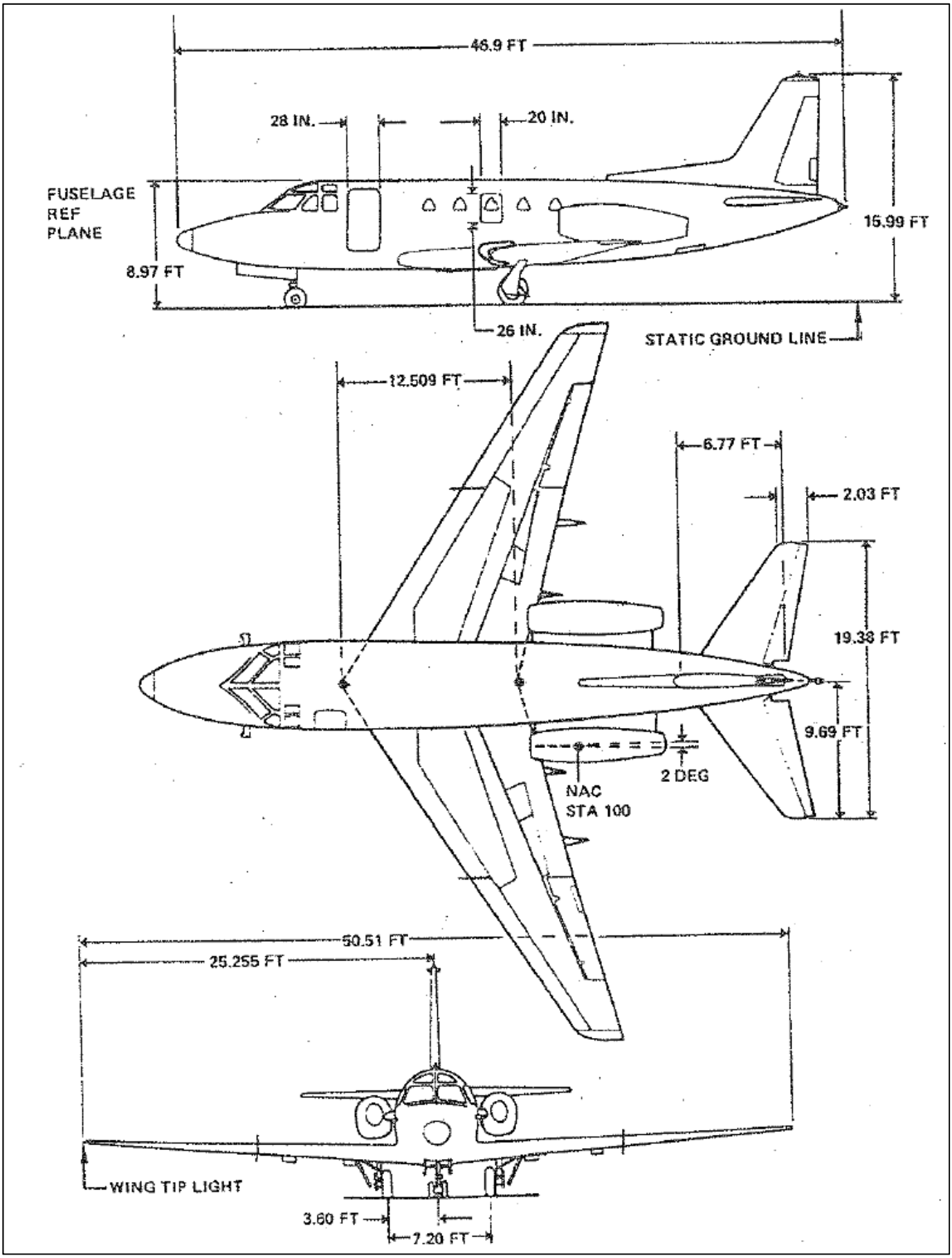

Figure 1. NA265-60SC diagrams, from Reference 3.

Figure 2. Pre-accident photo of Sabreliner N442RM (EAGLE1). Copyright © Gerhard Plomitzer; used with permission.

Figure 3. Pre-accident photograph of N1285U. Copyright © Terry Fletcher; used with permission.

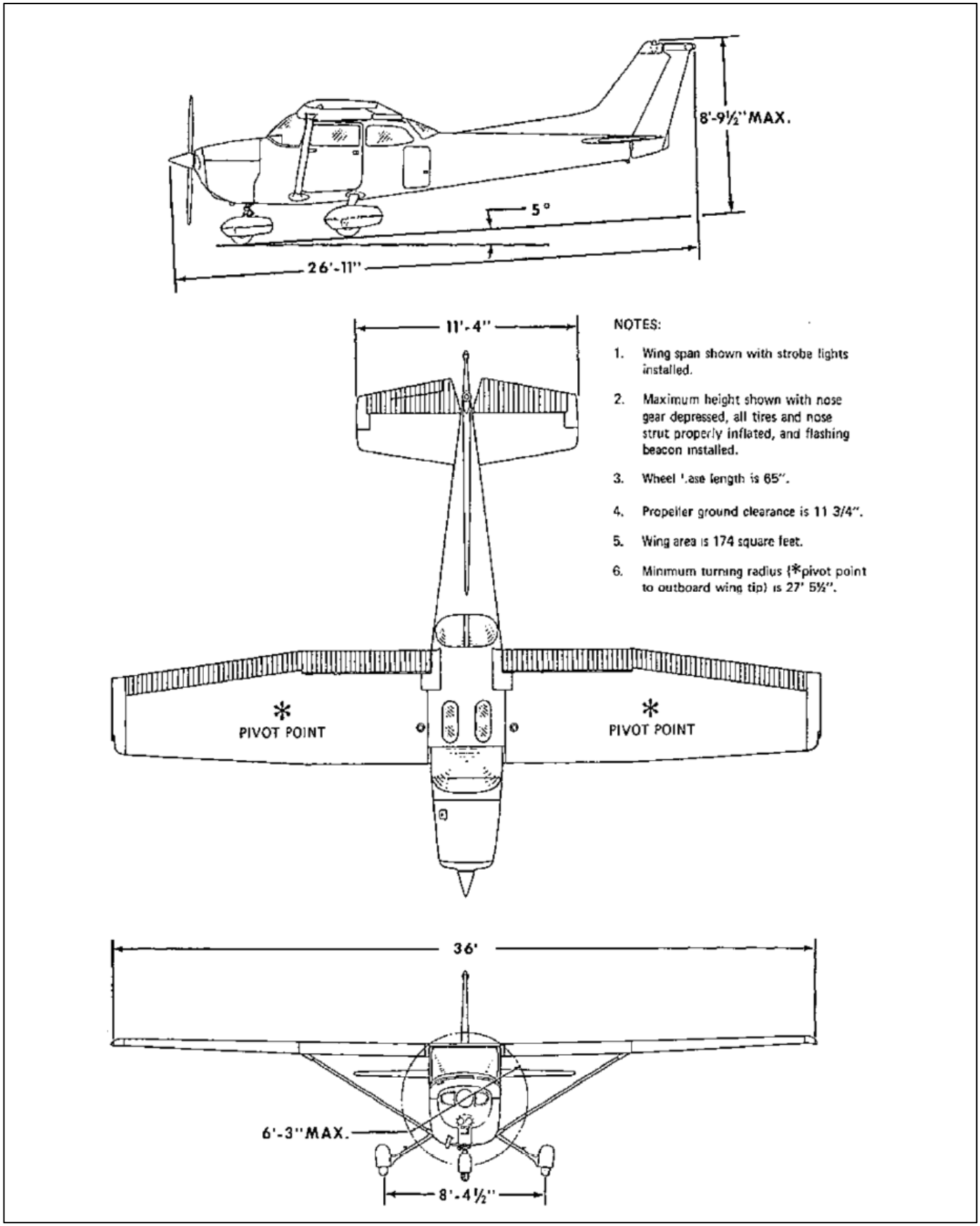

Figure 4. 3-view of Cessna 172M, from Reference 4.

WPR15FA243AB: Midair collision, Sabreliner EAGLE1 / C172 N1285U, San Diego, CA, 8/16/2015

Plan view of EAGLE1 and N1285U trajectories

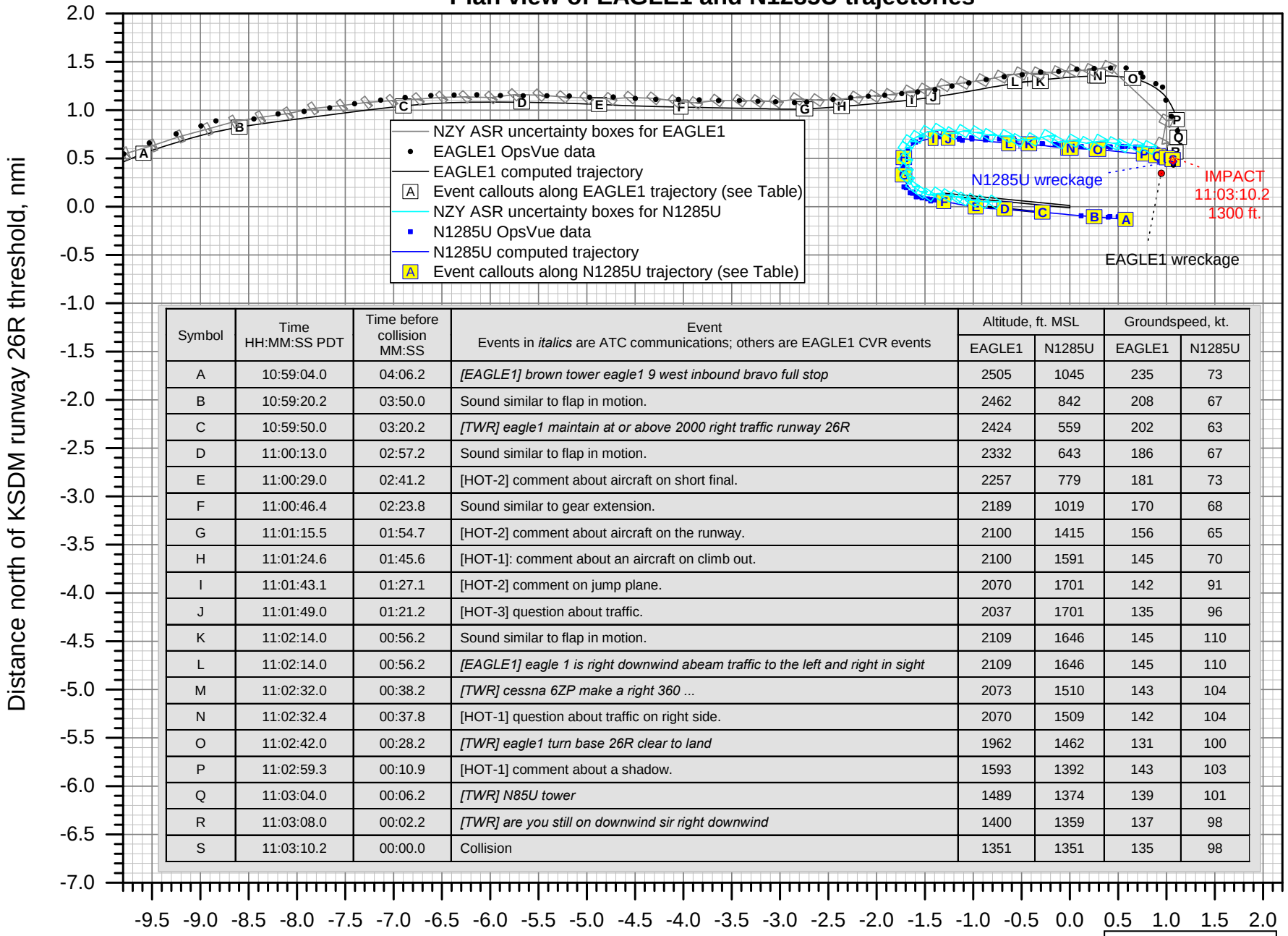

Symbol	Time HH:MM:SS PDT	Time before collision MM:SS	Event Events in *italics* are ATC communications; others are EAGLE1 CVR events	Altitude, ft. MSL		Groundspeed, kt.	
				EAGLE1	N1285U	EAGLE1	N1285U
A	10:59:04.0	04:06.2	*[EAGLE1] brown tower eagle1 9 west inbound bravo full stop*	2505	1045	235	73
B	10:59:20.2	03:50.0	Sound similar to flap in motion.	2462	842	208	67
C	10:59:50.0	03:20.2	*[TWR] eagle1 maintain at or above 2000 right traffic runway 26R*	2424	559	202	63
D	11:00:13.0	02:57.2	Sound similar to flap in motion.	2332	643	186	67
E	11:00:29.0	02:41.2	[HOT-2] comment about aircraft on short final.	2257	779	181	73
F	11:00:46.4	02:23.8	Sound similar to gear extension.	2189	1019	170	68
G	11:01:15.5	01:54.7	[HOT-2] comment about aircraft on the runway.	2100	1415	156	65
H	11:01:24.6	01:45.6	[HOT-1]: comment about an aircraft on climb out.	2100	1591	145	70
I	11:01:43.1	01:27.1	[HOT-2] comment on jump plane.	2070	1701	142	91
J	11:01:49.0	01:21.2	[HOT-3] question about traffic.	2037	1701	135	96
K	11:02:14.0	00:56.2	Sound similar to flap in motion.	2109	1646	145	110
L	11:02:14.0	00:56.2	*[EAGLE1] eagle 1 is right downwind abeam traffic to the left and right in sight*	2109	1646	145	110
M	11:02:32.0	00:38.2	*[TWR] cessna 6ZP make a right 360 ...*	2073	1510	143	104
N	11:02:32.4	00:37.8	[HOT-1] question about traffic on right side.	2070	1509	142	104
O	11:02:42.0	00:28.2	*[TWR] eagle1 turn base 26R clear to land*	1962	1462	131	100
P	11:02:59.3	00:10.9	[HOT-1] comment about a shadow.	1593	1392	143	103
Q	11:03:04.0	00:06.2	*[TWR] N85U tower*	1489	1374	139	101
R	11:03:08.0	00:02.2	*[TWR] are you still on downwind sir right downwind*	1400	1359	137	98
S	11:03:10.2	00:00.0	Collision	1351	1351	135	98

Figure 5a.

WPR15FA243AB: Midair collision, Sabreliner EAGLE1 / C172 N1285U, San Diego, CA, 8/16/2015

Plan view of EAGLE1 and N1285U trajectories (detail)

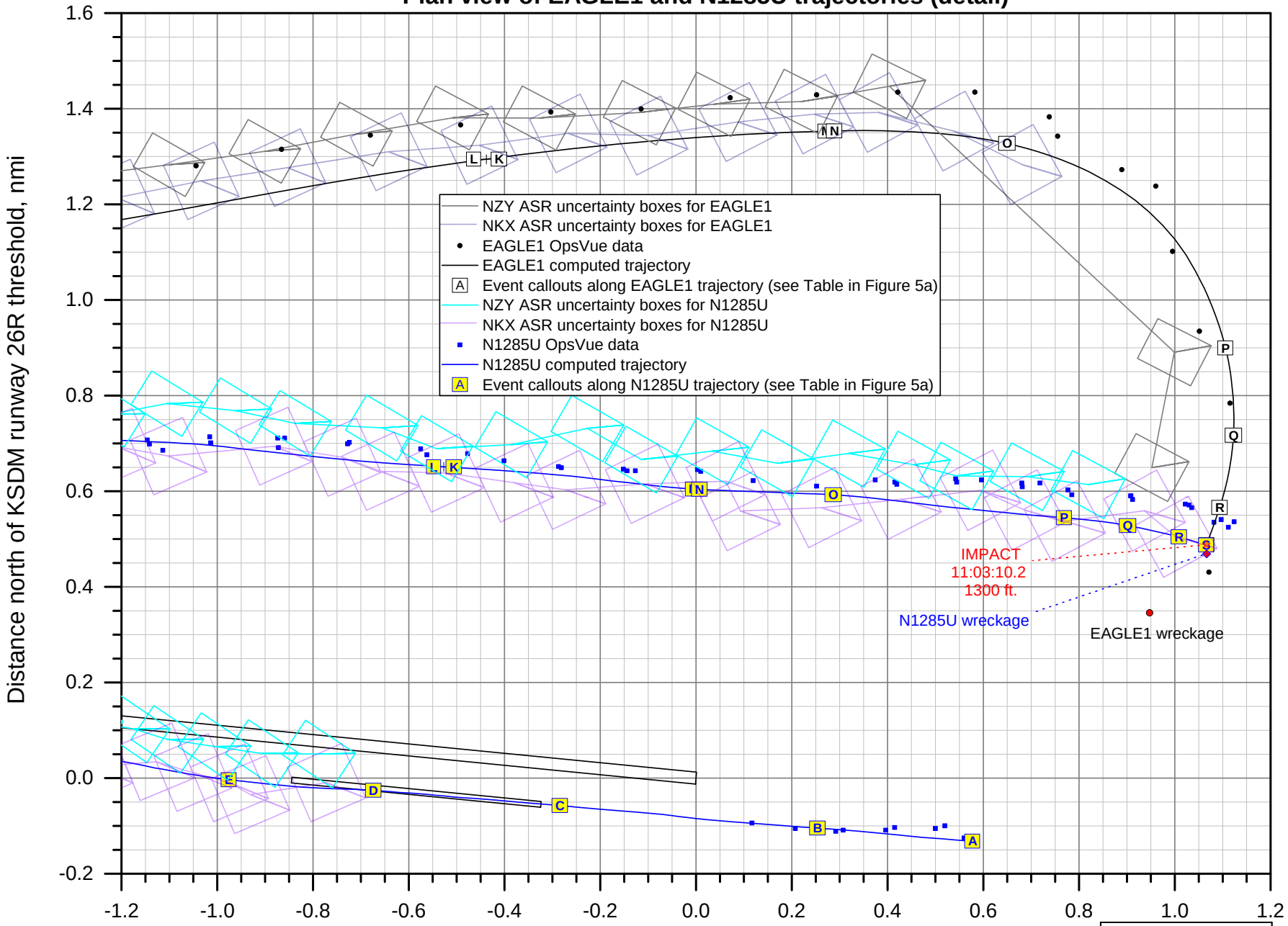

Figure 5b.

WPR15FA243AB: Midair collision, Sabreliner EAGLE1 / C172 N1285U, San Diego, CA, 8/16/2015

Plan view of EAGLE1 and N1285U trajectories

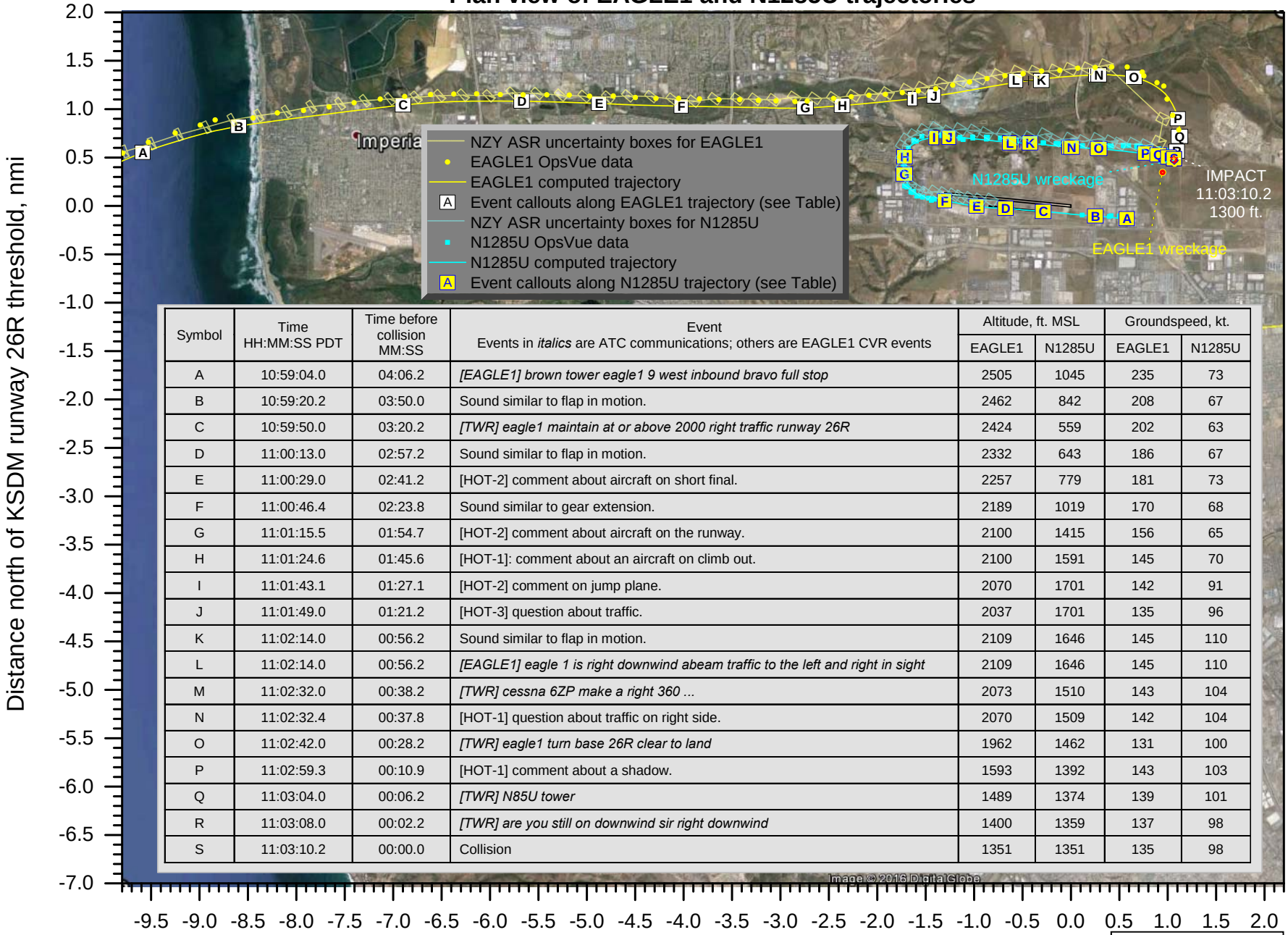

Symbol	Time HH:MM:SS PDT	Time before collision MM:SS	Event Events in *italics* are ATC communications; others are EAGLE1 CVR events	Altitude, ft. MSL		Groundspeed, kt.	
				EAGLE1	N1285U	EAGLE1	N1285U
A	10:59:04.0	04:06.2	*[EAGLE1] brown tower eagle1 9 west inbound bravo full stop*	2505	1045	235	73
B	10:59:20.2	03:50.0	Sound similar to flap in motion.	2462	842	208	67
C	10:59:50.0	03:20.2	*[TWR] eagle1 maintain at or above 2000 right traffic runway 26R*	2424	559	202	63
D	11:00:13.0	02:57.2	Sound similar to flap in motion.	2332	643	186	67
E	11:00:29.0	02:41.2	[HOT-2] comment about aircraft on short final.	2257	779	181	73
F	11:00:46.4	02:23.8	Sound similar to gear extension.	2189	1019	170	68
G	11:01:15.5	01:54.7	[HOT-2] comment about aircraft on the runway.	2100	1415	156	65
H	11:01:24.6	01:45.6	[HOT-1]: comment about an aircraft on climb out.	2100	1591	145	70
I	11:01:43.1	01:27.1	[HOT-2] comment on jump plane.	2070	1701	142	91
J	11:01:49.0	01:21.2	[HOT-3] question about traffic.	2037	1701	135	96
K	11:02:14.0	00:56.2	Sound similar to flap in motion.	2109	1646	145	110
L	11:02:14.0	00:56.2	*[EAGLE1] eagle 1 is right downwind abeam traffic to the left and right in sight*	2109	1646	145	110
M	11:02:32.0	00:38.2	*[TWR] cessna 6ZP make a right 360 ...*	2073	1510	143	104
N	11:02:32.4	00:37.8	[HOT-1] question about traffic on right side.	2070	1509	142	104
O	11:02:42.0	00:28.2	*[TWR] eagle1 turn base 26R clear to land*	1962	1462	131	100
P	11:02:59.3	00:10.9	[HOT-1] comment about a shadow.	1593	1392	143	103
Q	11:03:04.0	00:06.2	*[TWR] N85U tower*	1489	1374	139	101
R	11:03:08.0	00:02.2	*[TWR] are you still on downwind sir right downwind*	1400	1359	137	98
S	11:03:10.2	00:00.0	Collision	1351	1351	135	98

Figure 6a.

WPR15FA243AB: Midair collision, Sabreliner EAGLE1 / C172 N1285U, San Diego, CA, 8/16/2015

Plan view of EAGLE1 and N1285U trajectories (detail)

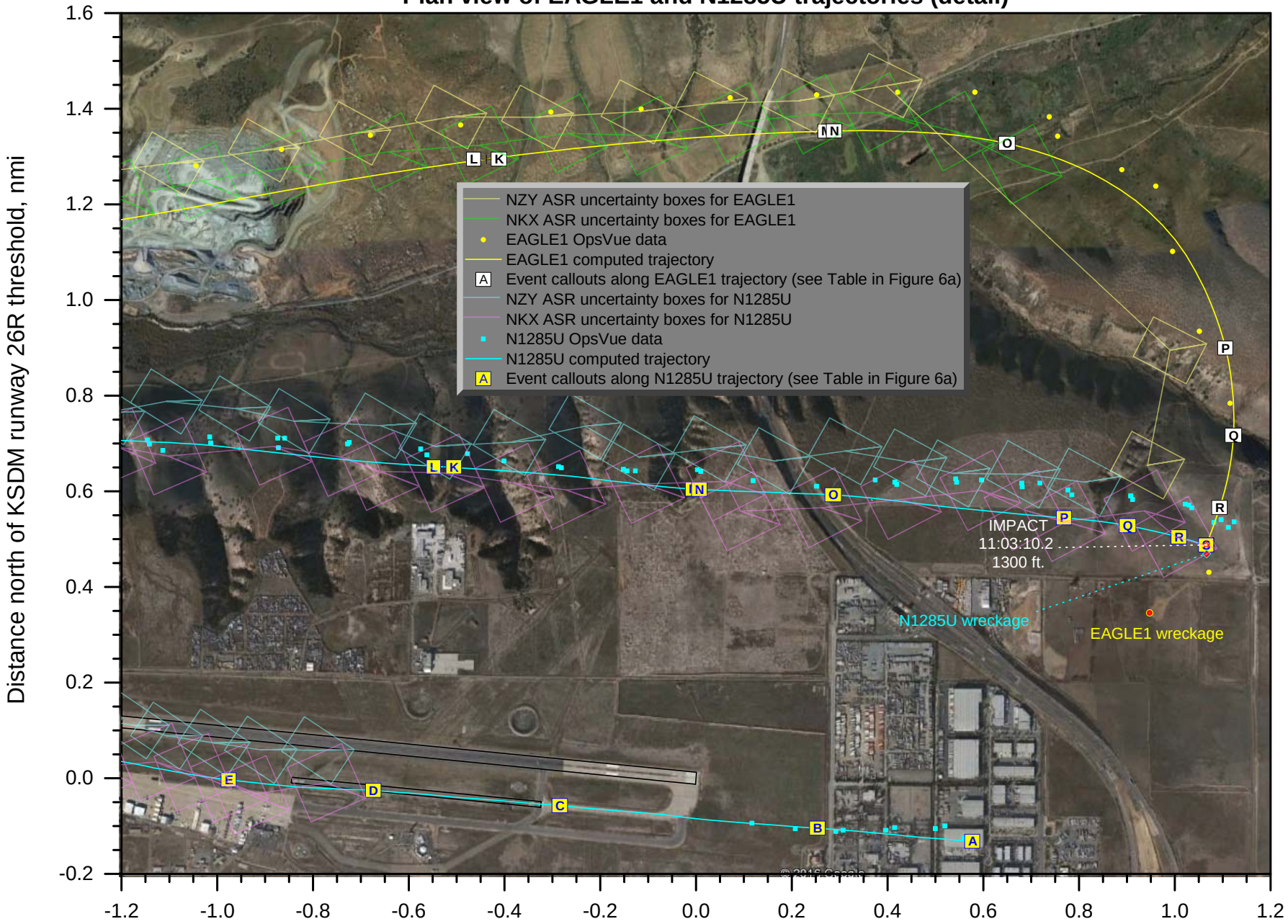

Figure 6b.

WPR15FA243AB: Midair collision, Sabreliner EAGLE1 / C172 N1285U, San Diego, CA, 8/16/2015

Aircraft in KSDM traffic pattern, 10:59:04 - 11:01:30 PDT

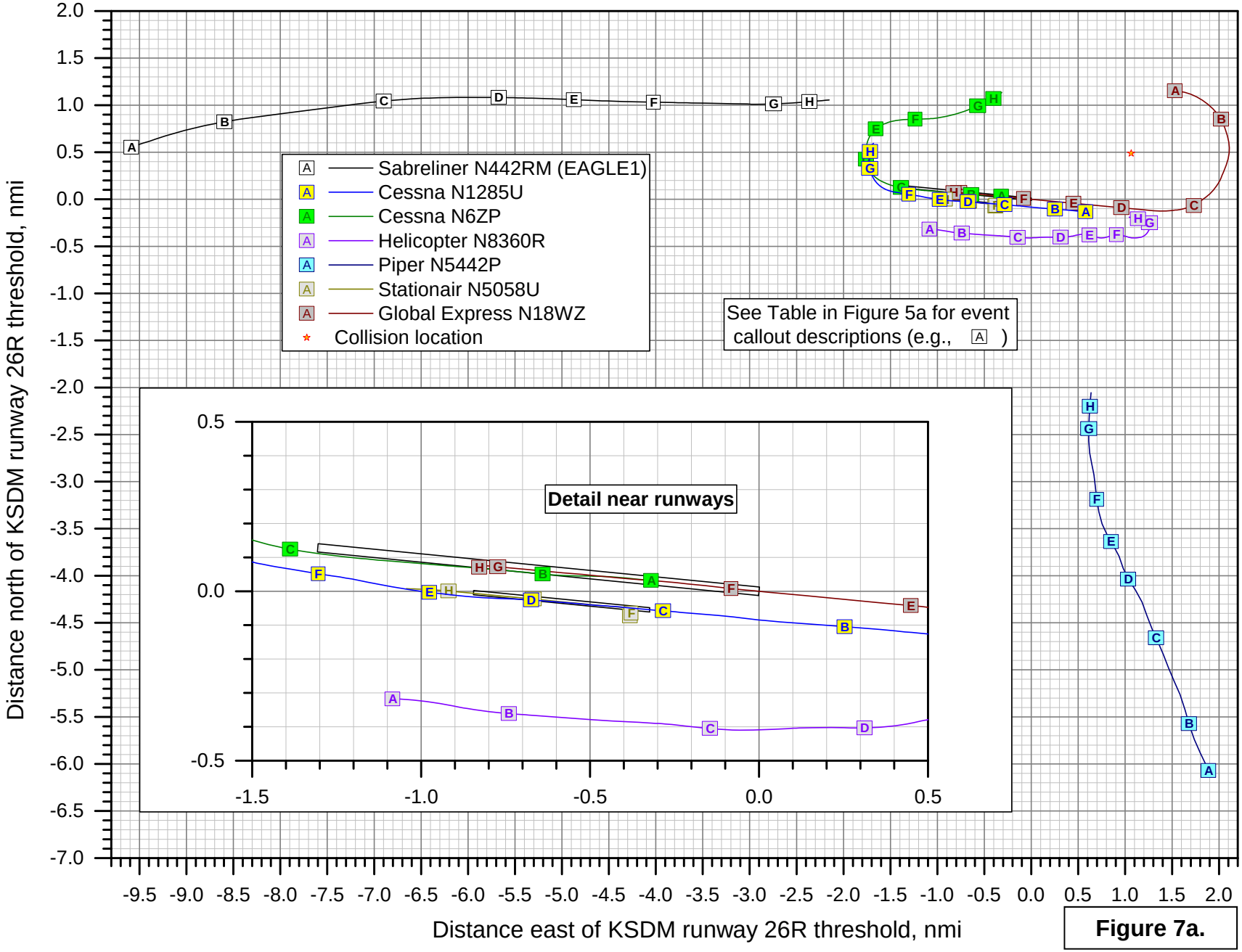

Figure 7a.

WPR15FA243AB: Midair collision, Sabreliner EAGLE1 / C172 N1285U, San Diego, CA, 8/16/2015

Aircraft in KSDM traffic pattern, 11:01:30 - 11:03:11 PDT

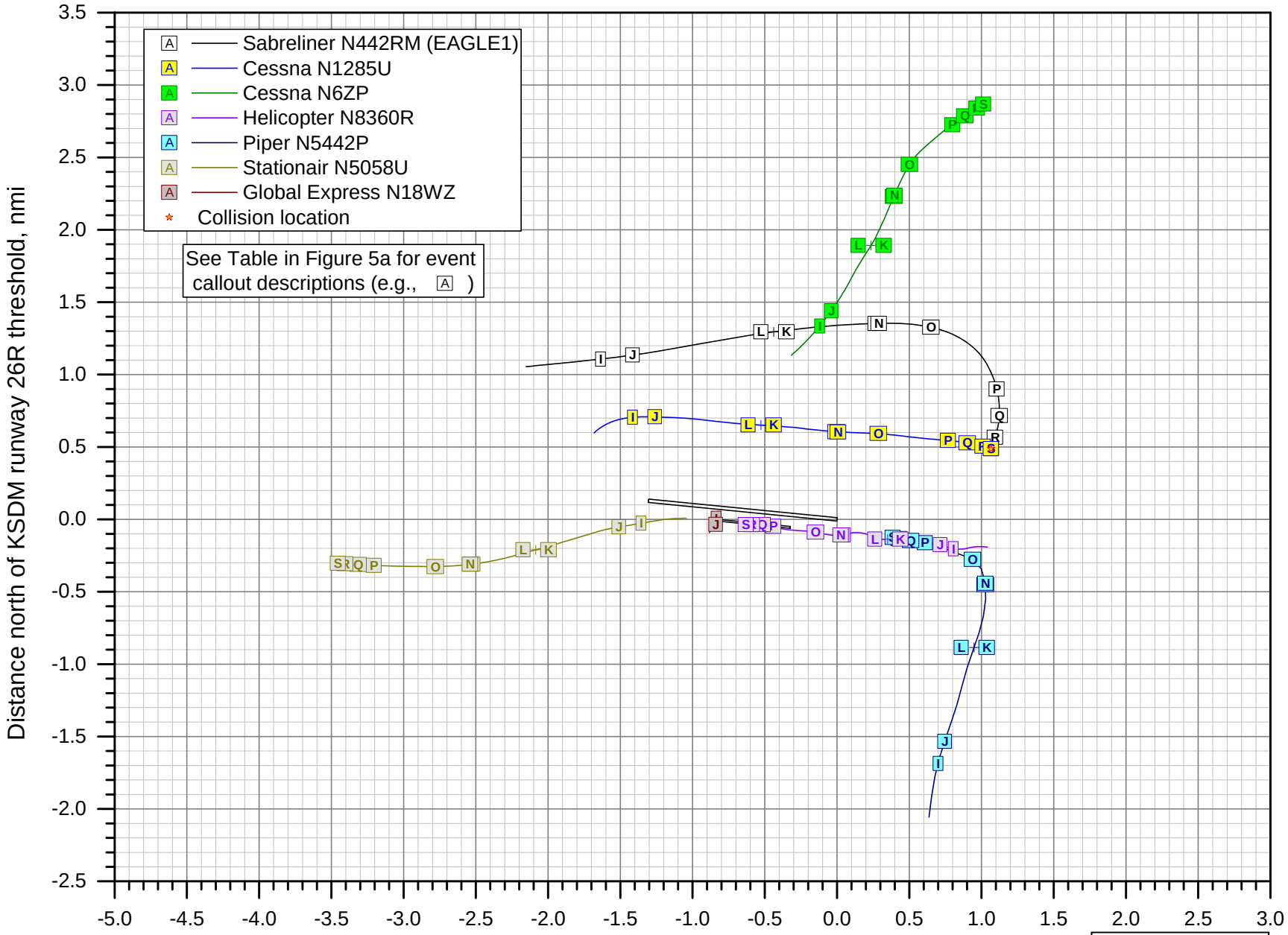

Figure 7b.

WPR15FA243AB: Midair collision, Sabreliner EAGLE1 / C172 N1285U, San Diego, CA, 8/16/2015

Summary of KSDM aircraft operations, 10:49:00 – 11:03:10 PDT

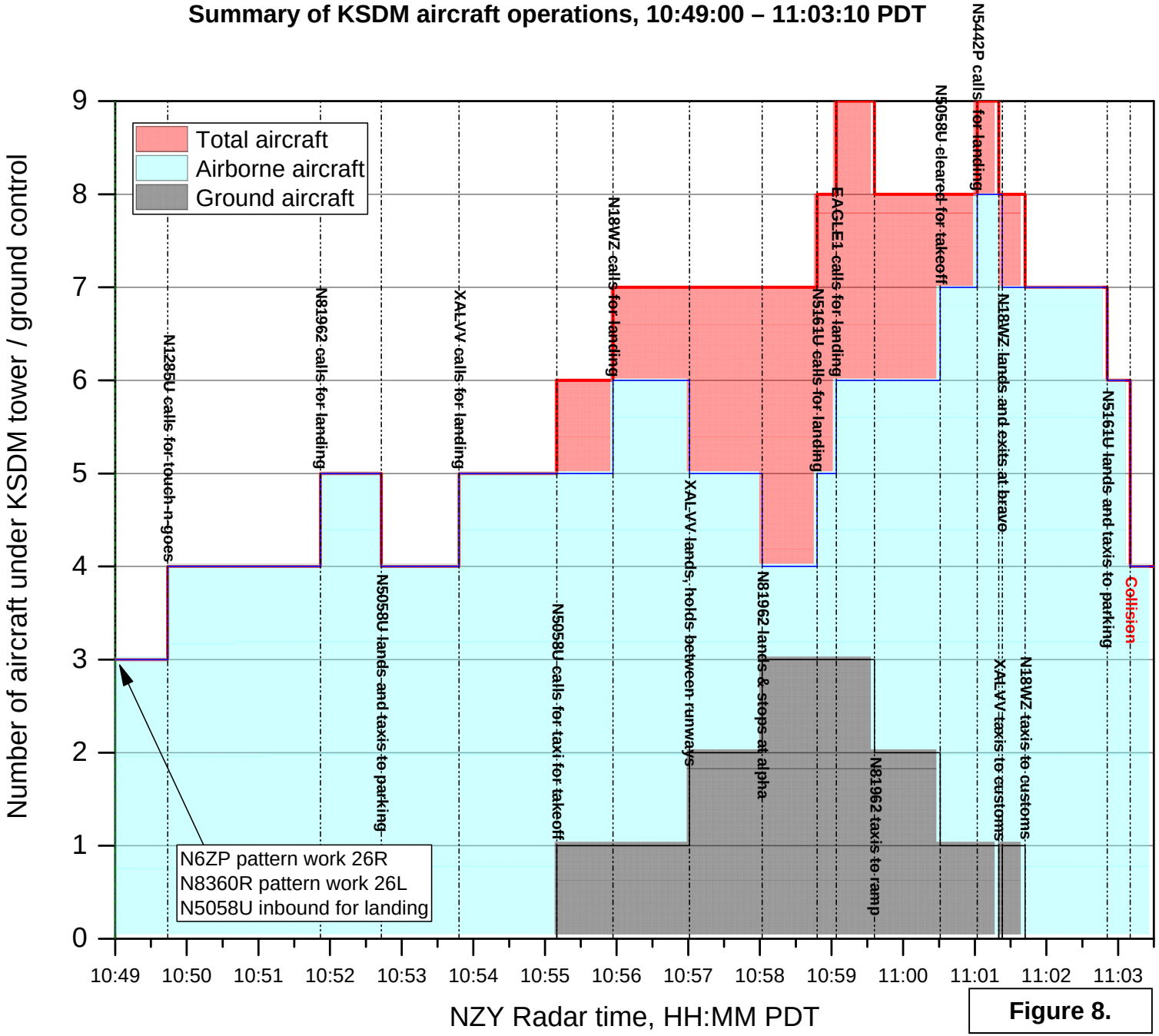

Figure 8.

WPR15FA243AB: Midair collision, Sabreliner EAGLE1 / C172 N1285U, San Diego, CA, 8/16/2015

Winds aloft based on 18:00 UTC (11:00 PDT) NAM computer model

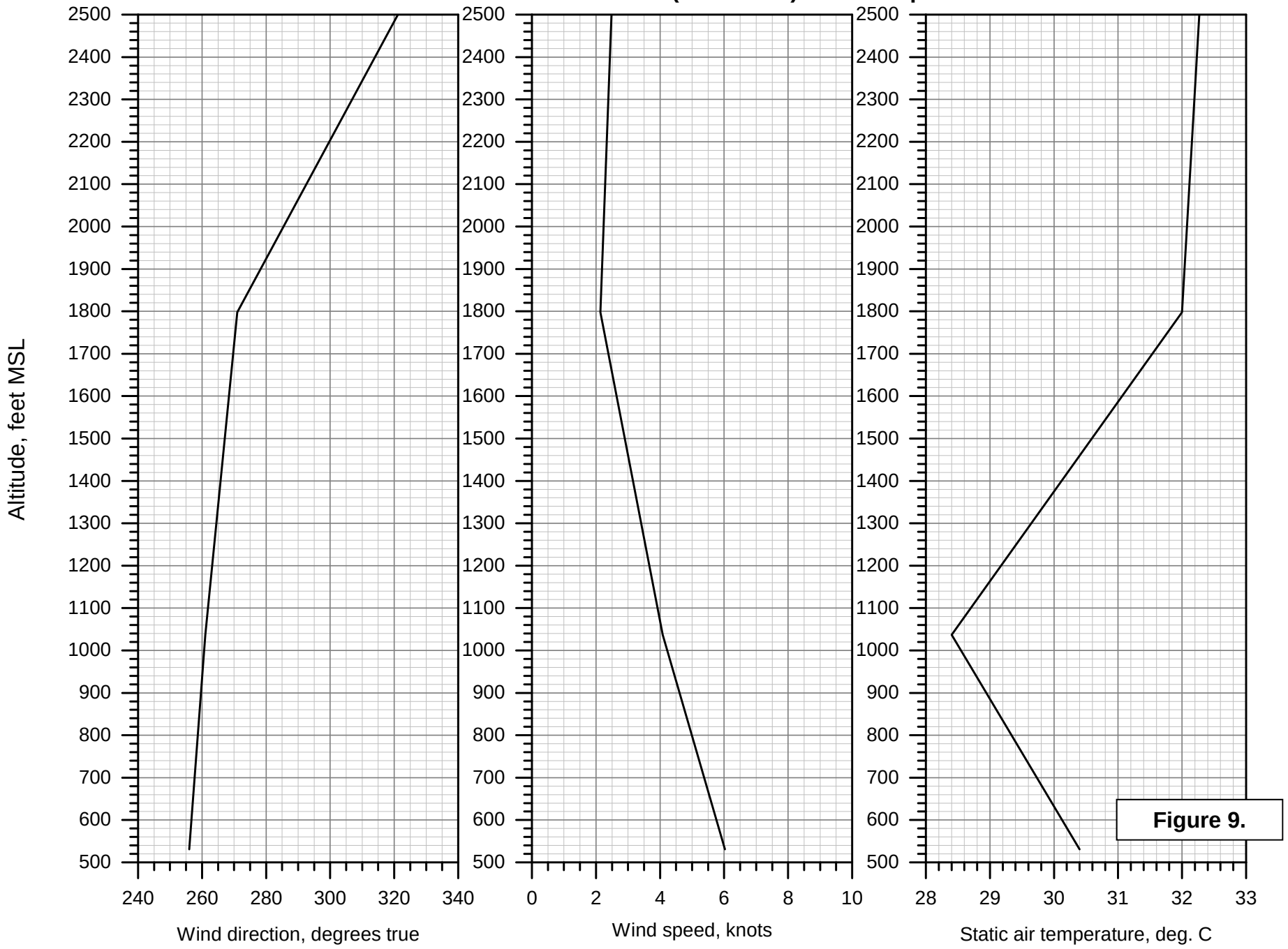

Figure 9.

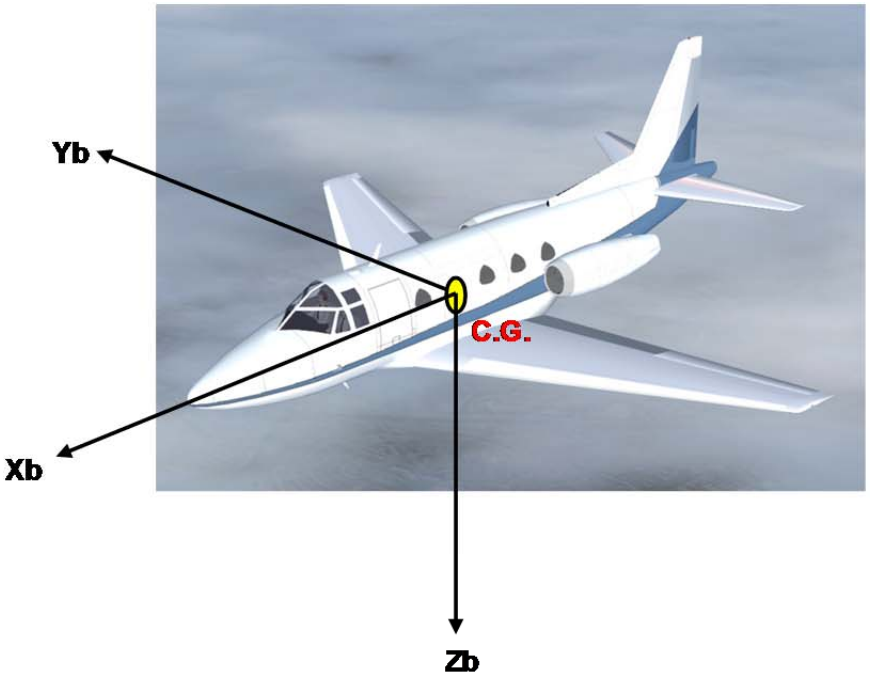

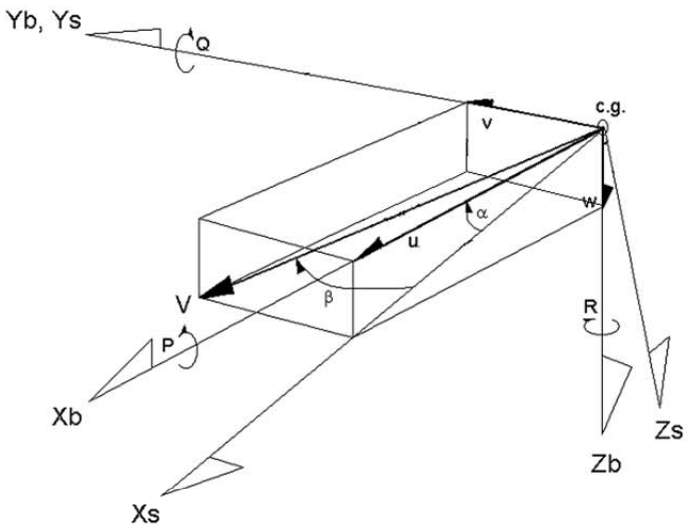

C.G. = center of gravity

{Xb, Yb, Zb} = body axis system

{Xs, Ys, Zs} = stability axis system

V = velocity vector

α = angle of attack

β = sideslip angle

P = body axis roll rate

Q = body axis pitch rate

R = body axis yaw rate

u = component of V along Xb

v = component of V along Yb

w = component of V along Zb

Figure 10.

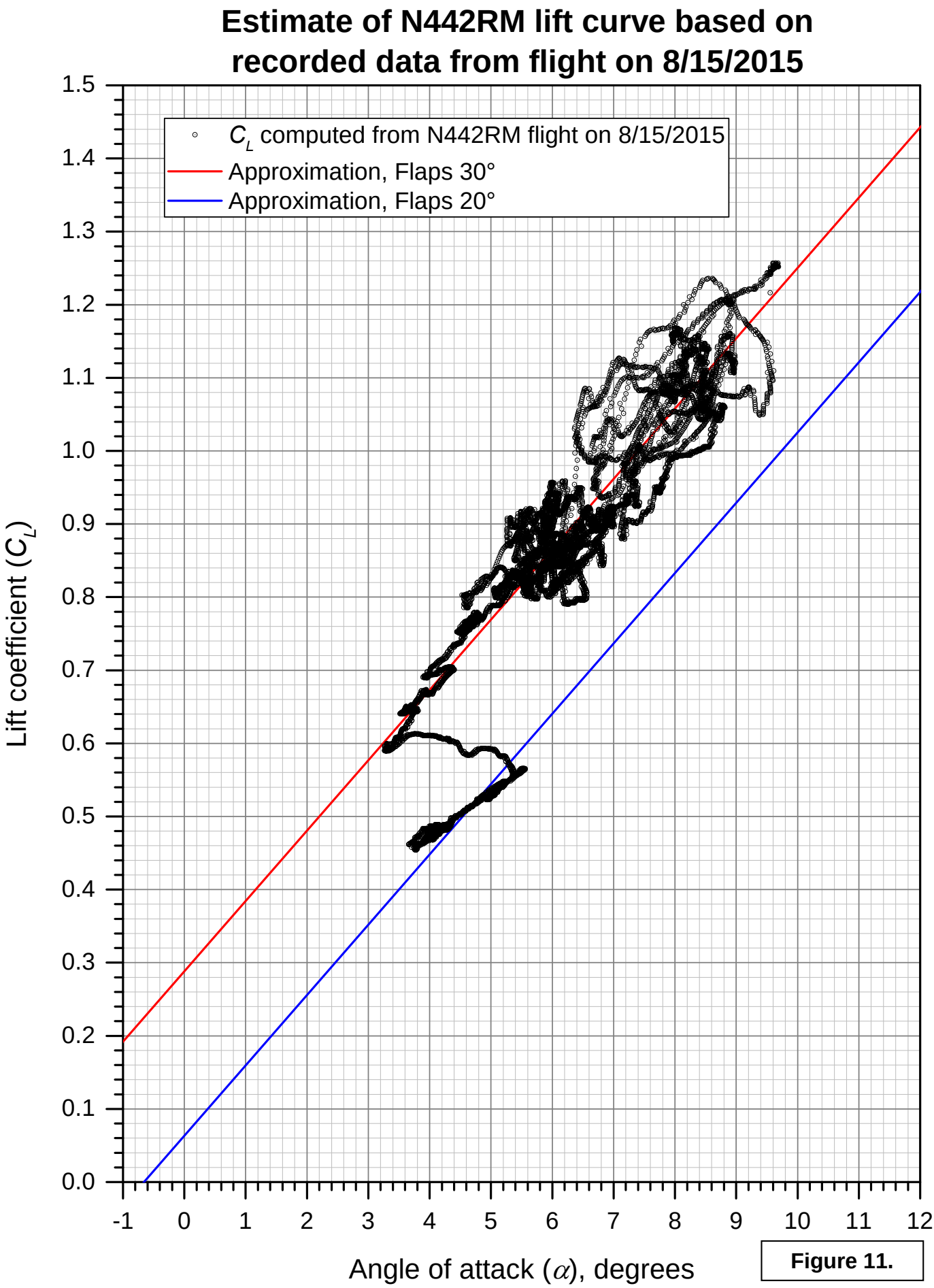
Estimate of N442RM lift curve based on recorded data from flight on 8/15/2015
C_L computed from N442RM flight on 8/15/2015
Approximation, Flaps 30°
Approximation, Flaps 20°
Lift coefficient (C_L)
Angle of attack (α), degrees
1.5
1.4
1.3
1.2
1.1
1.0
0.9
0.8
0.7
0.6
0.5
0.4
0.3
0.2
0.1
0.0
-1
0
1
2
3
4
5
6
7
8
9
10
11
12

Figure 11.

WPR15FA243AB: Midair collision, Sabreliner EAGLE1 / C172 N1285U, San Diego, CA, 8/16/2015

EAGLE1 and N1285U north and east positions vs. time

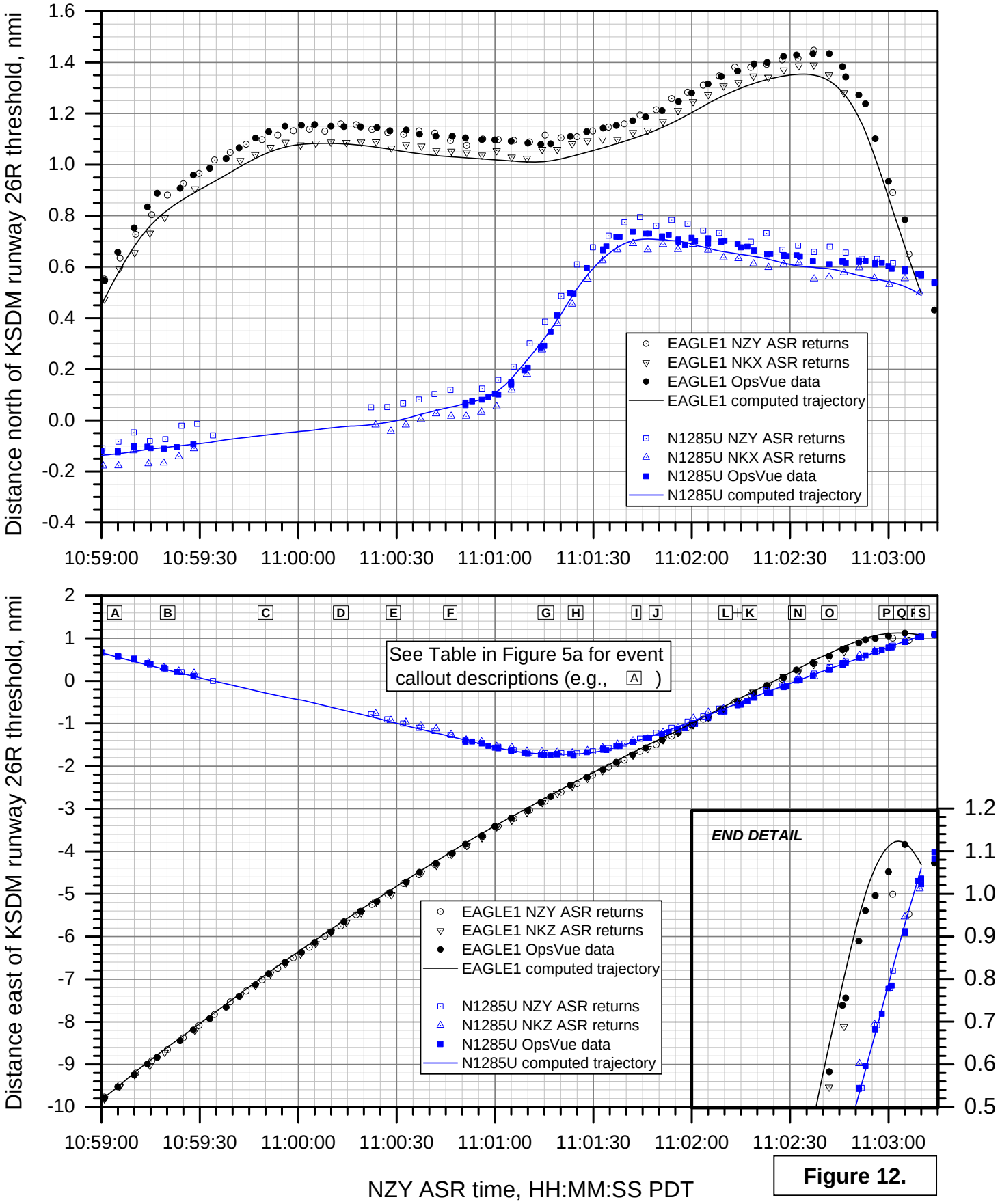

Figure 12.

WPR15FA243AB: Midair collision, Sabreliner EAGLE1 / C172 N1285U, San Diego, CA, 8/16/2015

Altitudes of aircraft in KSDM traffic pattern, 10:59:00 - 11:03:15 PDT

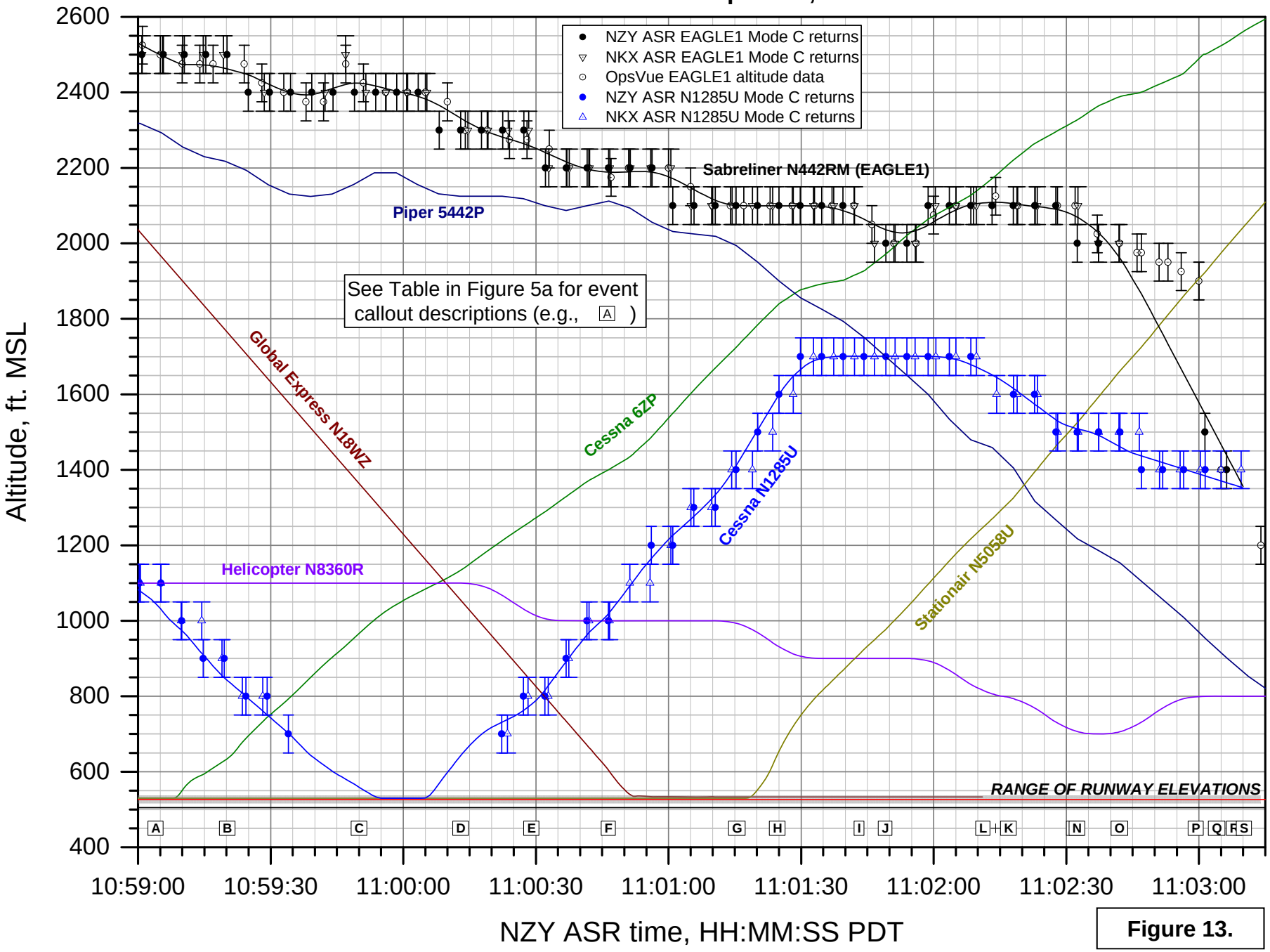

Figure 13.

WPR15FA243AB: Midair collision, Sabreliner EAGLE1 / C172 N1285U, San Diego, CA, 8/16/2015

EAGLE1 and N1285U speeds and rates of climb

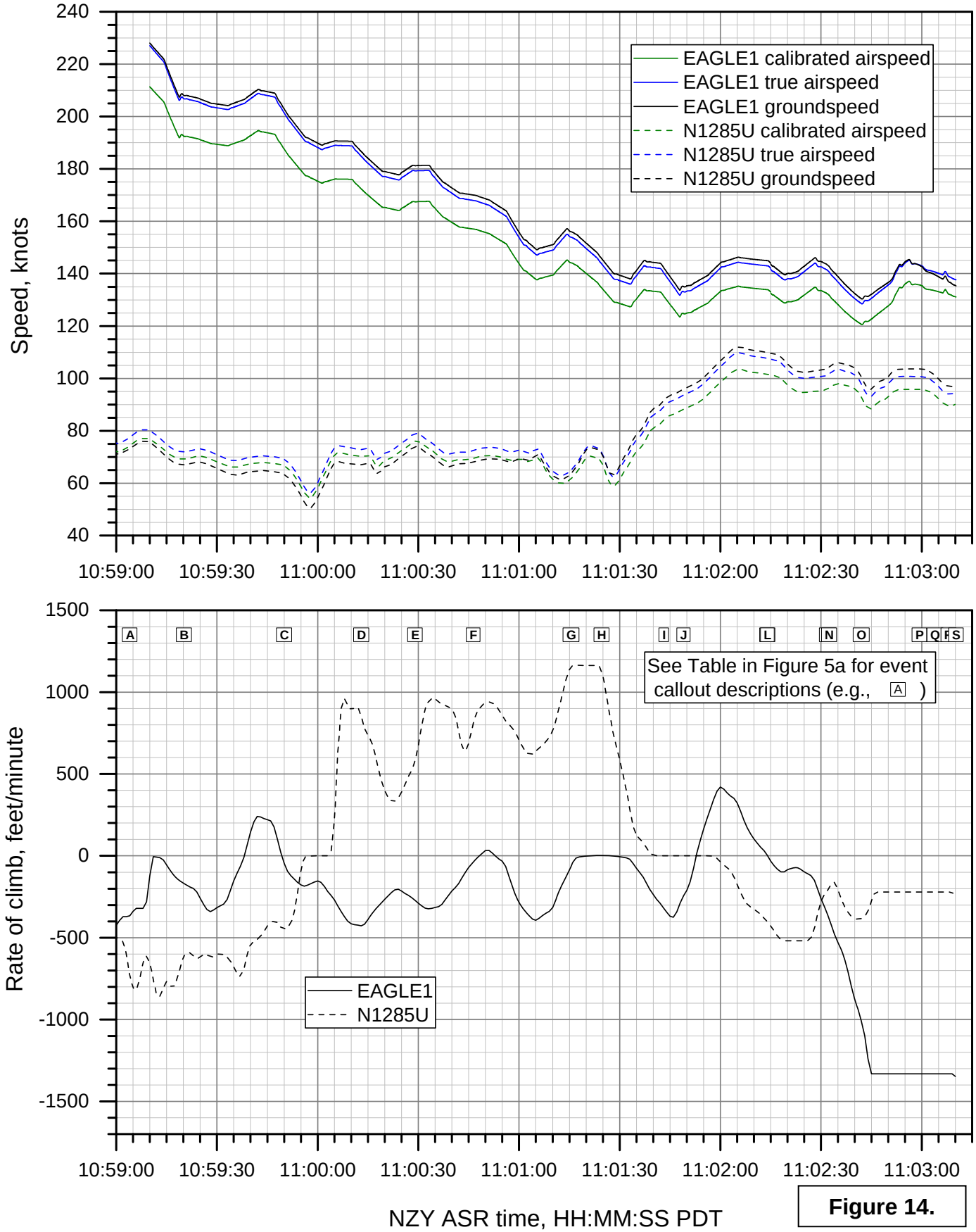

Figure 14.

WPR15FA243AB: Midair collision, Sabreliner EAGLE1 / C172 N1285U, San Diego, CA, 8/16/2015

EAGLE1 and N1285U separation distance and closure rate

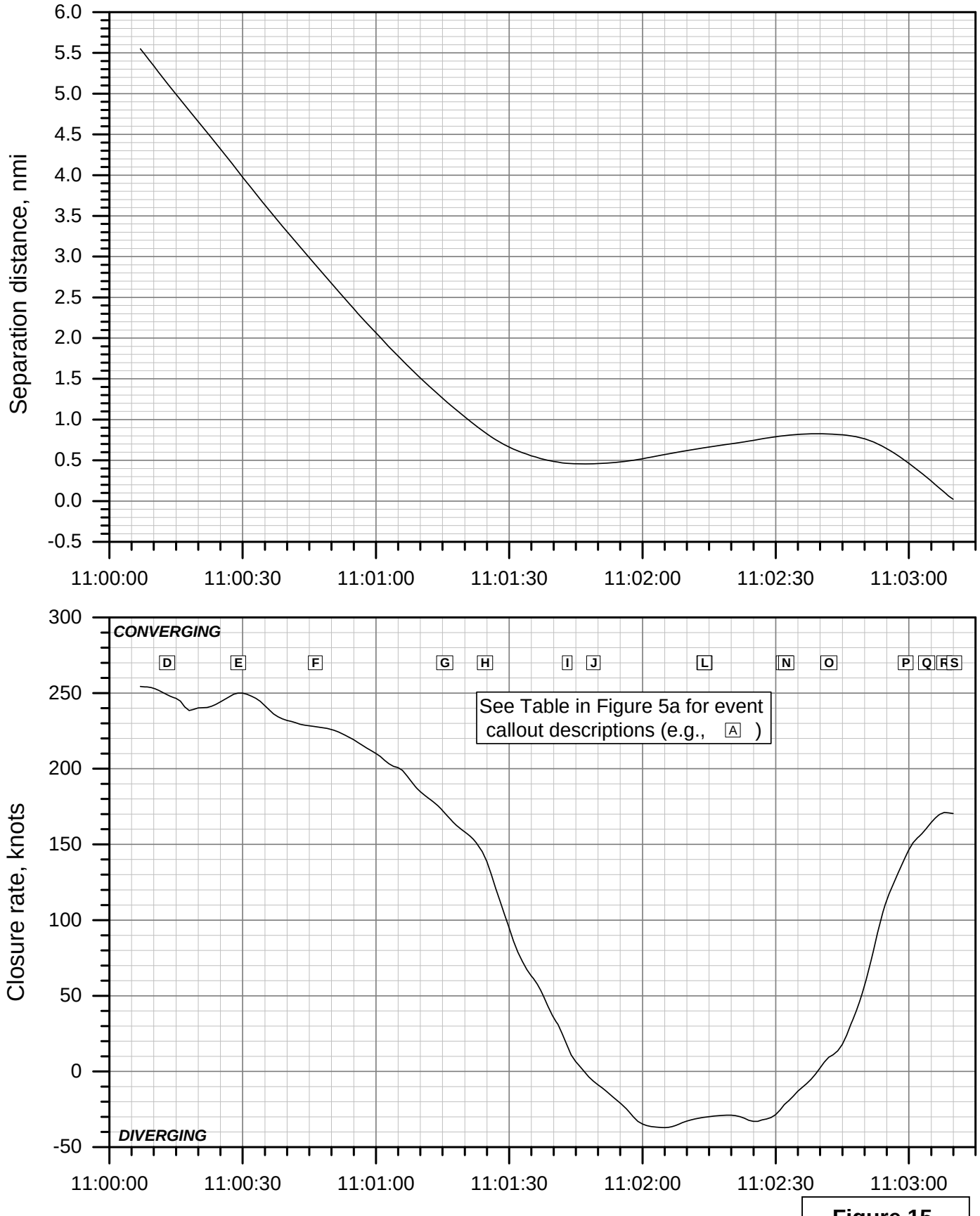

Figure 15.

WPR15FA243AB: Midair collision, Sabreliner EAGLE1 / C172 N1285U, San Diego, CA, 8/16/2015

EAGLE1 and N1285U Euler angles vs. time

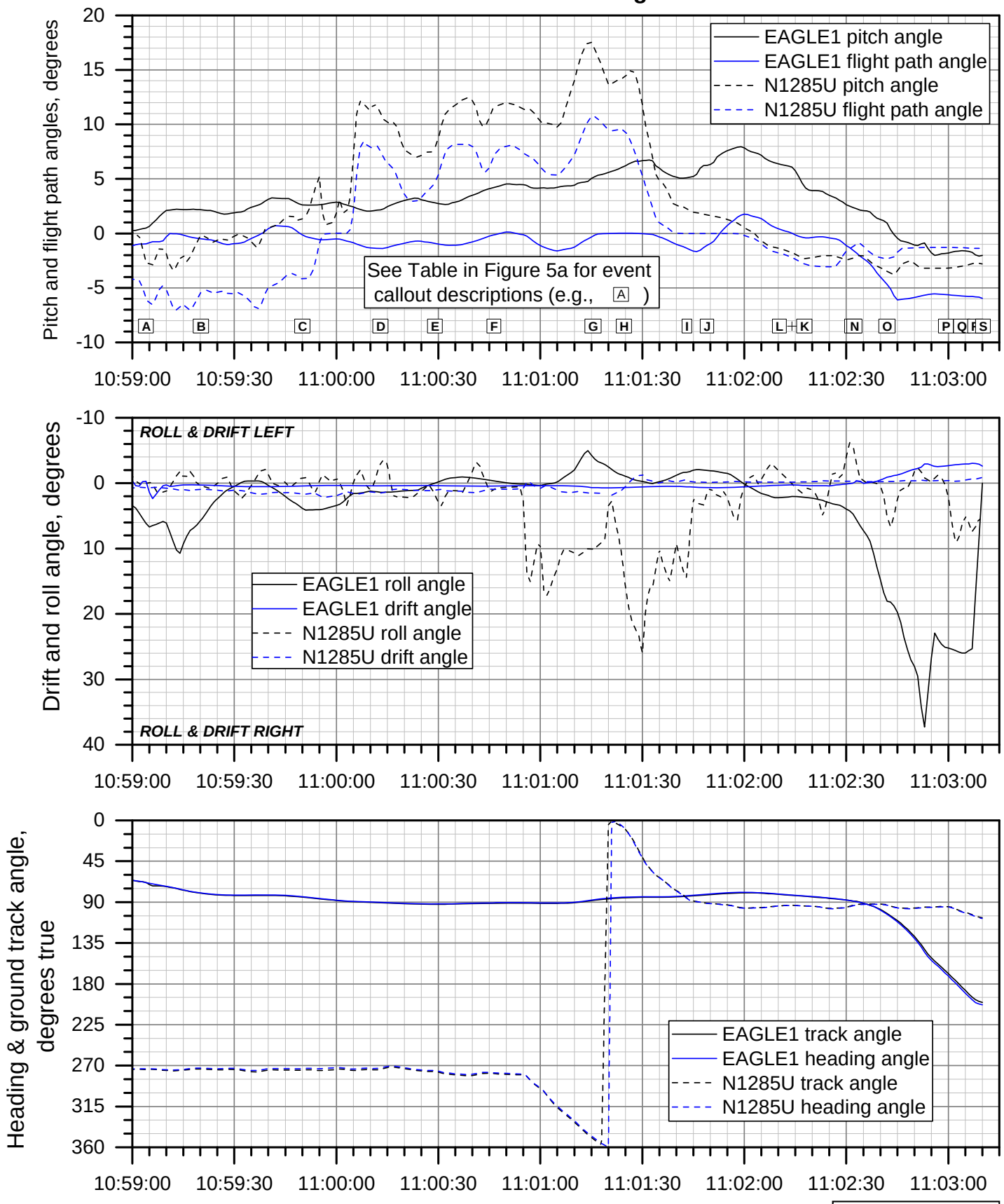

Figure 16.

WPR15FA243AB: Midair collision, Sabreliner EAGLE1 / C172 N1285U, San Diego, CA, 8/16/2015

Assumed EAGLE1 and N1285U airplane configurations

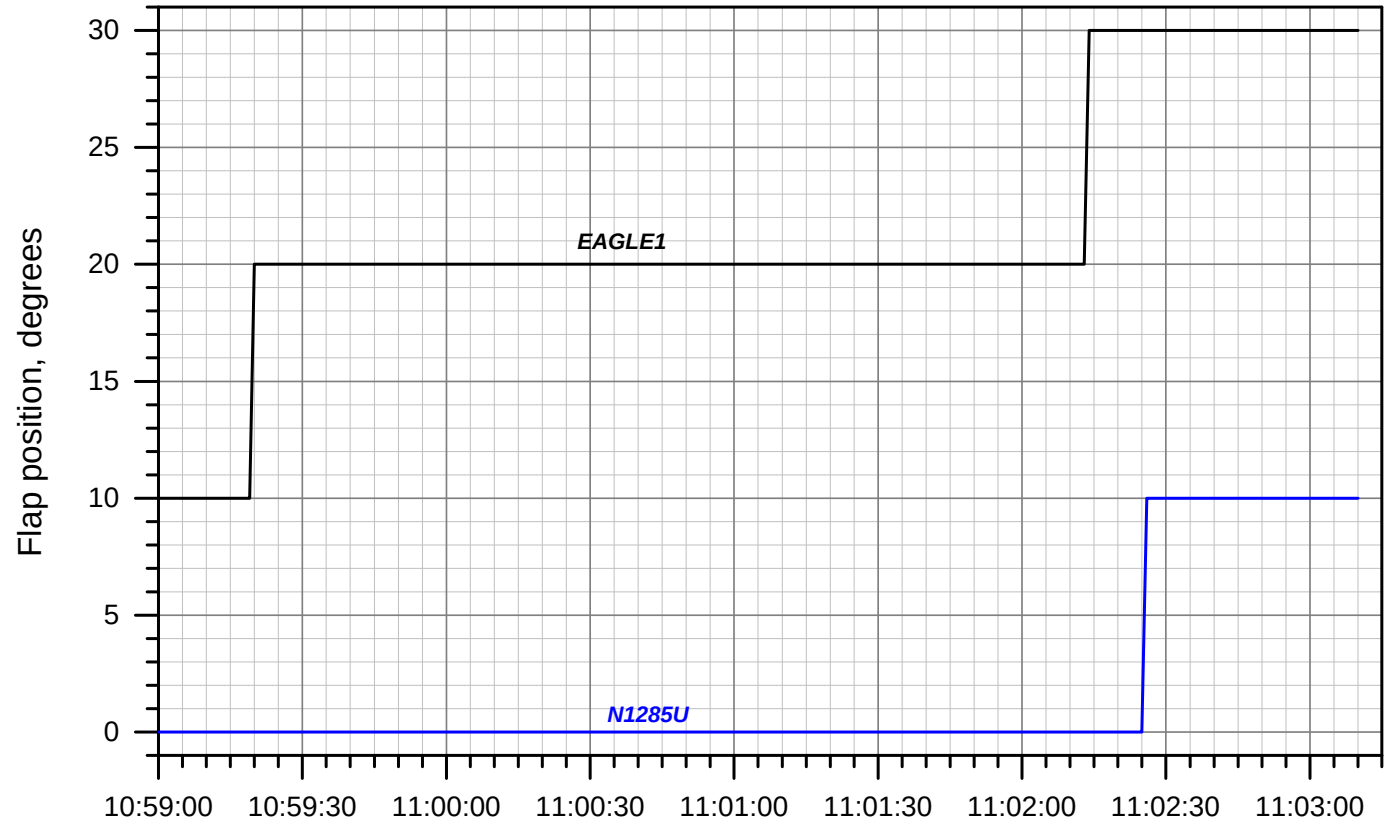

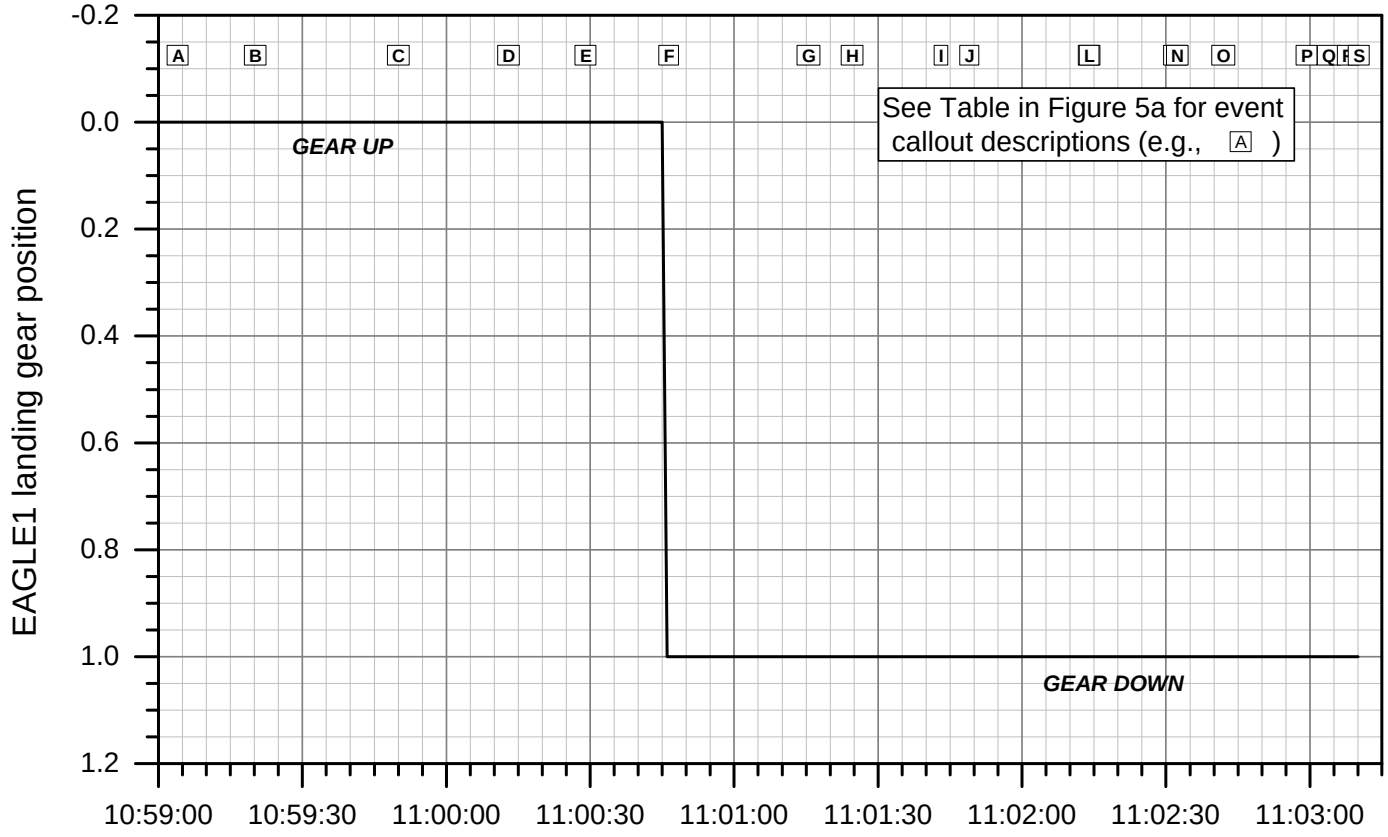

NZY ASR time, HH:MM:SS PDT

Figure 17.

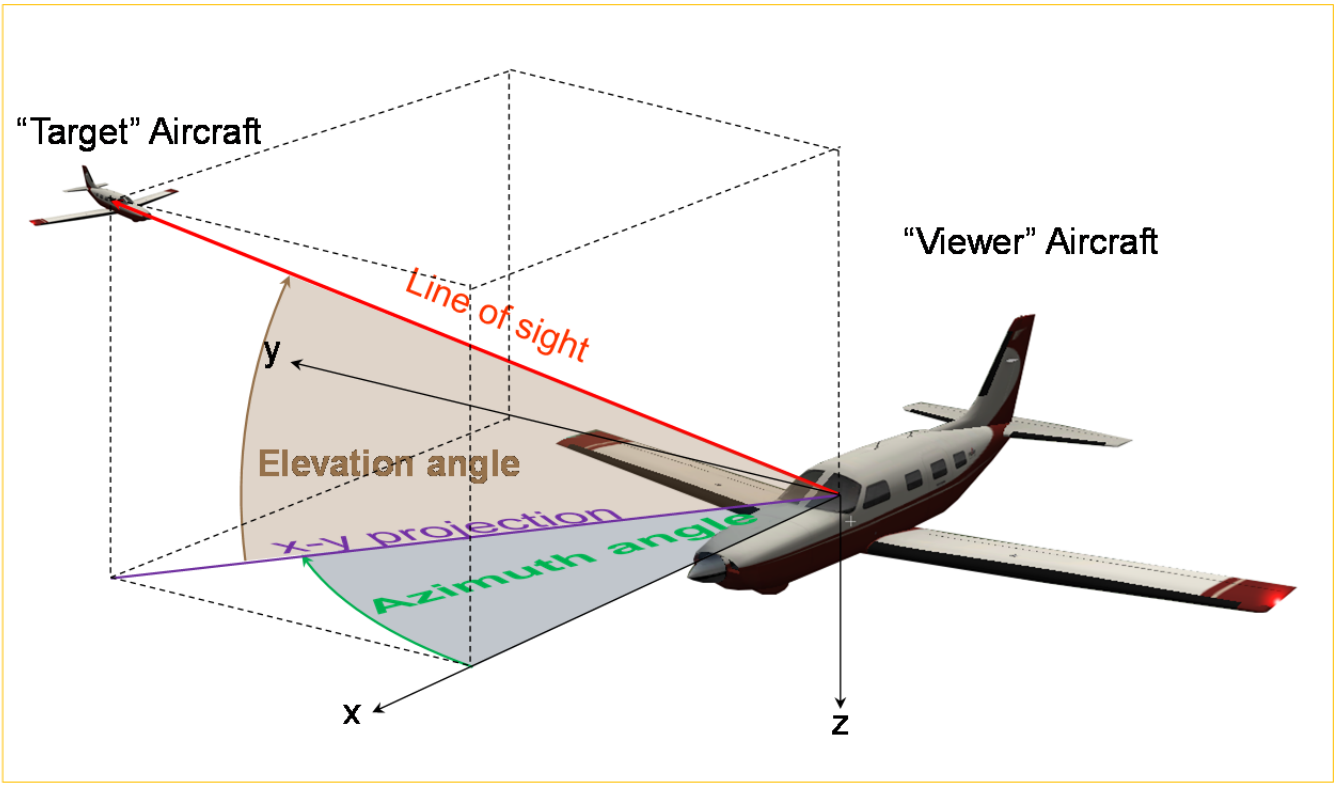

Figure 18. Azimuth and elevation angles from "viewer" airplane to "target" airplane.

WPR15FA243AB: Midair collision, Sabreliner EAGLE1 / C172 N1285U, San Diego, CA, 8/16/2015

EAGLE1 and N1285U azimuth & elevation viewing angles vs. time

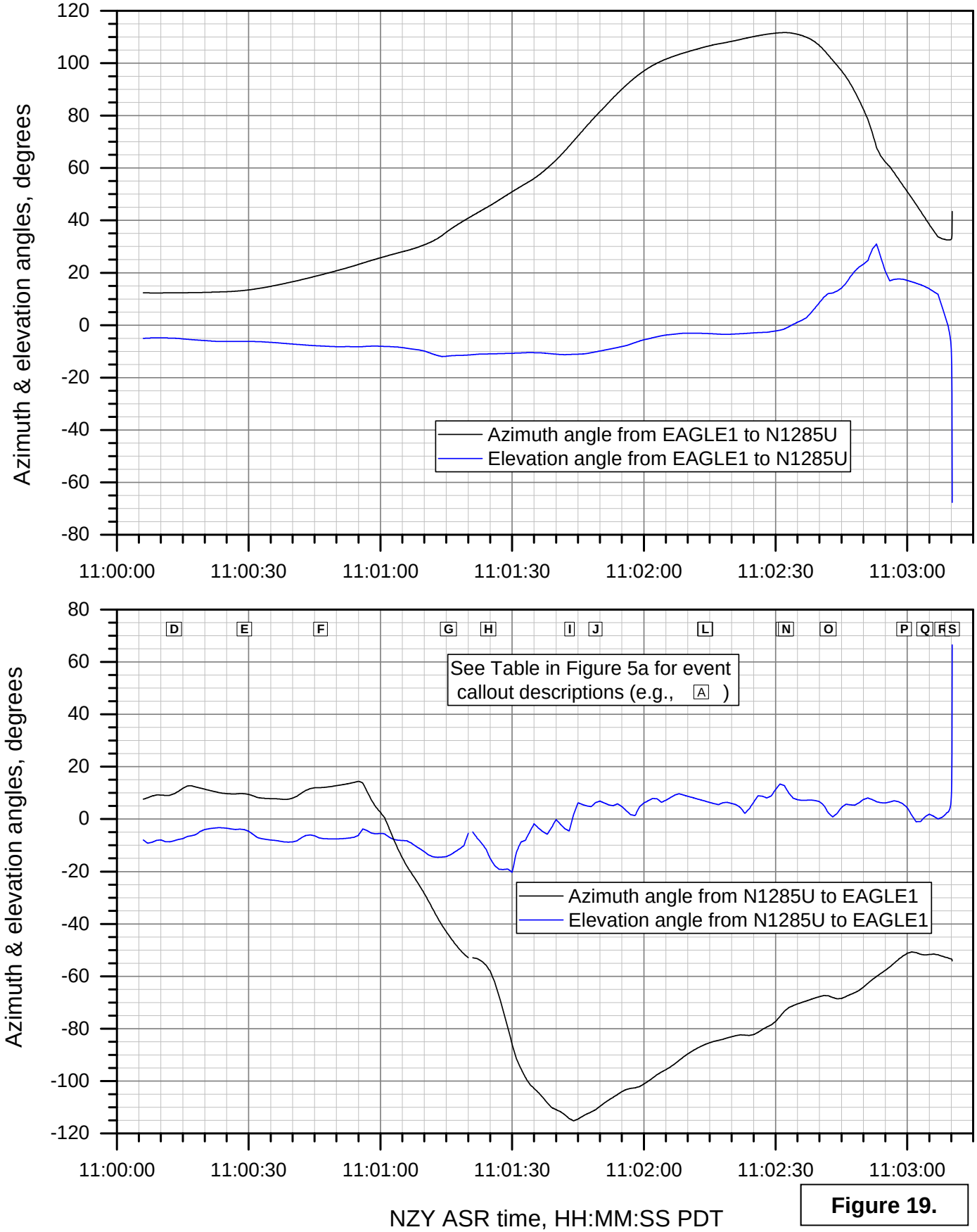

Figure 19.

WPR15FA243AB: Midair collision, Sabreliner EAGLE1 / C172 N1285U, San Diego, CA, 8/16/2015

EAGLE1 and N1285U: azimuth & elevation viewing angles

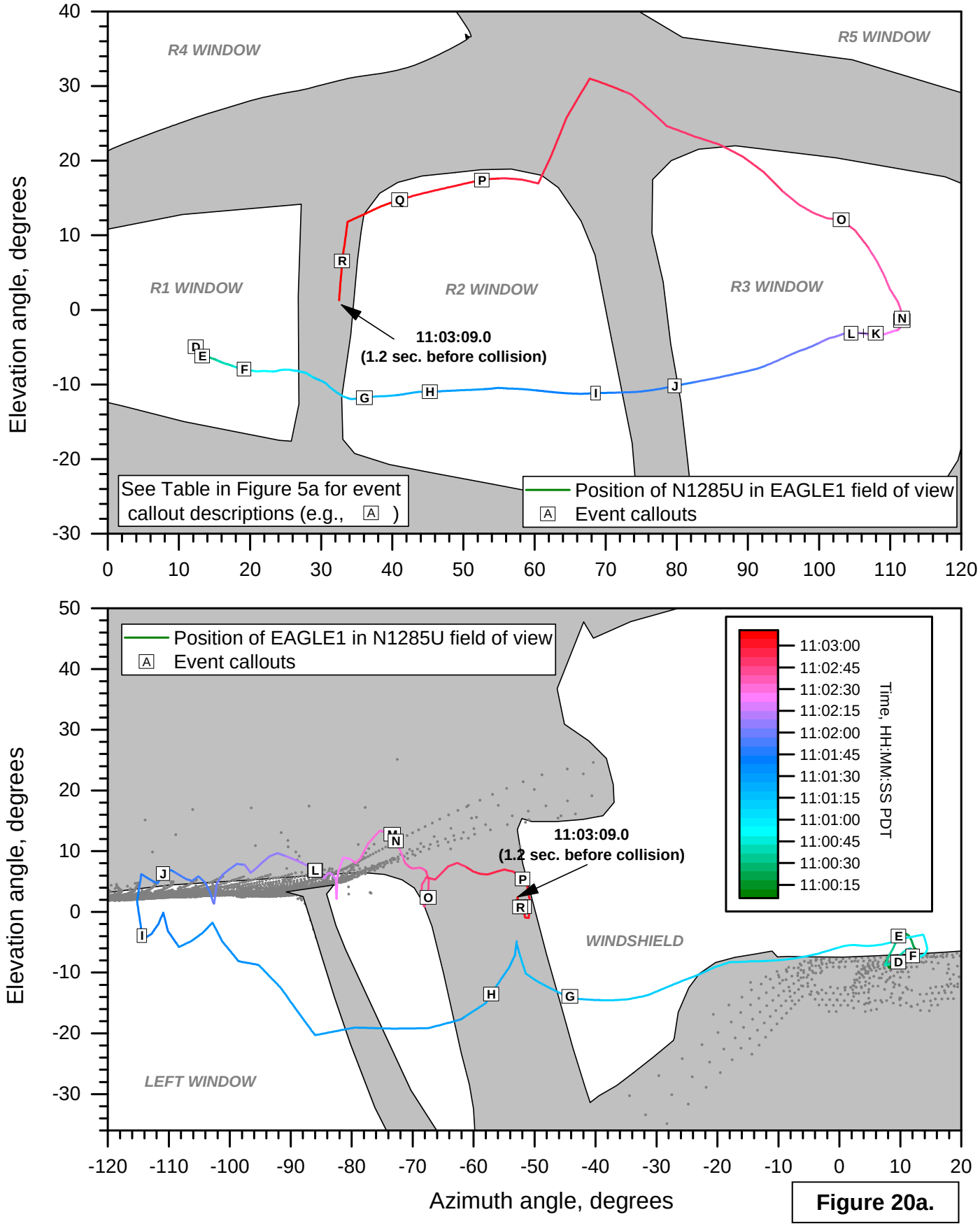

Figure 20a.

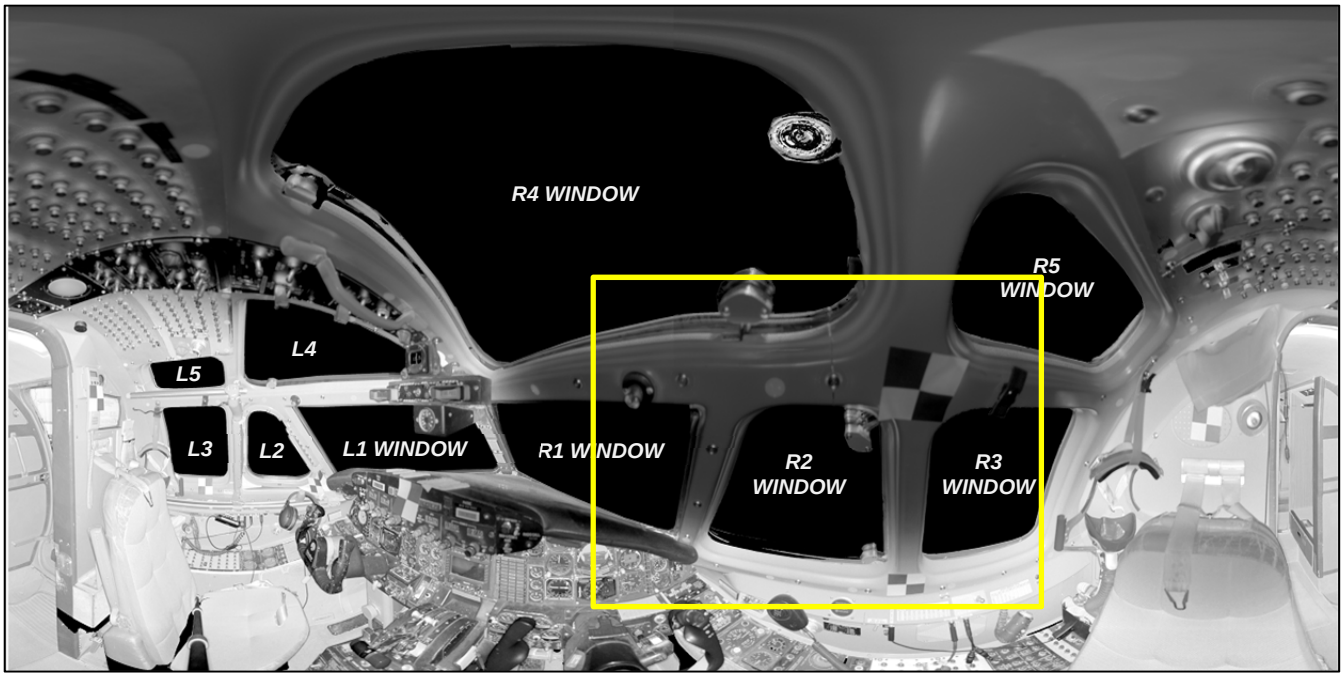

"Fish eye" photograph of the cockpit of an exemplar Sabreliner. The highlighted area is plotted in Figure 20a.

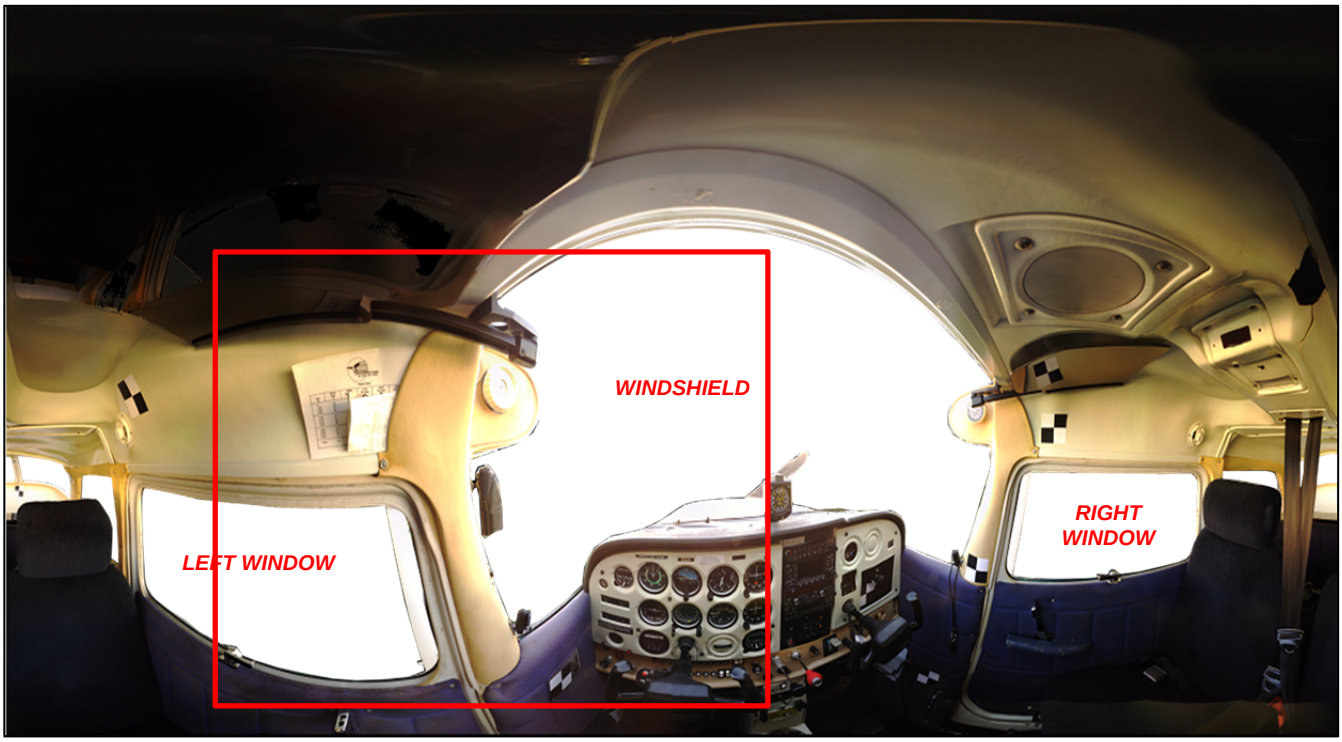

"Fish eye" photograph of the cockpit of an exemplar Cessna 172. The highlighted area is plotted in Figure 20a.

Figure 20b.

WPR15FA243AB: Midair collision, Sabreliner EAGLE1 / C172 N1285U, San Diego, CA, 8/16/2015

EAGLE1 and N1285U: azimuth & elevation angles of the sun

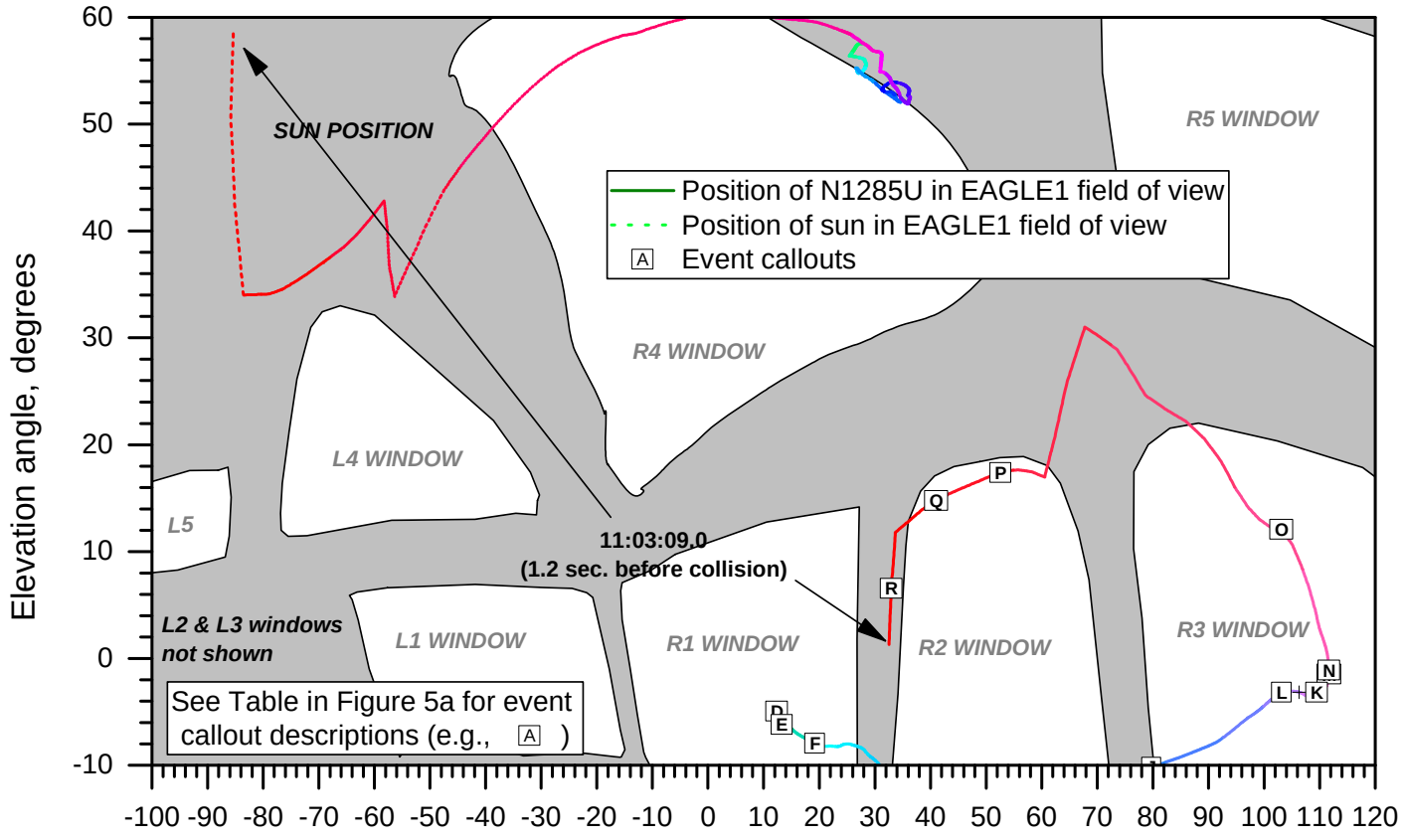

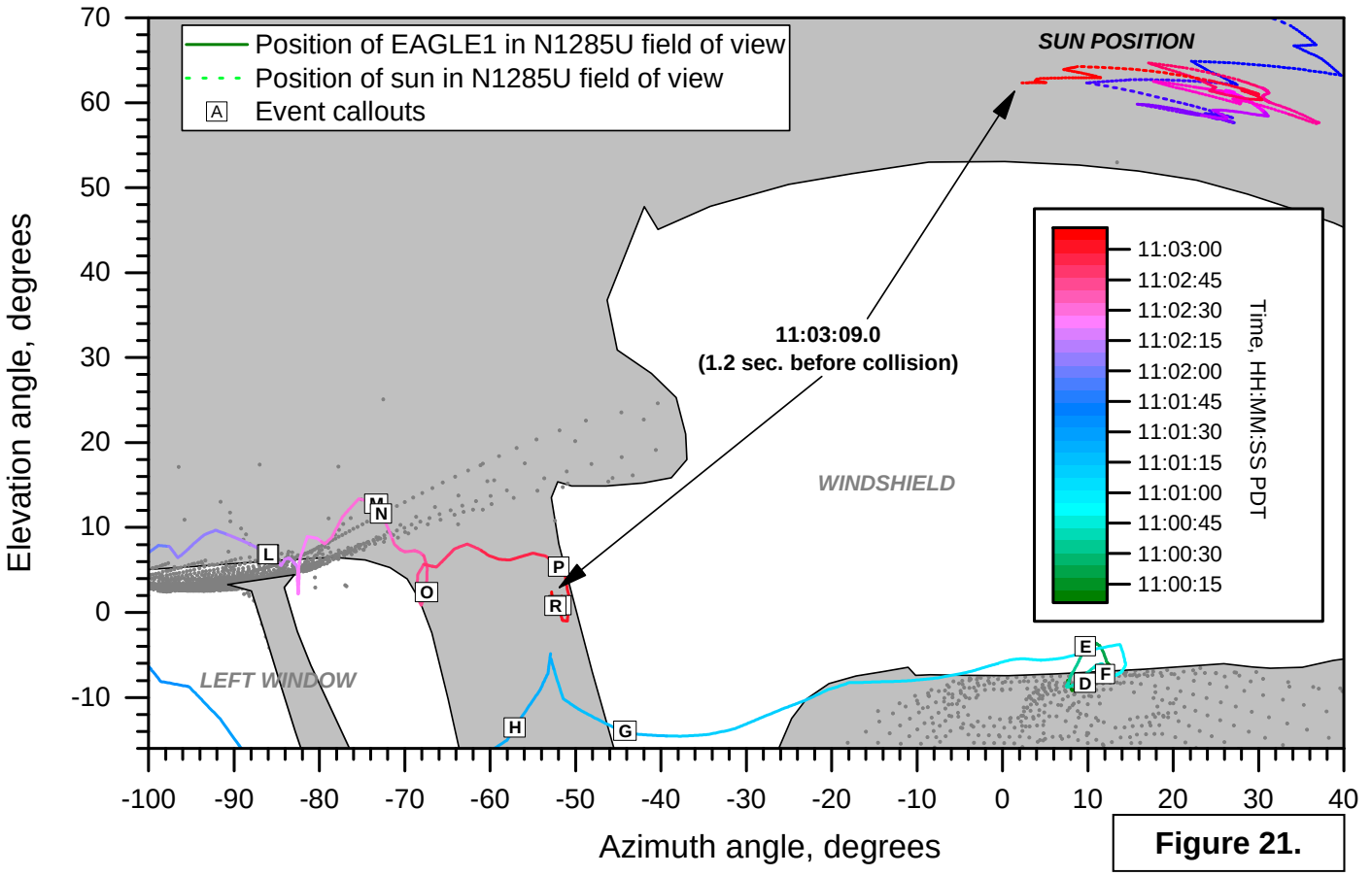

Figure 21.

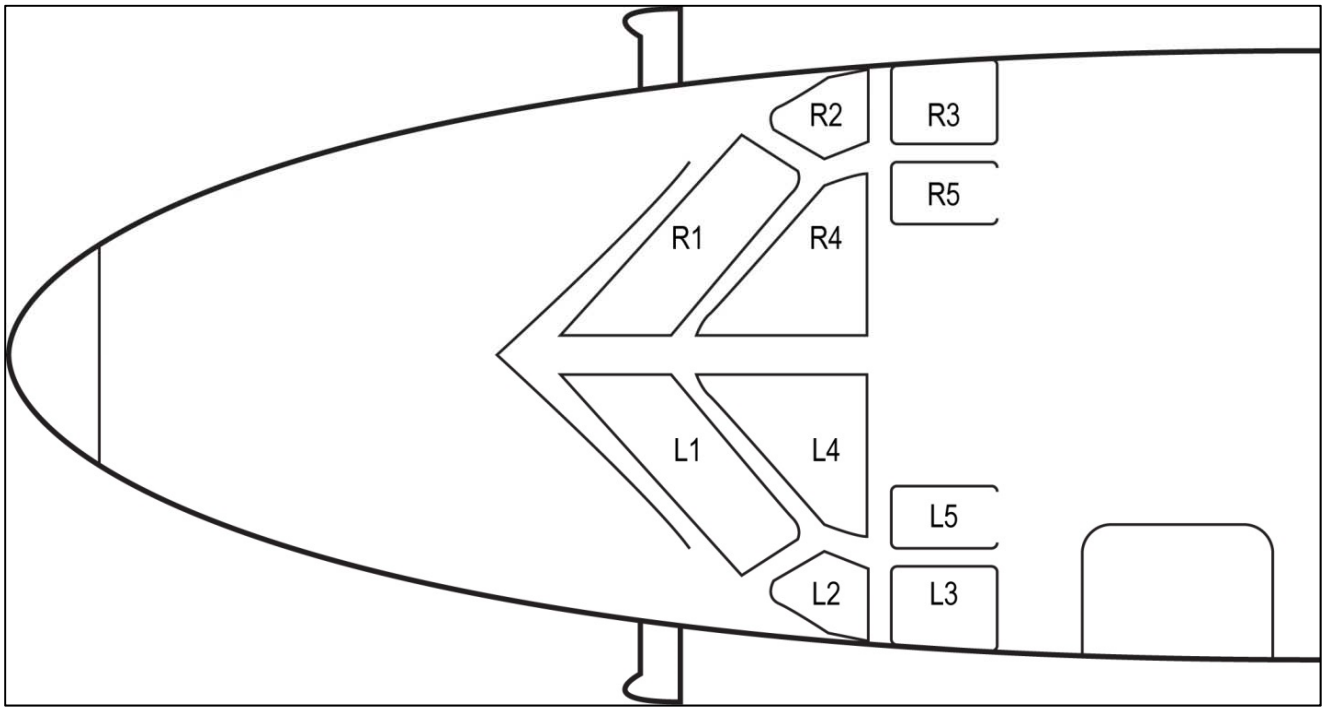

Figure 22a. Top-down view of NA265-60SC forward fuselage, showing labels used to identify cockpit windows.

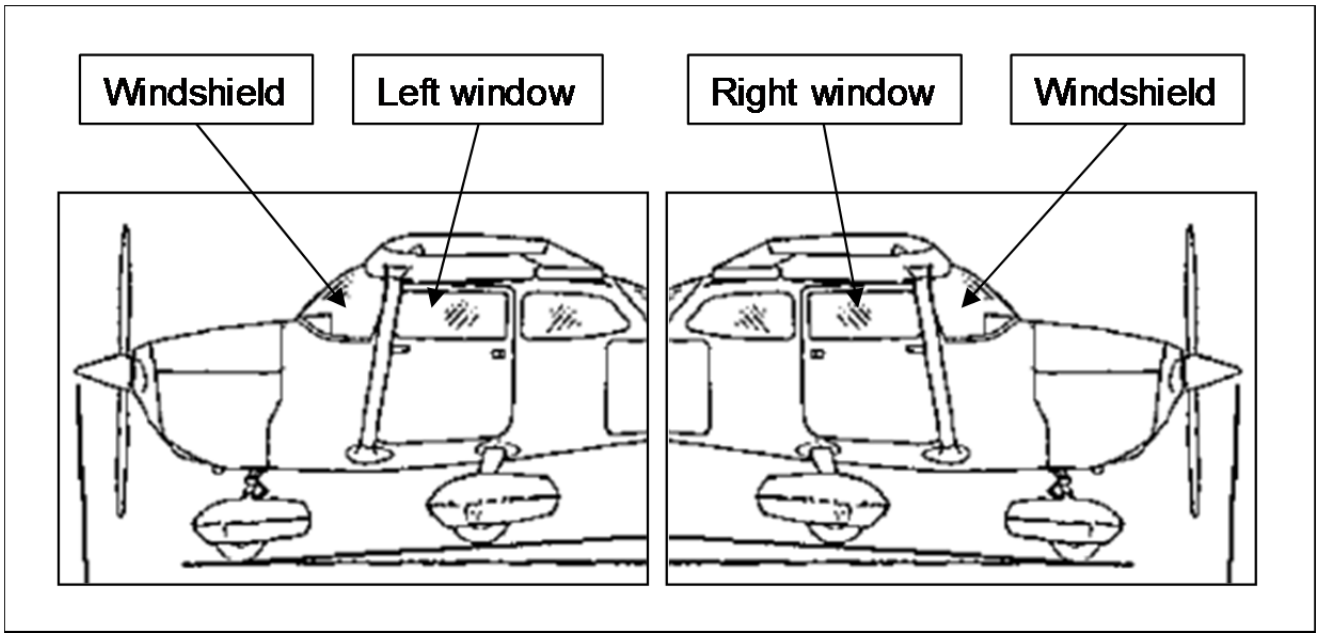

Figure 22b . Side view of Cessna 172 forward fuselage, showing labels used to identify cockpit windows.

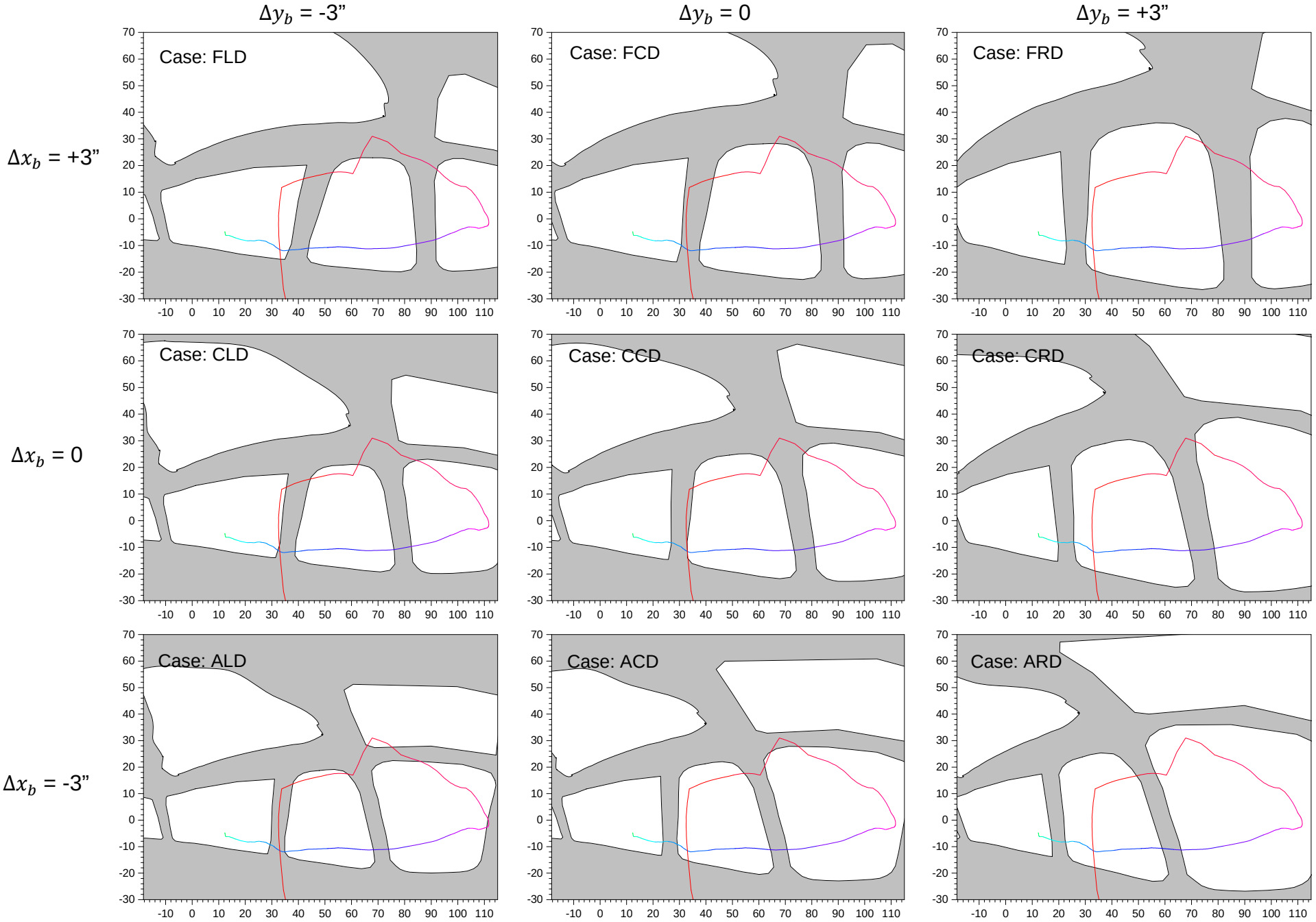

Figure 23a. Viewing angles for EAGLE1 at Δz_b = +1.5 inches (i.e., down). Plots are elevation angle vs. azimuth angle (in degrees).

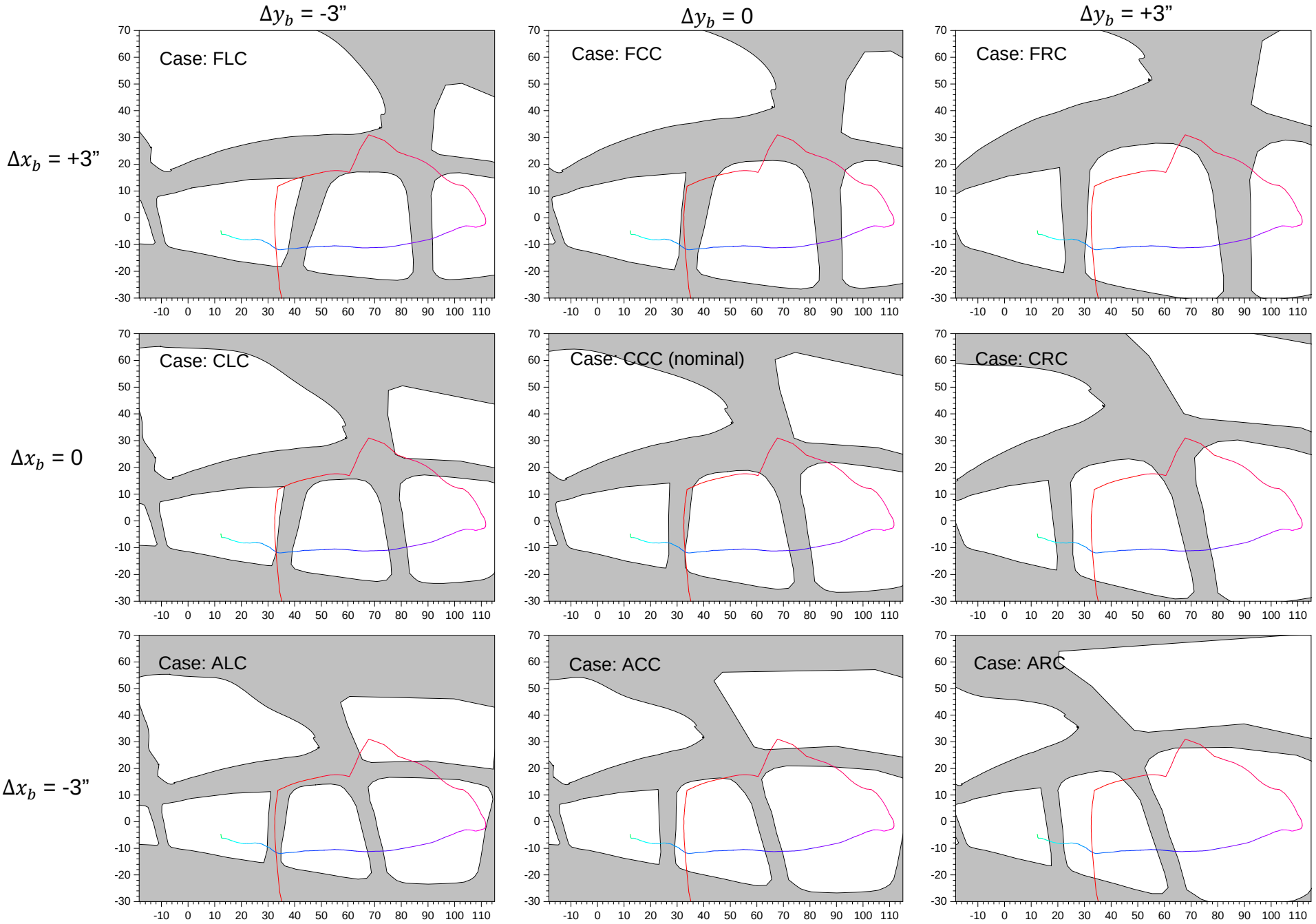

Figure 23b. Viewing angles for EAGLE1 at Δz_b = 0. Plots are elevation angle vs. azimuth angle (in degrees).

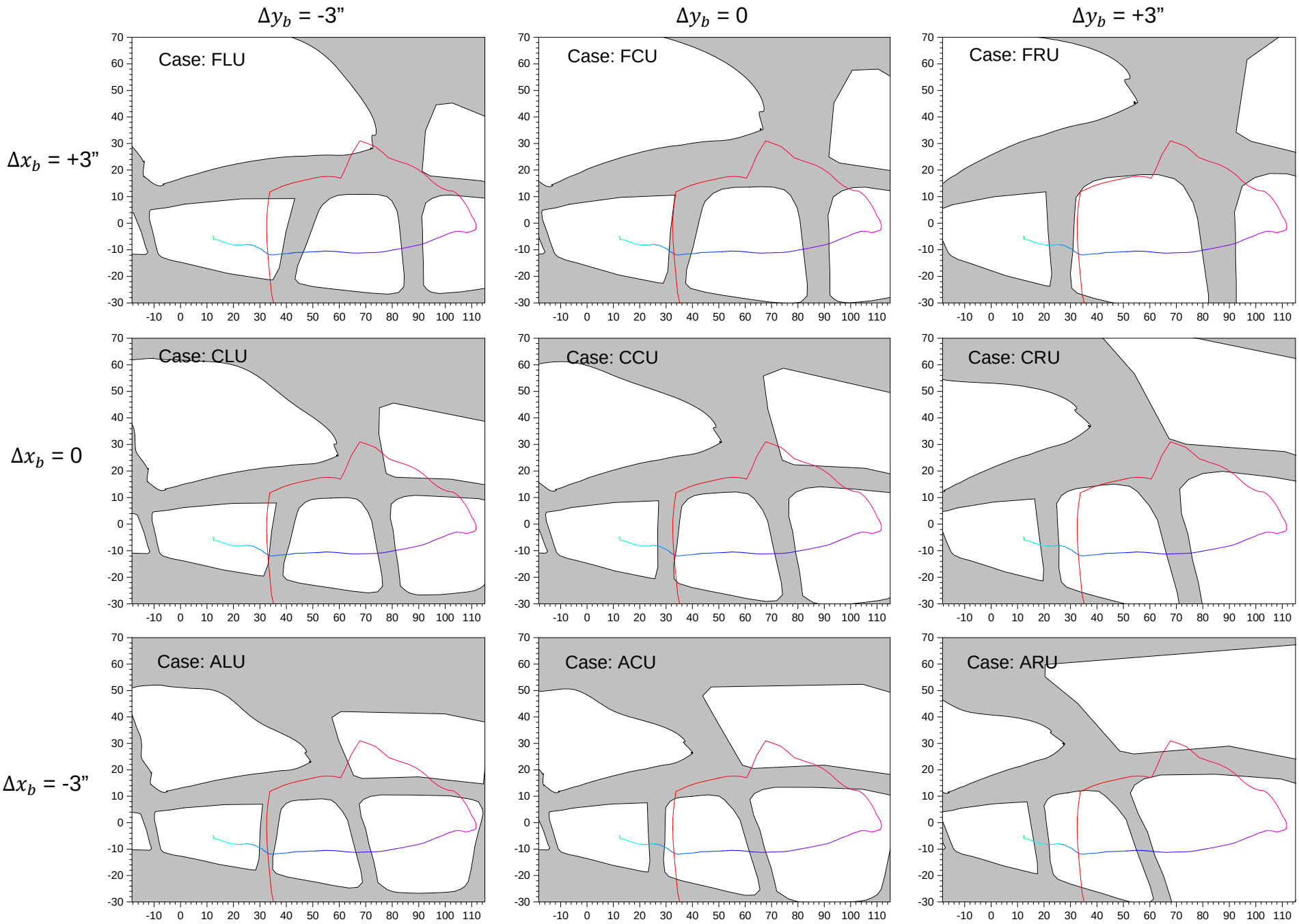

Figure 23c. Viewing angles for EAGLE1 at Δz_b = -1.5 inches (i.e., up). Plots are elevation angle vs. azimuth angle (in degrees).

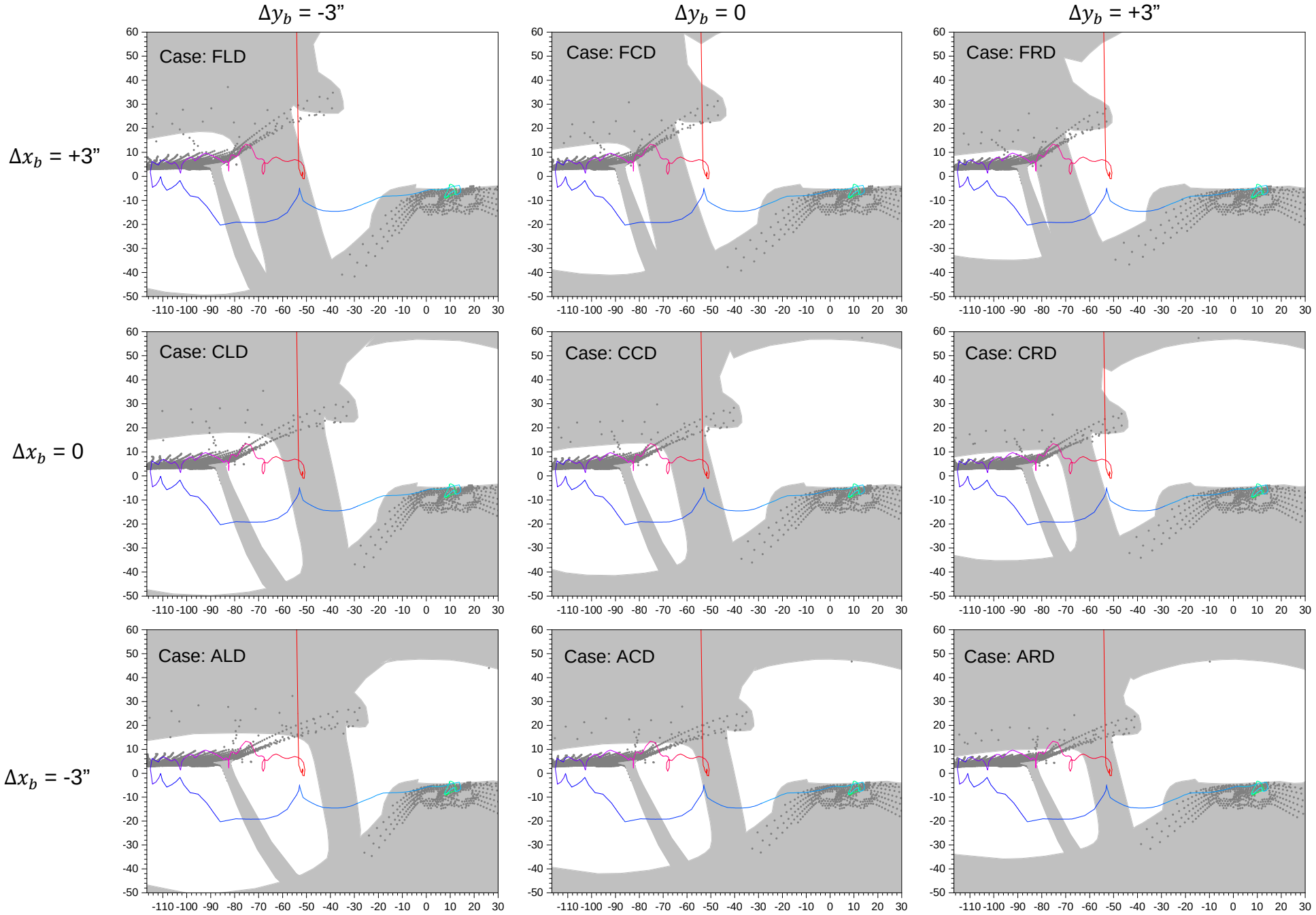

Figure 24a. Viewing angles for N1285u at Δz_b = +1.5 inches (i.e., down). Plots are elevation angle vs. azimuth angle (in degrees).

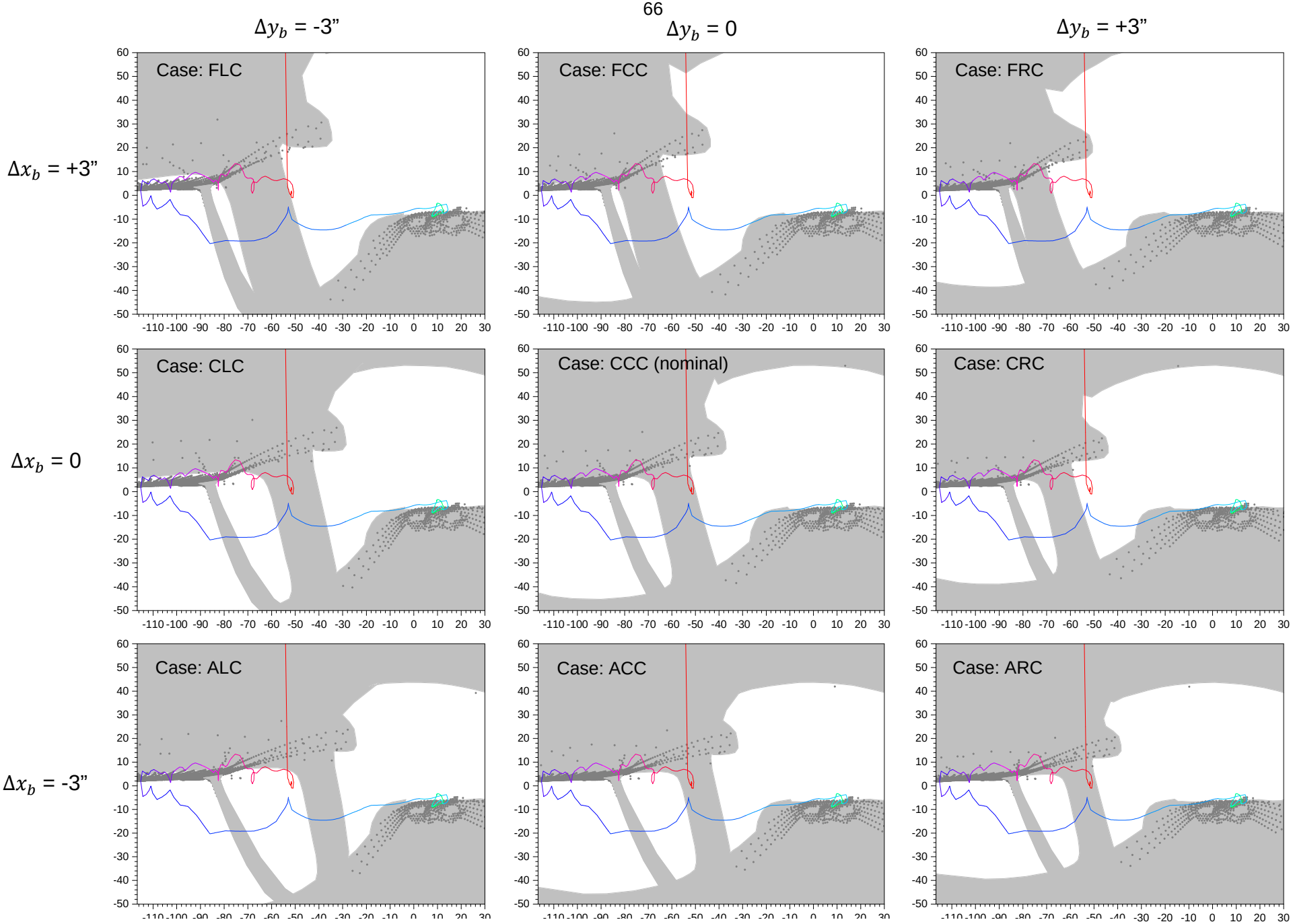

Figure 24b. Viewing angles for N1285U at Δz_b = 0. Plots are elevation angle vs. azimuth angle (in degrees).

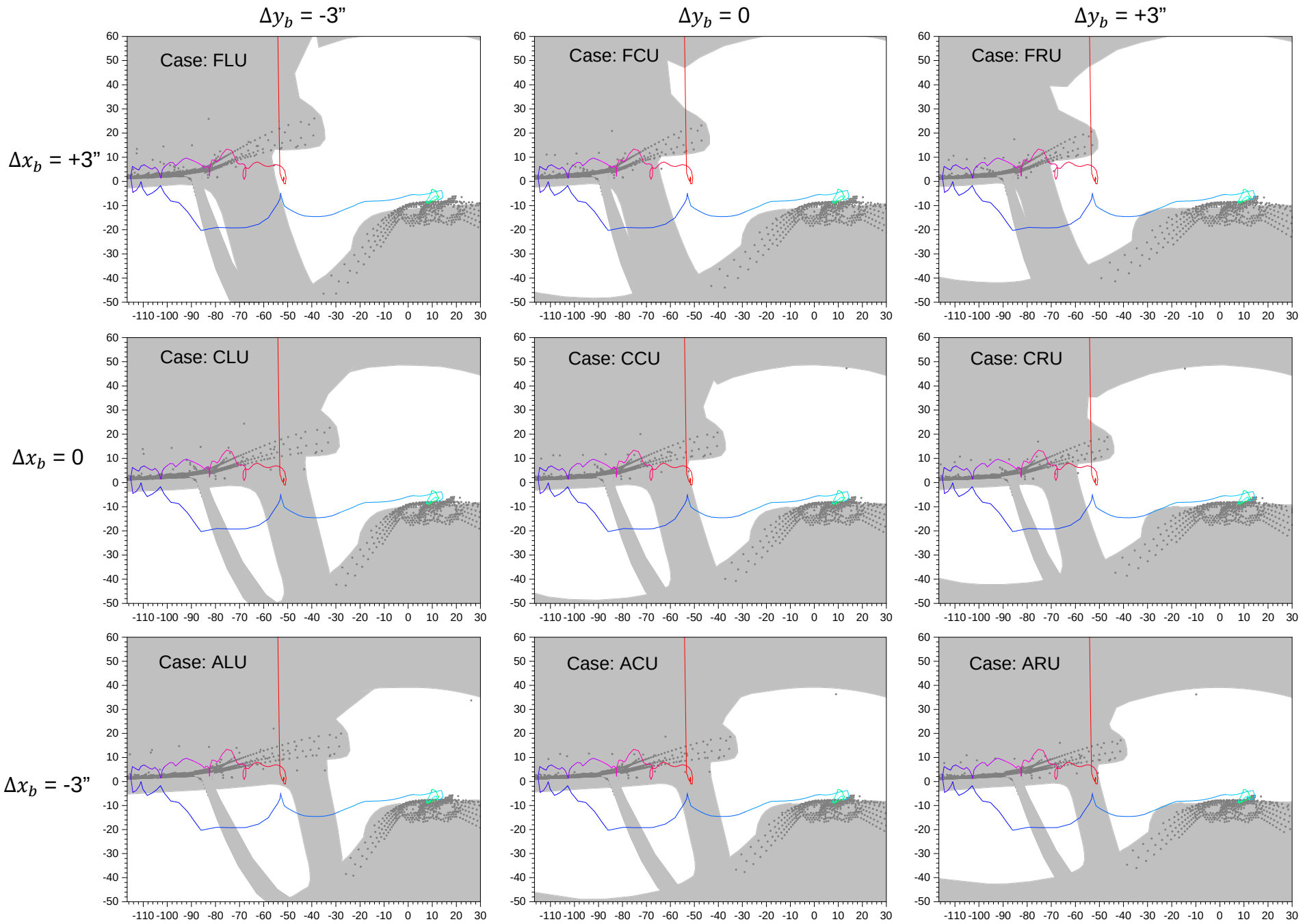

Figure 24c. Viewing angles for N1285U at Δz_b = -1.5 inches (i.e., up). Plots are elevation angle vs. azimuth angle (in degrees).

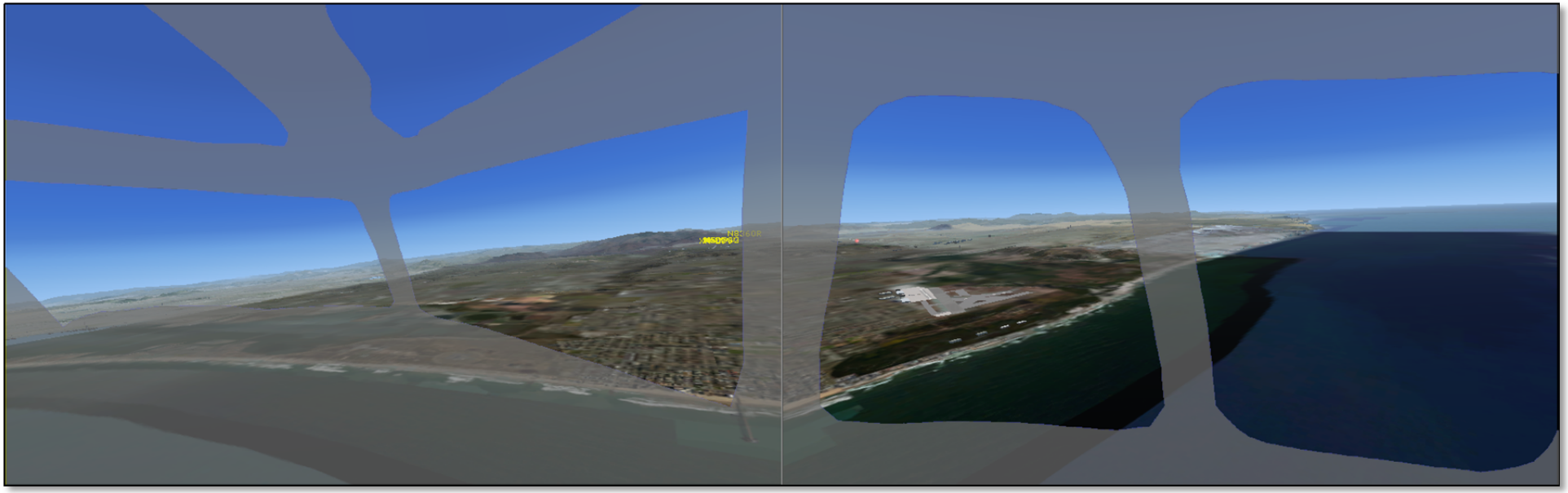

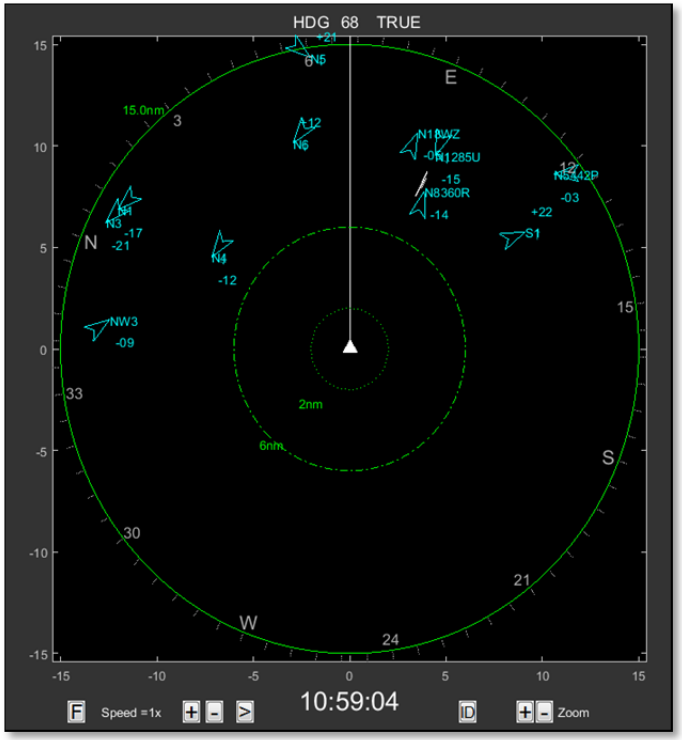

10:59:04 PDT
(04:06.2 min:sec before collision)

[EAGLE1] brown tower eagle1 9 west inbound bravo full stop

Events in *italics* are ATC communications; others are EAGLE1 CVR events

Figure 25a.

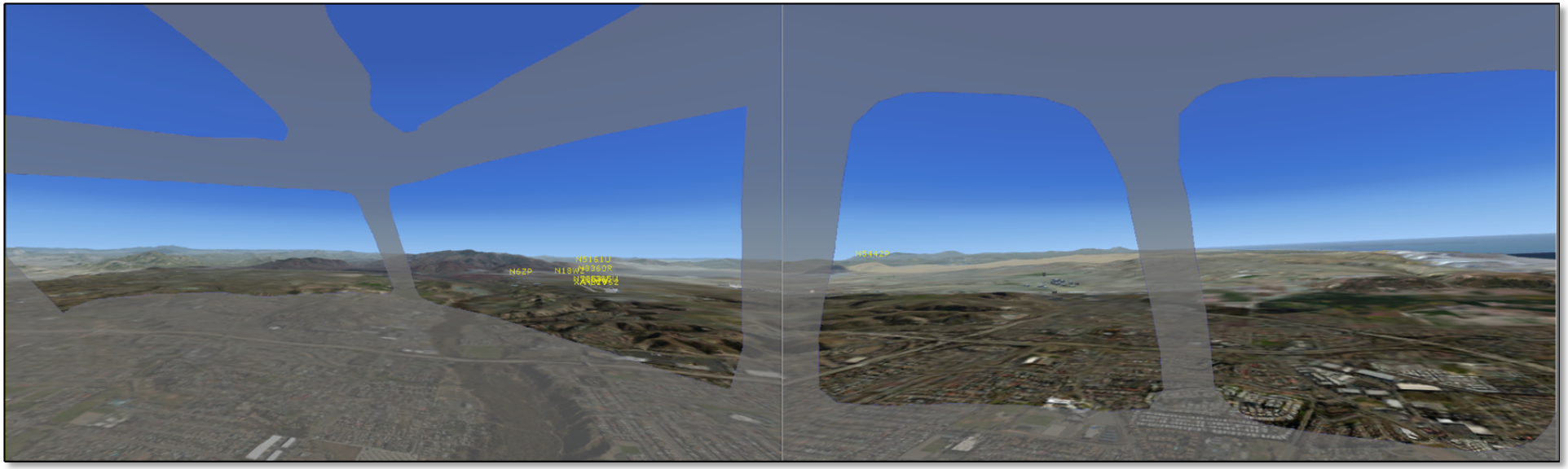

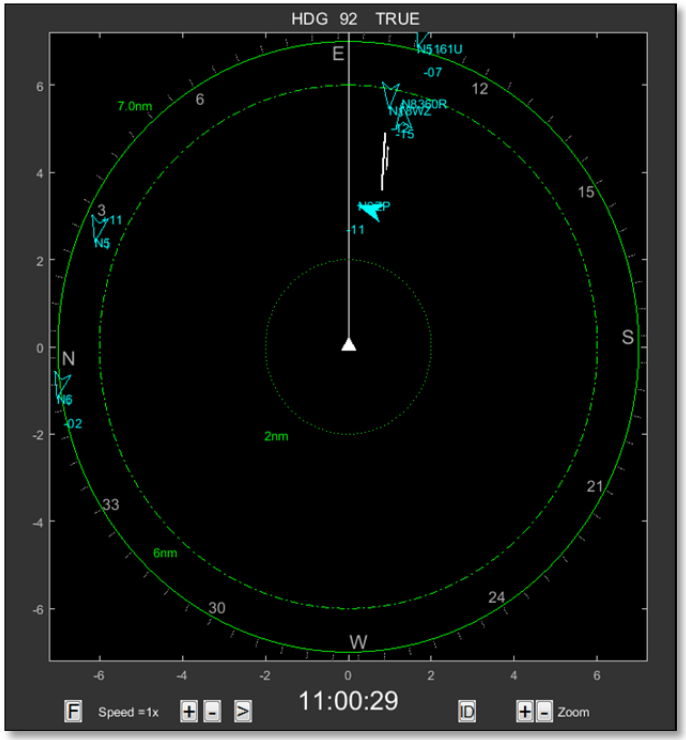

11:00:29 PDT
(02:41.2 min:sec before collision)

[HOT-2] got one on short final.

Events in *italics* are ATC communications; others are EAGLE1 CVR events

Figure 25b.

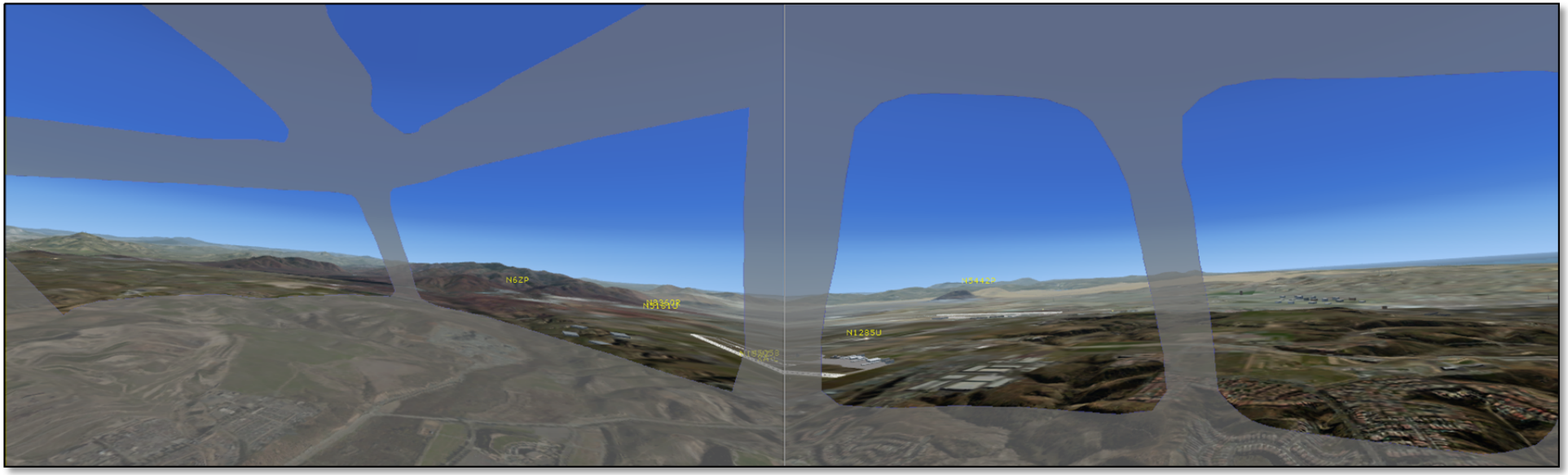

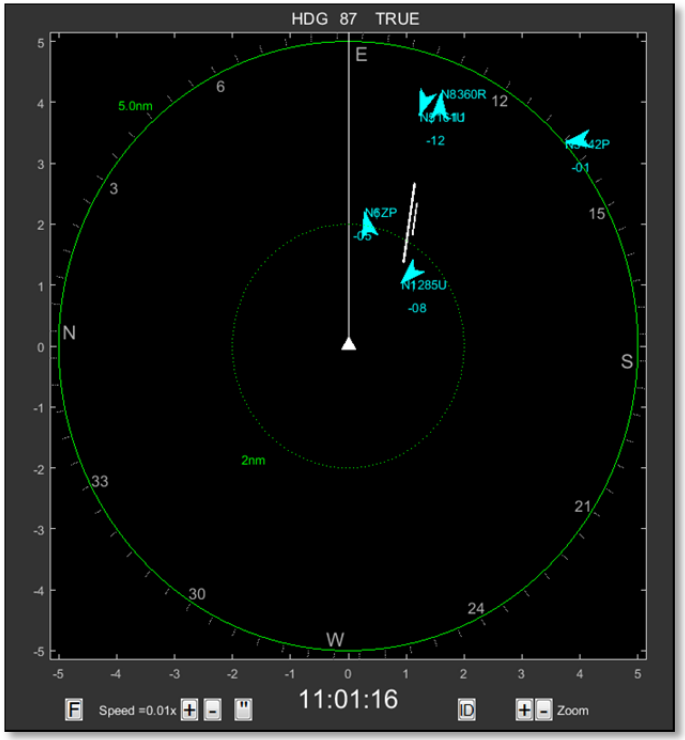

11:01:15.5 PDT
(01:54.7 min:sec before collision)

[HOT-2] got one on the runway.

Events in *italics* are ATC communications; others are EAGLE1 CVR events

Figure 25c.

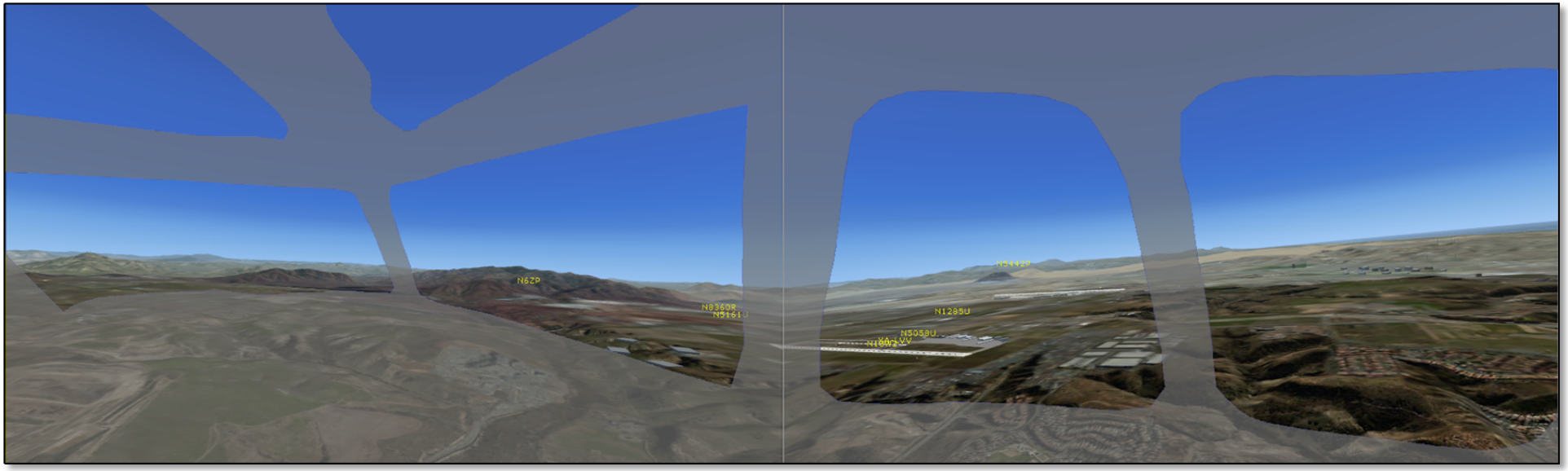

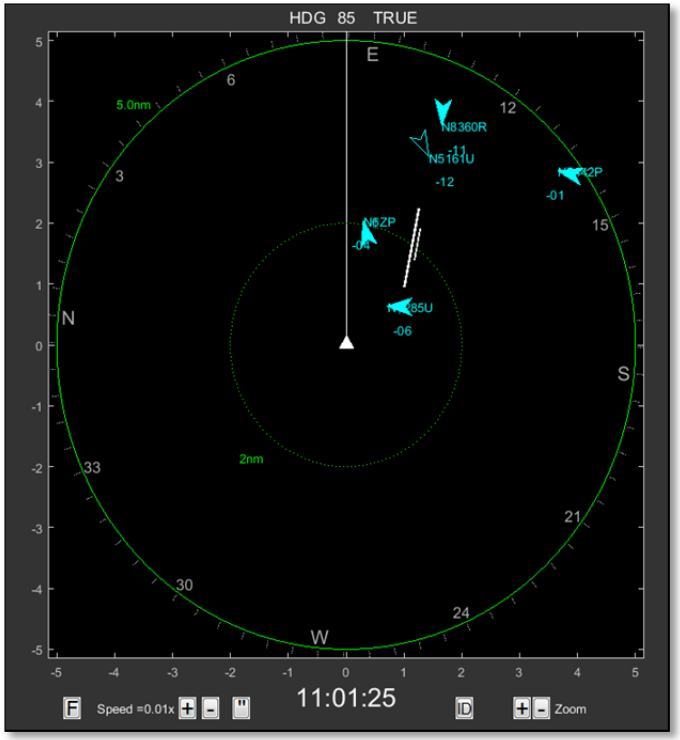

11:01:24.6 PDT
(01:45.6 min:sec before collision)

[HOT-1] I got twelve o'clock on a climb out.

Events in *italics* are ATC communications; others are EAGLE1 CVR events

Figure 25d.

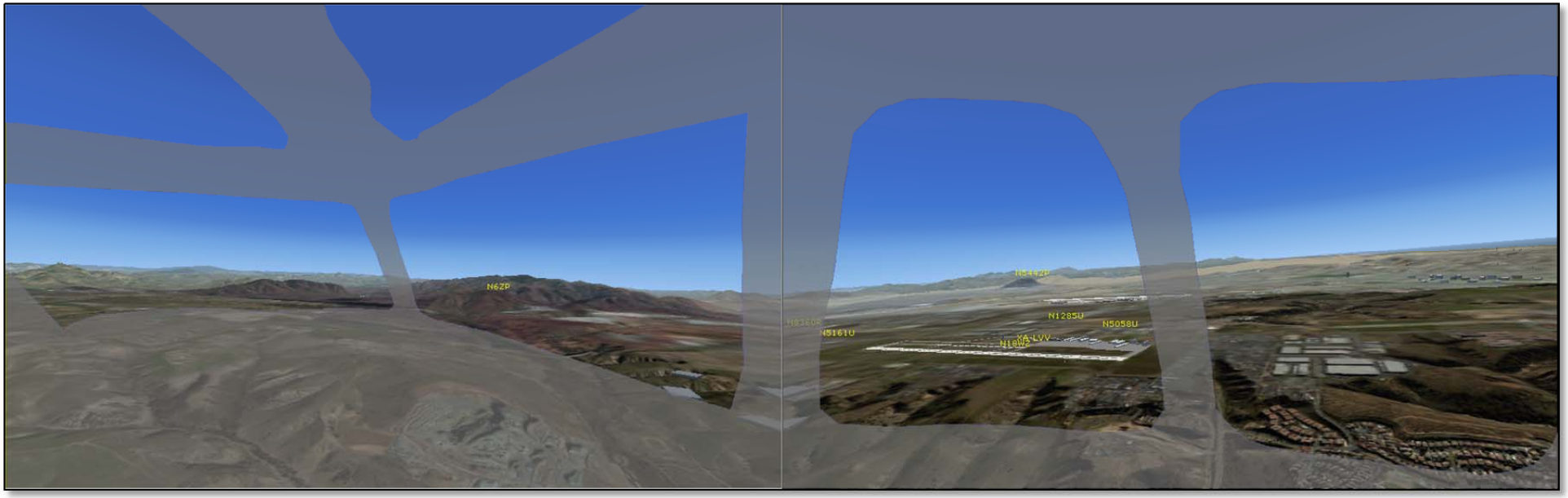

11:01:38 PDT
(01:32.2 min:sec before collision)

ATAS aural alert: "*Traffic, 2 o'clock, low, less than 1 mile, climbing.*"

Events in *italics* are ATC communications; others are EAGLE1 CVR events

Figure 25e.

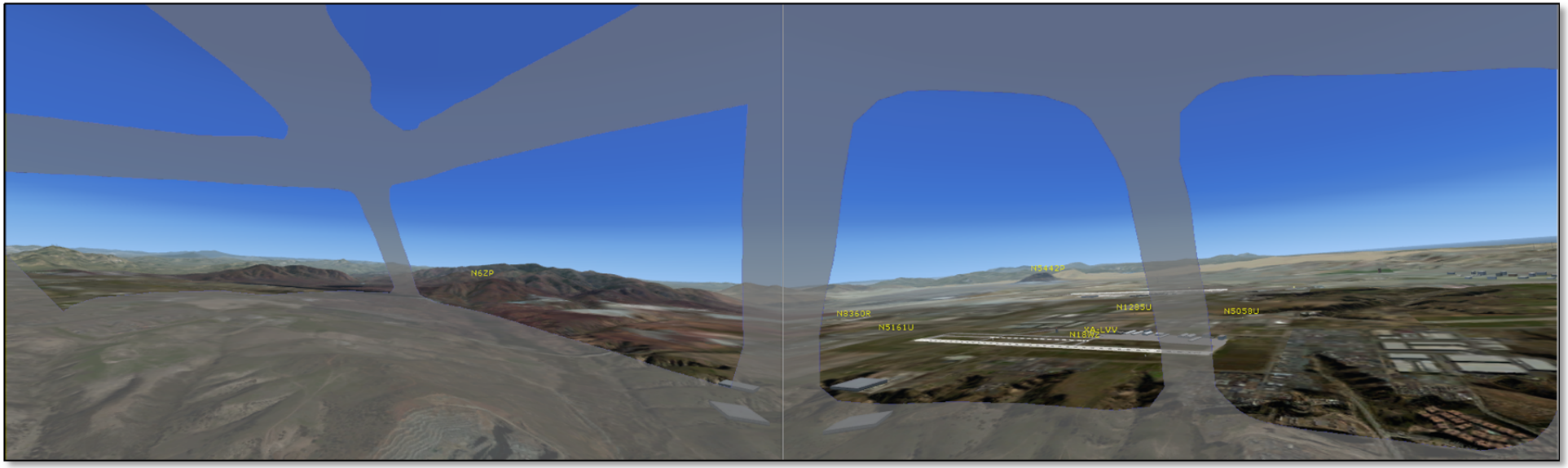

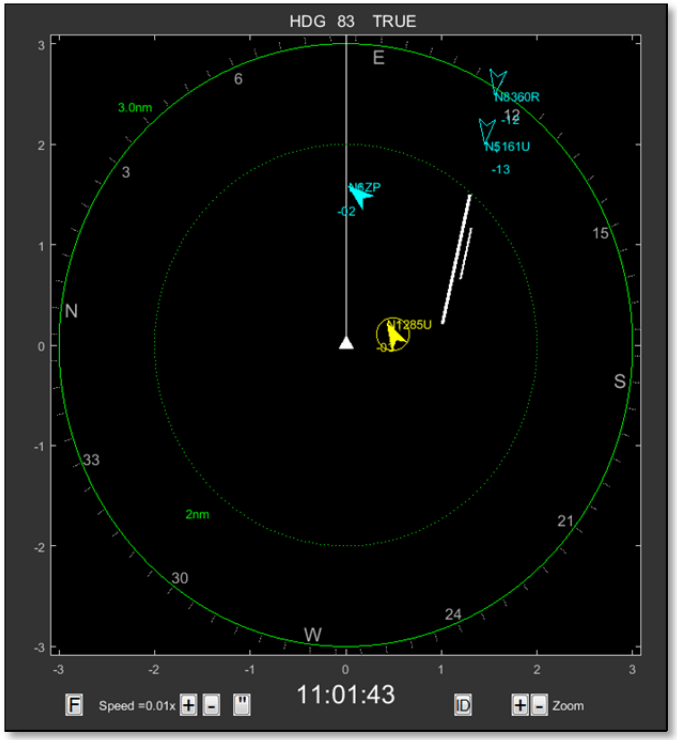

11:01:43.1 PDT
(01:27.1 min:sec before collision)

[HOT-2] (must be) the jump plane.

Events in *italics* are ATC communications; others are EAGLE1 CVR events

Figure 25f.

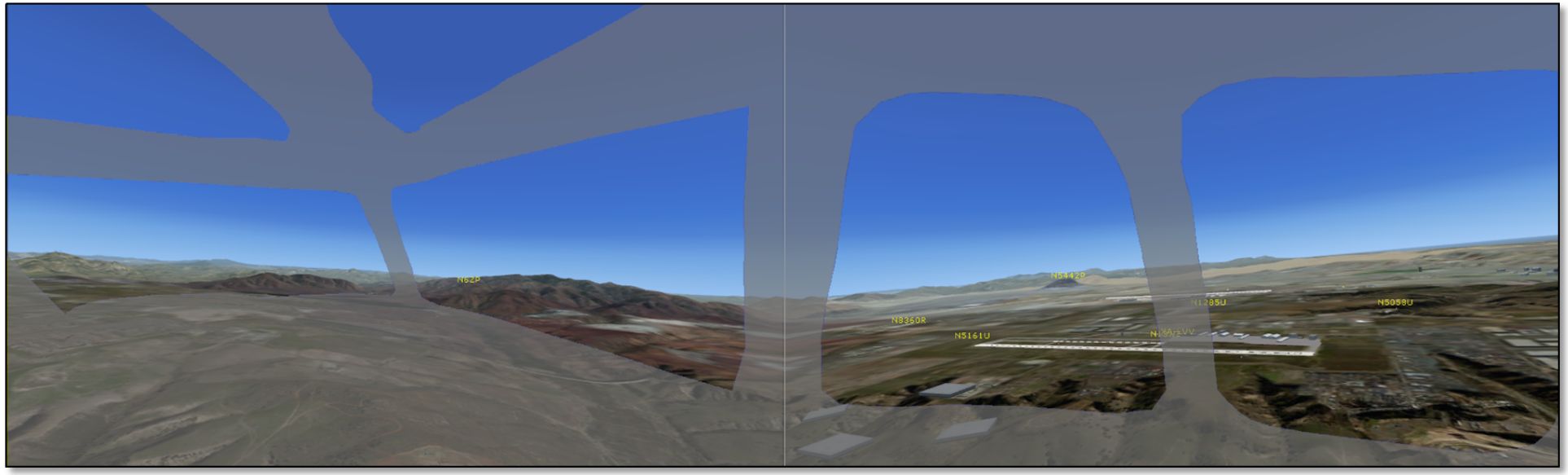

11:01:49 PDT
(01:21.2 min:sec before collision)

[HOT-3] see him right there?

Events in *italics* are ATC communications; others are EAGLE1 CVR events

Figure 25g.

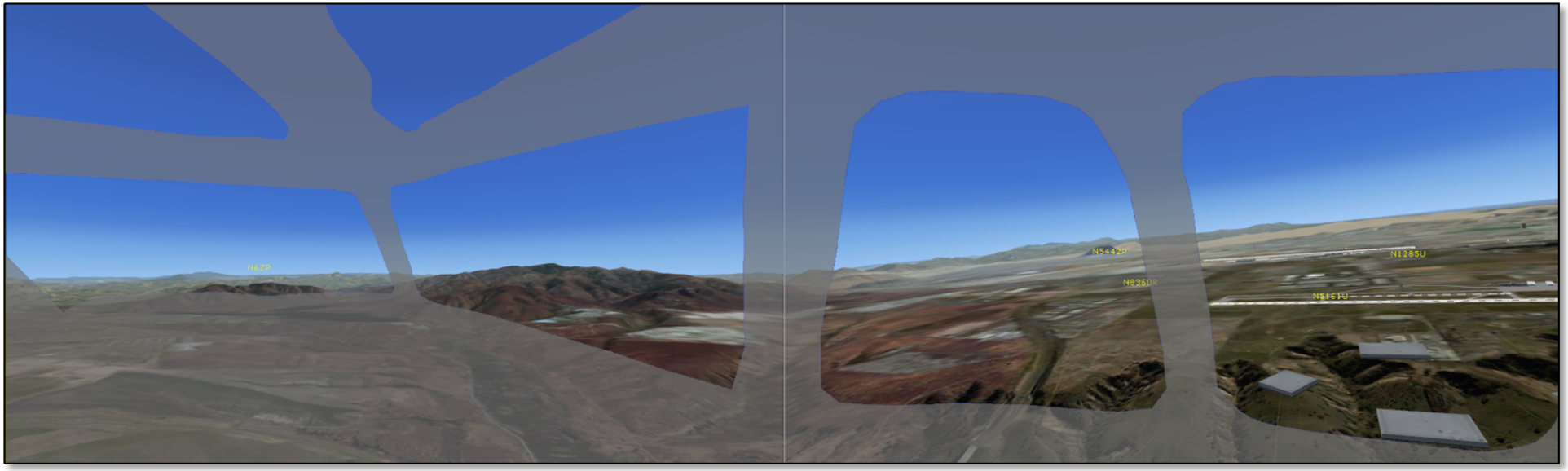

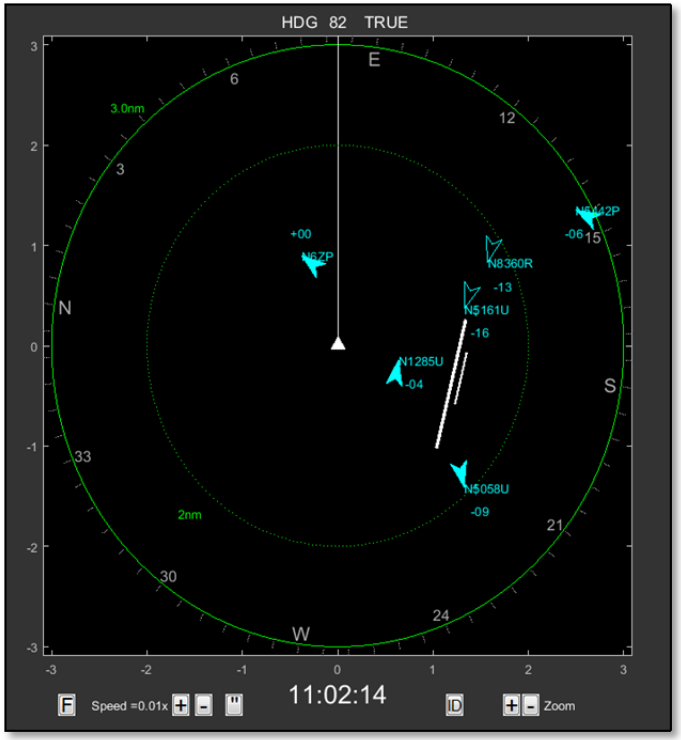

11:02:14 PDT
(00:56.2 min:sec before collision)

[EAGLE1] eagle 1 is right downwind abeam traffic to the left and right in sight

Events in *italics* are ATC communications; others are EAGLE1 CVR events

Figure 25h.

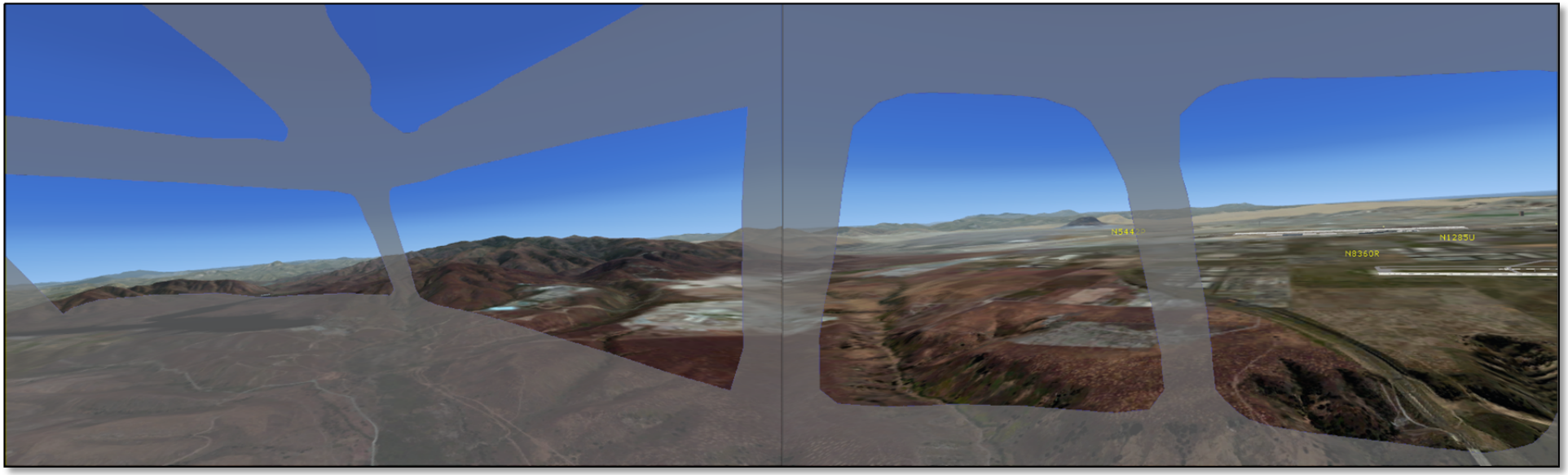

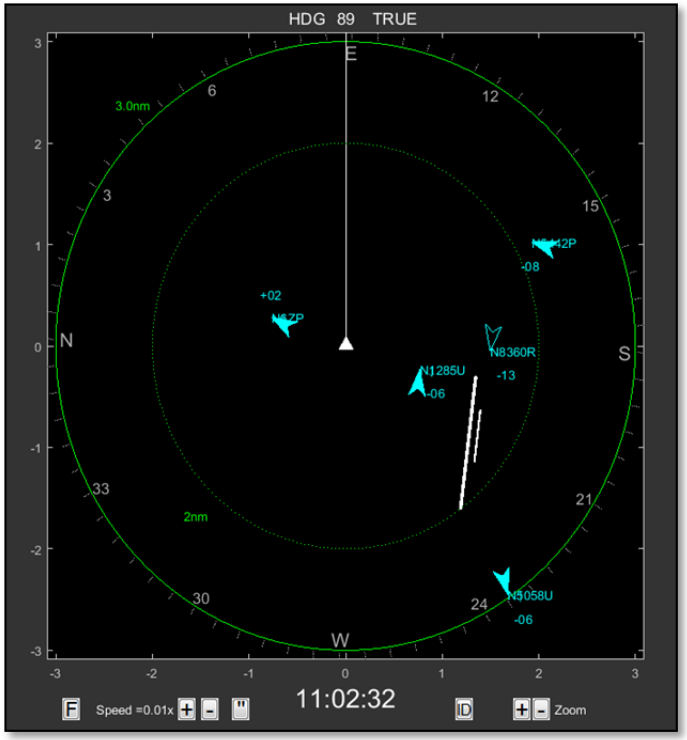

11:02:32.4 PDT
(00:37.8 min:sec before collision)

[TWR (@11:02:32.0)] cessna 6ZP make a right 360 right 360 rejoin the downwind

[HOT-1] you still got the guy on the right side?

Events in *italics* are ATC communications; others are EAGLE1 CVR events

Figure 25i.

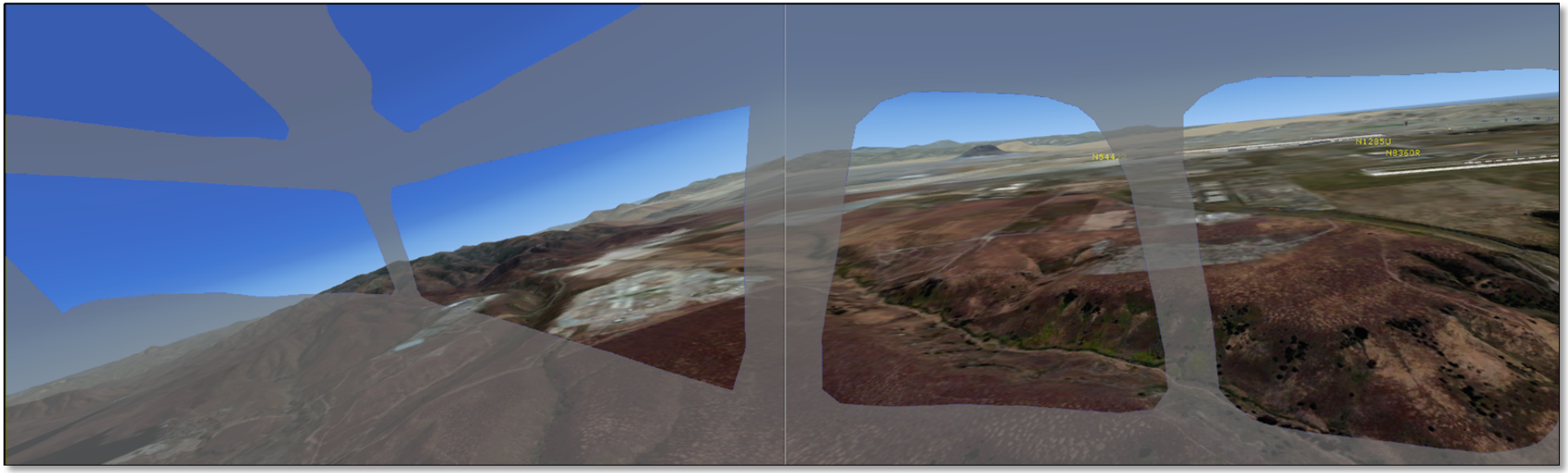

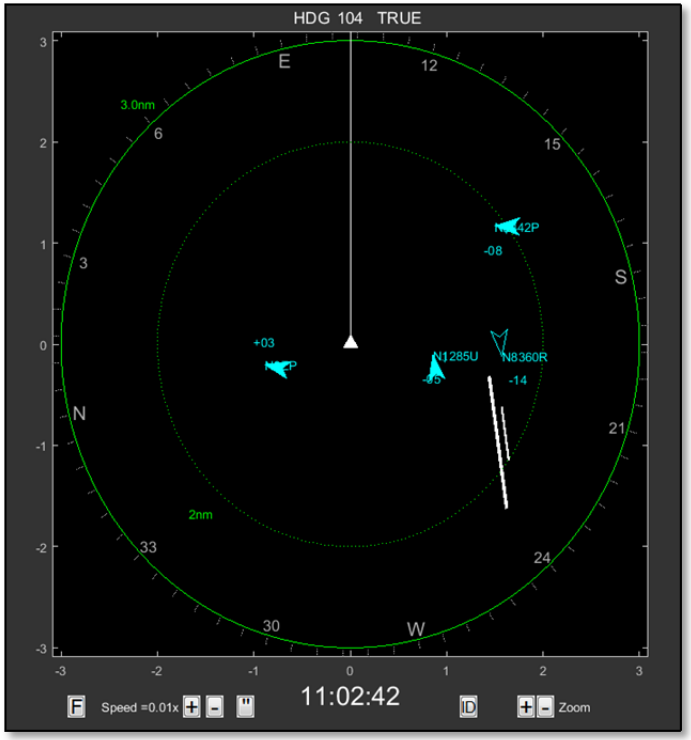

11:02:42 PDT
(00:28.2 min:sec before collision)

[TWR] eagle1 turn base 26R clear to land

Events in *italics* are ATC communications; others are EAGLE1 CVR events

Figure 25j.

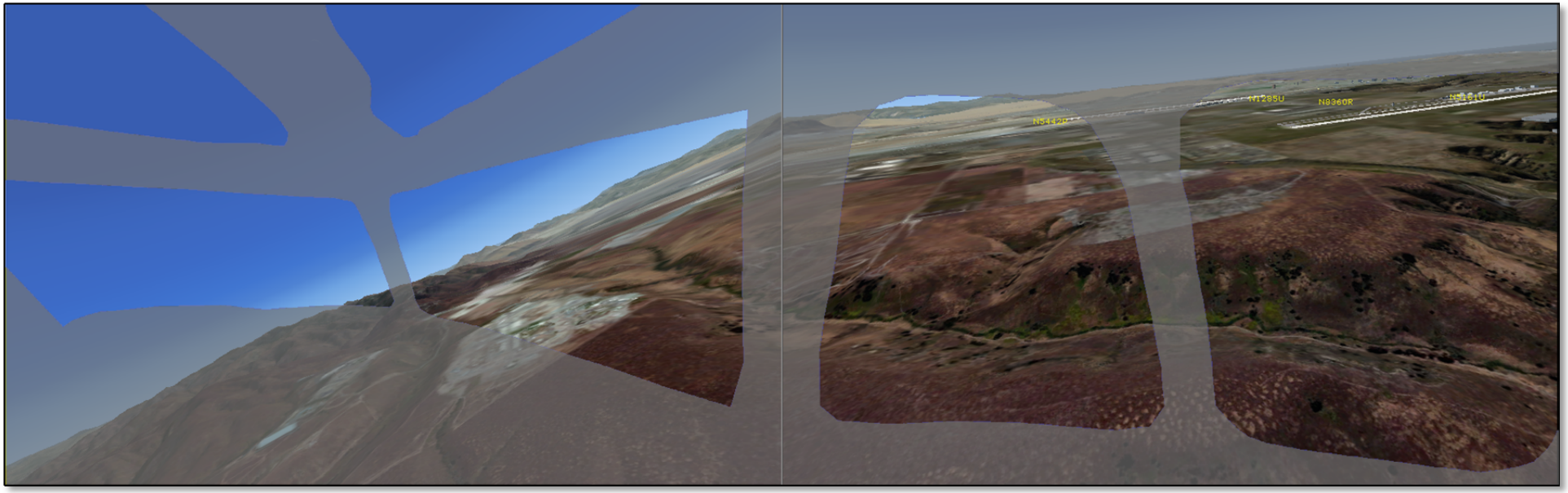

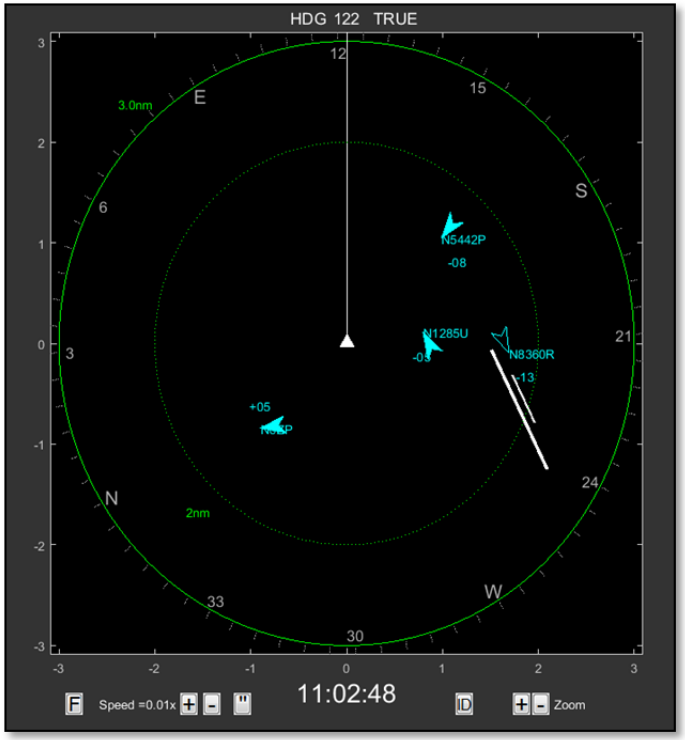

11:02:48 PDT
(00:22.2 min:sec before collision)

[N1285U would have received an ATAS aural alert concerning N5442P, if the airplane had been ATAS equipped; see Figure 26k]

Events in *italics* are ATC communications; others are EAGLE1 CVR events

Figure 25k.

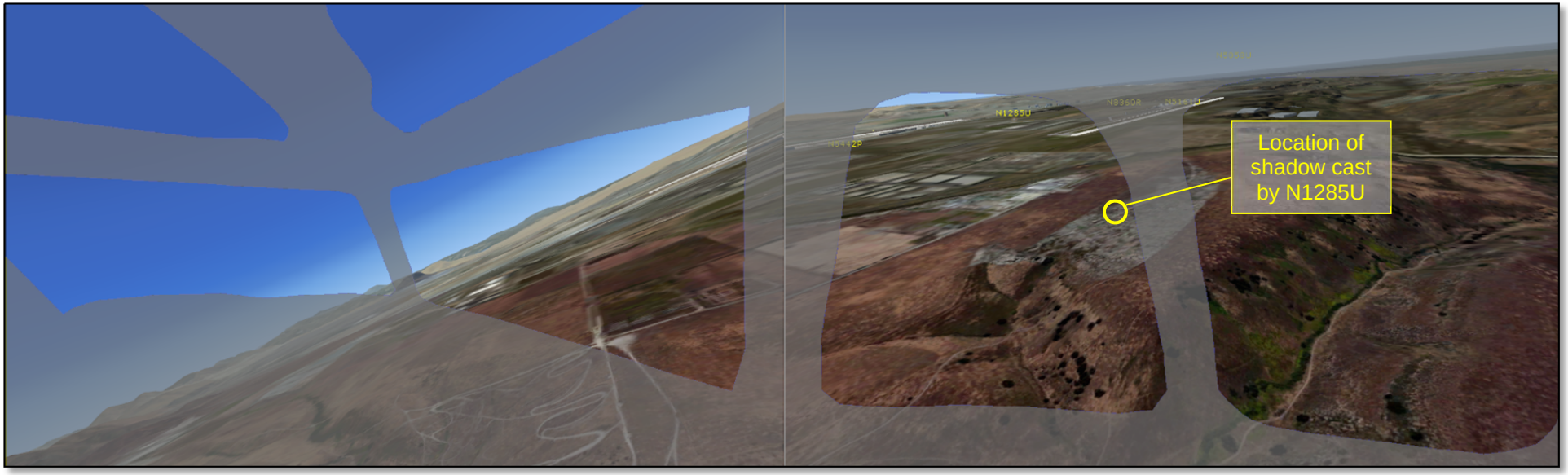

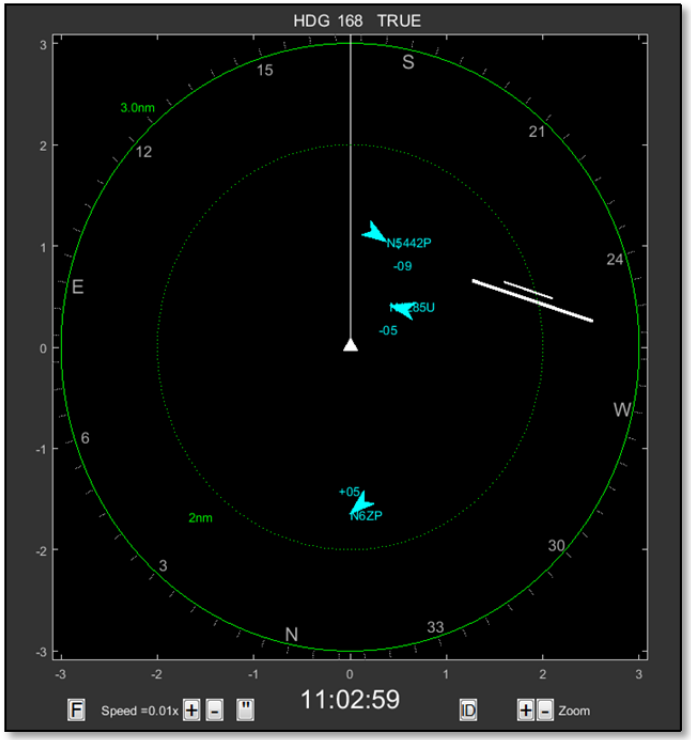

11:02:59.3 PDT
(00:10.9 min:sec before collision)

[HOT-1] I see the shadow but I don't see him.

Events in *italics* are ATC communications; others are EAGLE1 CVR events

Figure 25l.

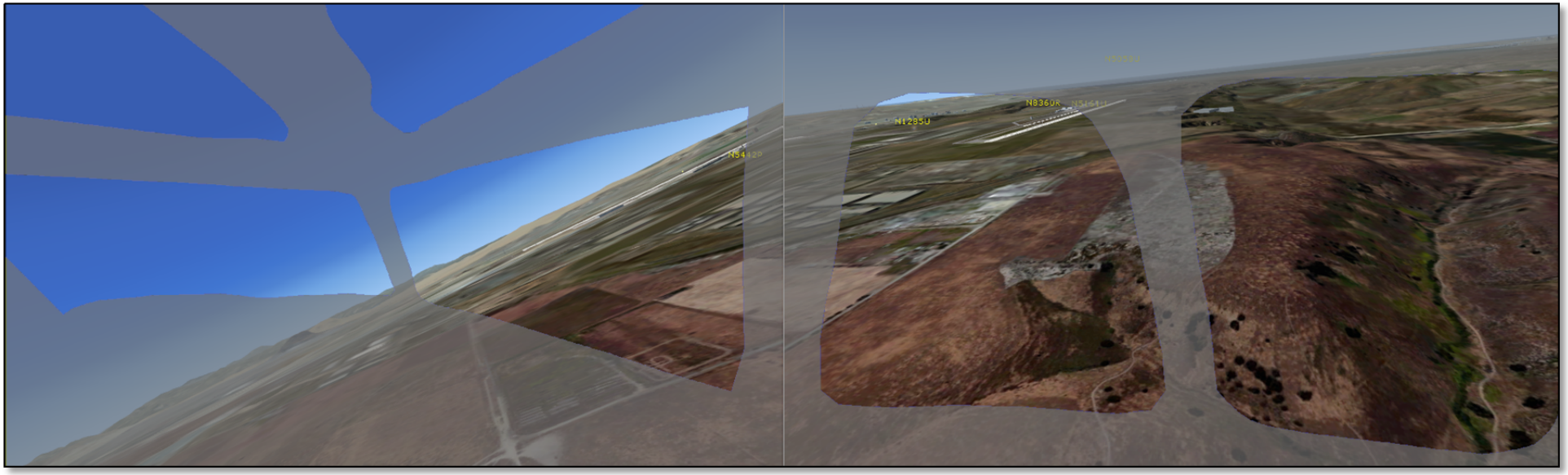

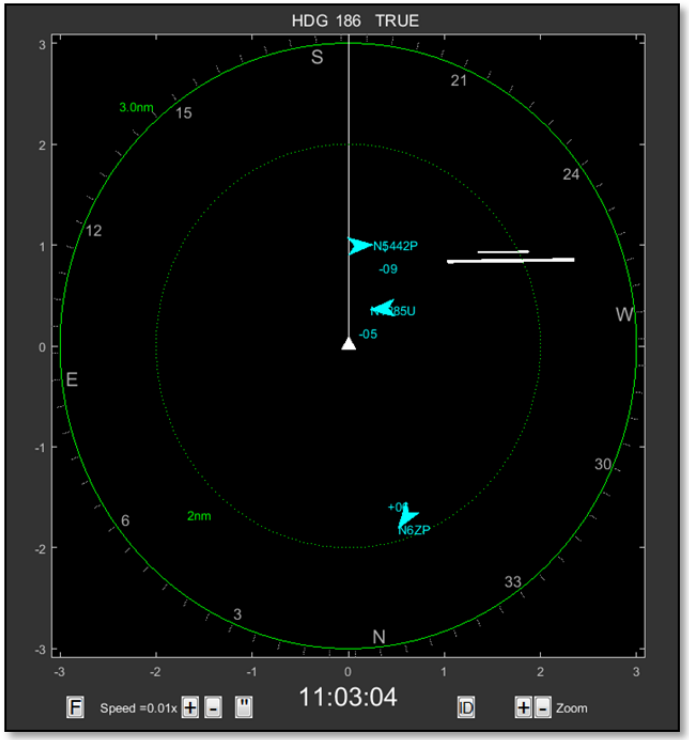

11:03:04 PDT
(00:06.2 min:sec before collision)

[TWR] N85U tower

Events in *italics* are ATC communications; others are EAGLE1 CVR events

Figure 25m.

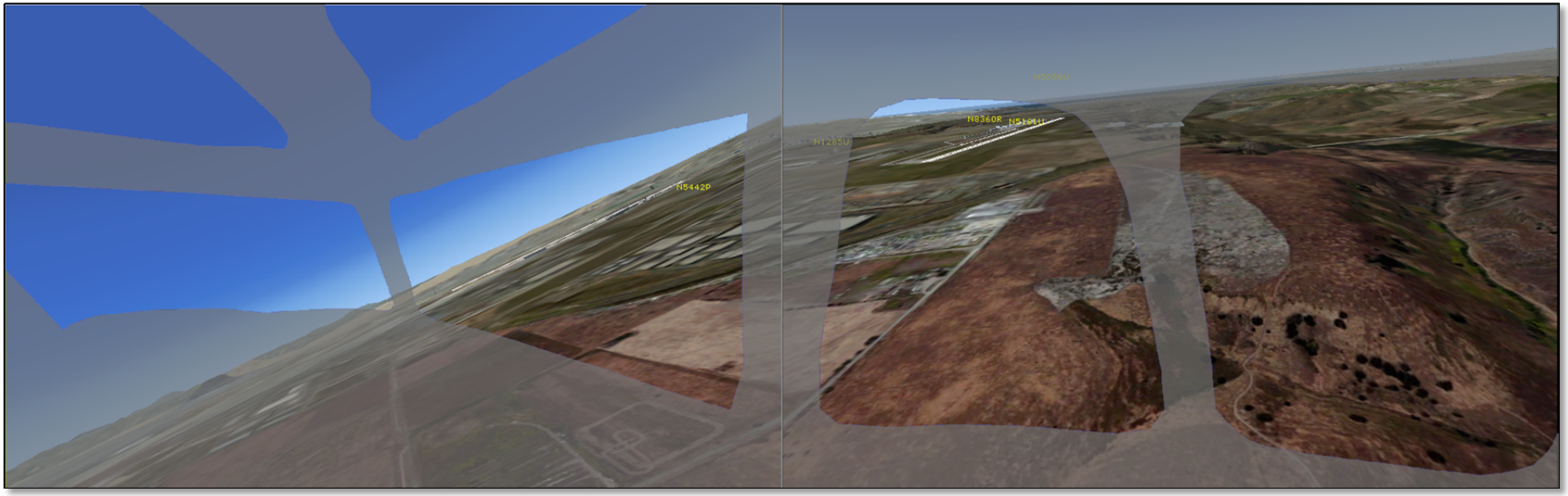

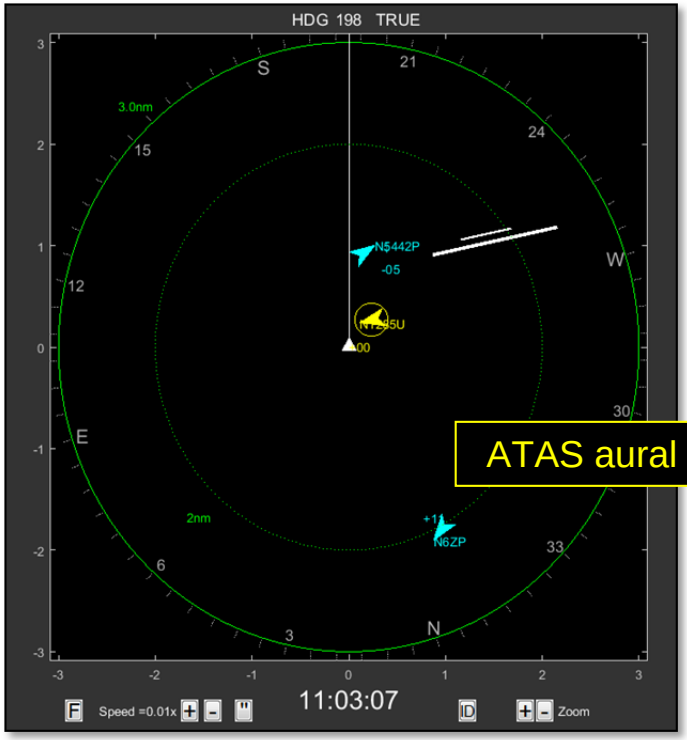

11:03:07 PDT
(00:03.2 min:sec before collision)

ATAS aural alert: "*Traffic, 1 o'clock, same altitude, zero miles*"

Events in *italics* are ATC communications; others are EAGLE1 CVR events

Figure 25n.

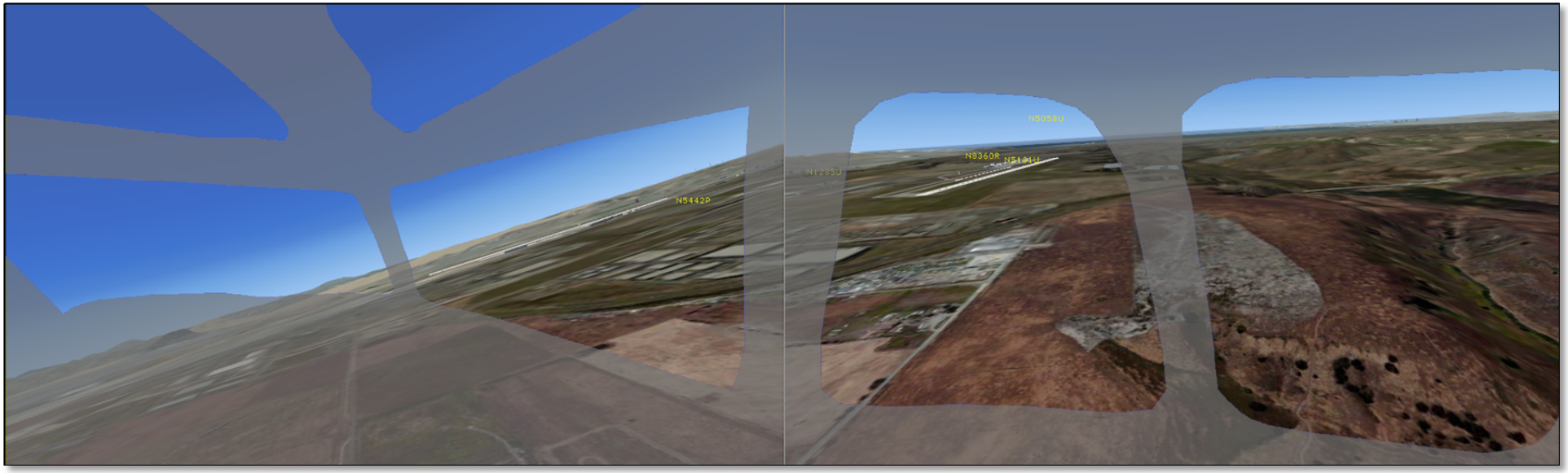

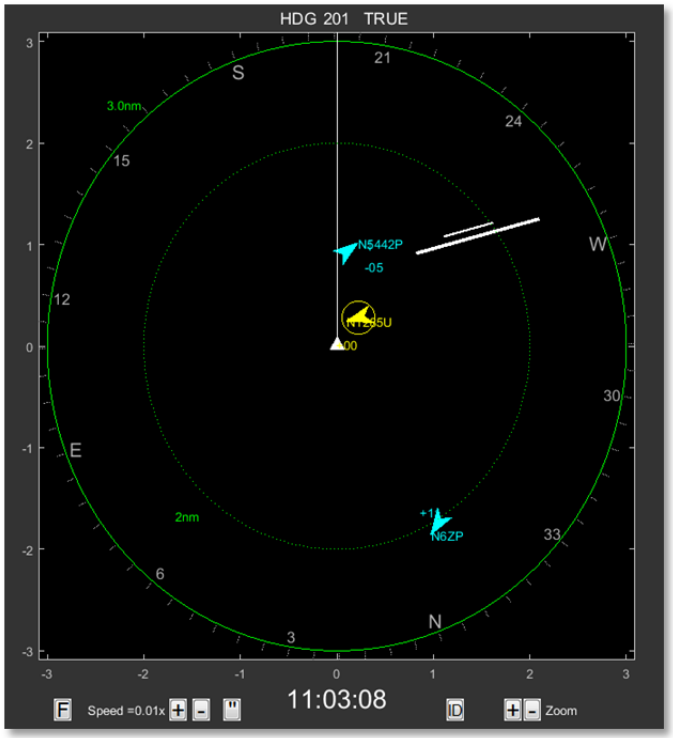

11:03:08 PDT
(00:02.2 min:sec before collision)

[TWR] are you still on downwind sir right downwind

Events in *italics* are ATC communications; others are EAGLE1 CVR events

Figure 25o.

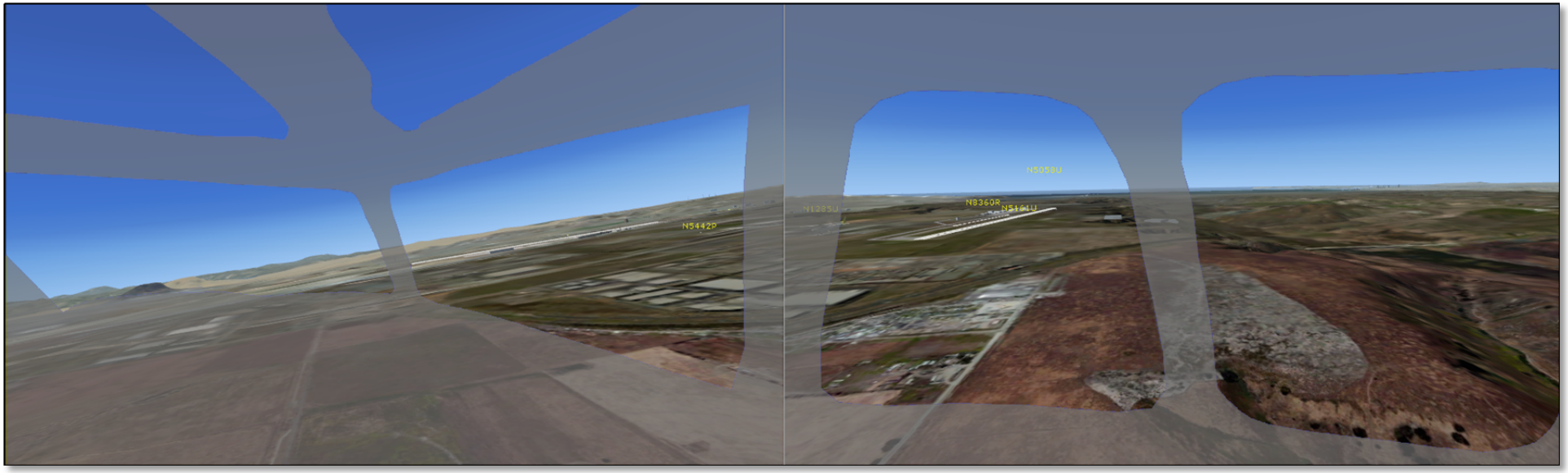

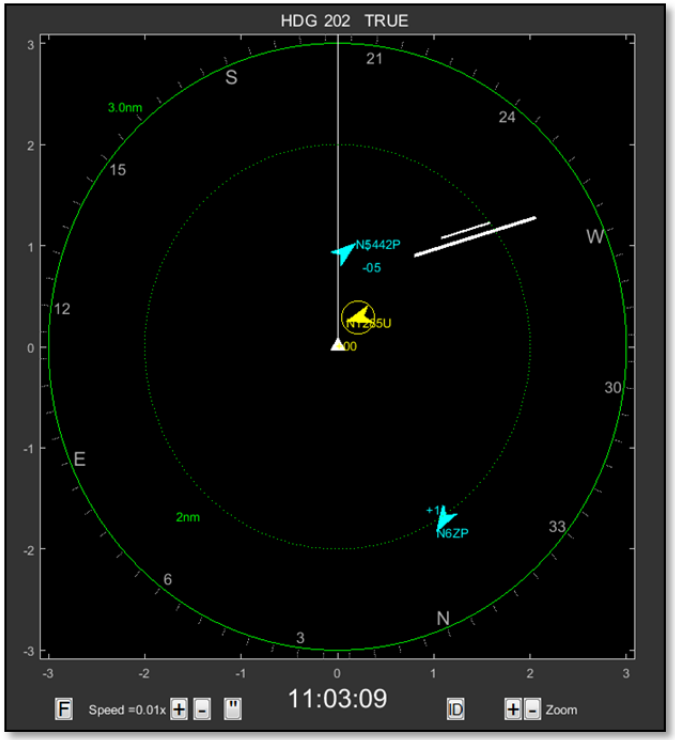

11:03:09 PDT
(00:01.2 min:sec before collision)

Figure 25p.

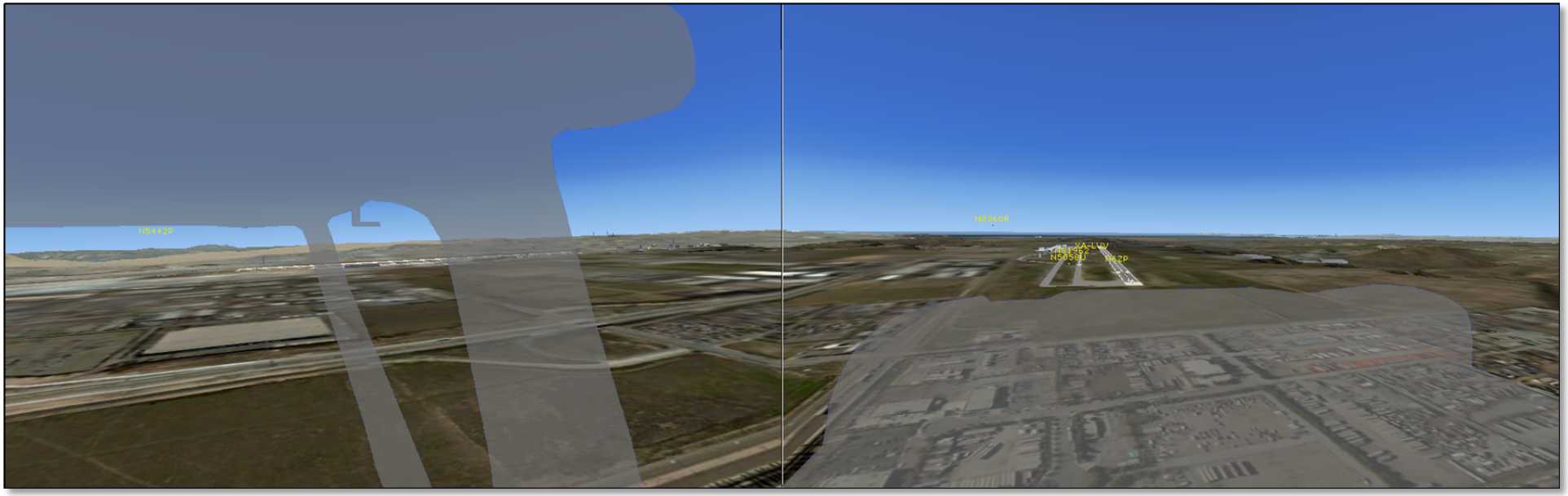

10:59:04 PDT
(04:06.2 min:sec before collision)

[EAGLE1] brown tower eagle1 9 west inbound bravo full stop

Events in *italics* are ATC communications; others are EAGLE1 CVR events

Figure 26a.

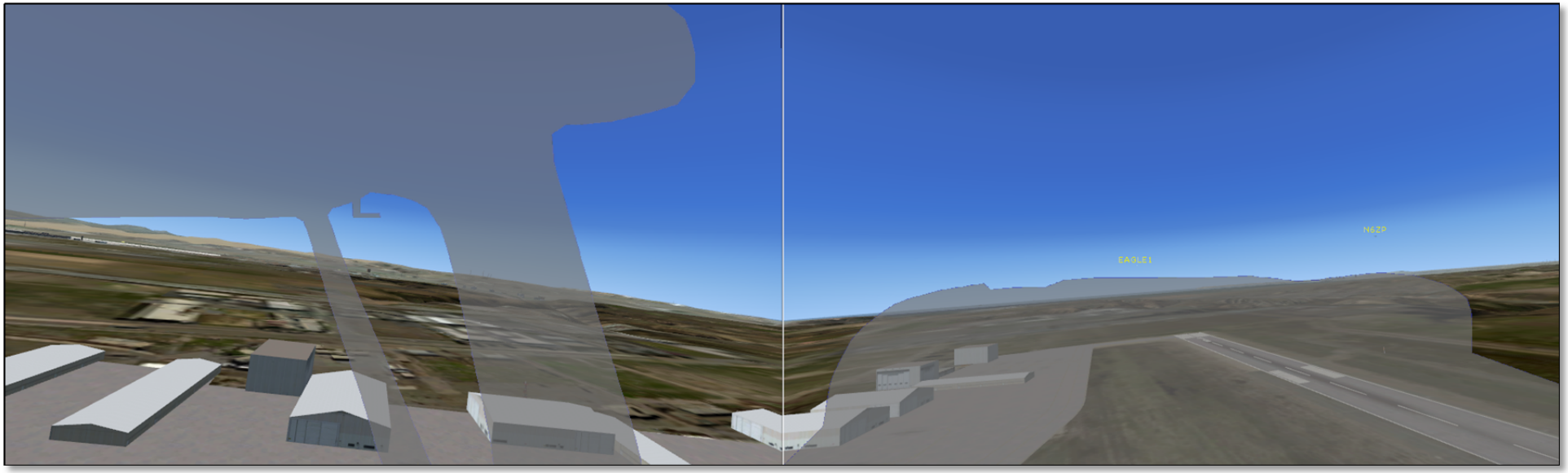

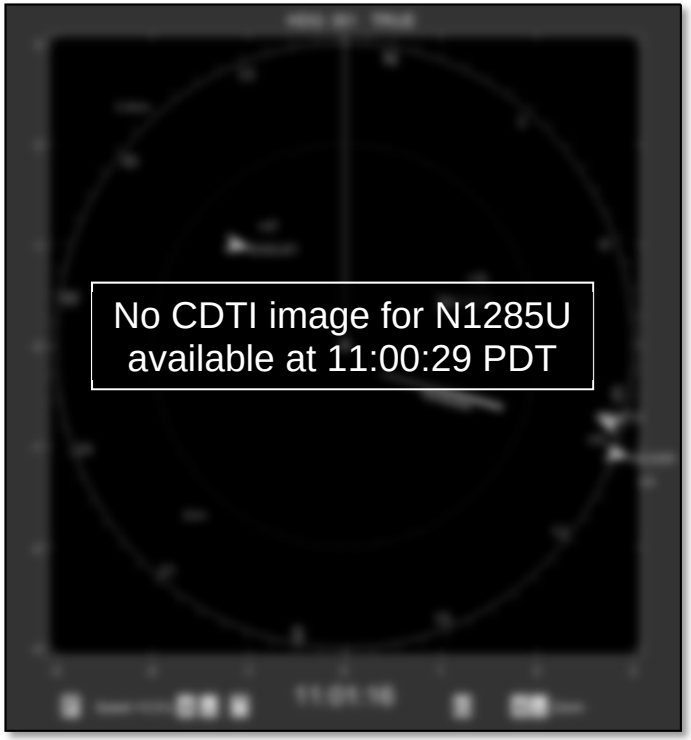

11:00:29 PDT
(02:41.2 min:sec before collision)

[HOT-2] got one on short final.

Events in *italics* are ATC communications; others are EAGLE1 CVR events

Figure 26b.

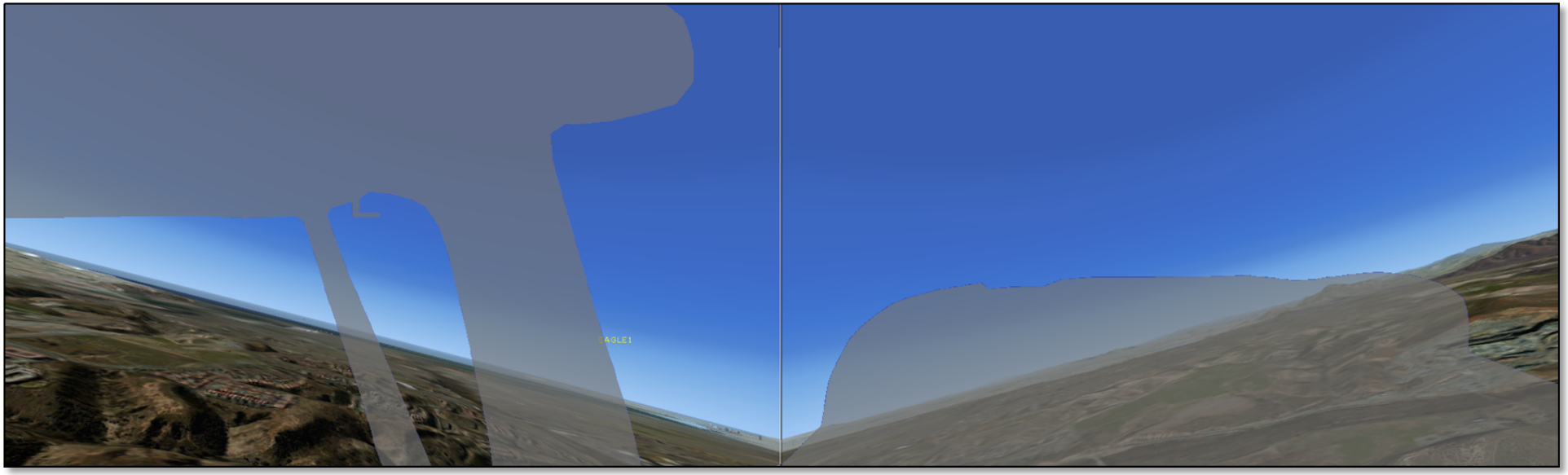

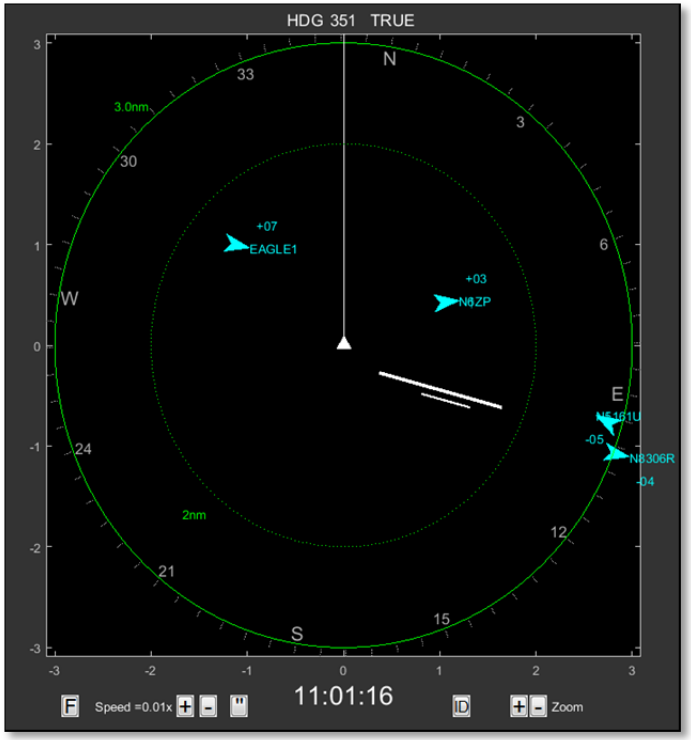

11:01:15.5 PDT
(01:54.7 min:sec before collision)

[HOT-2] got one on the runway.

Events in *italics* are ATC communications; others are EAGLE1 CVR events

Figure 26c.

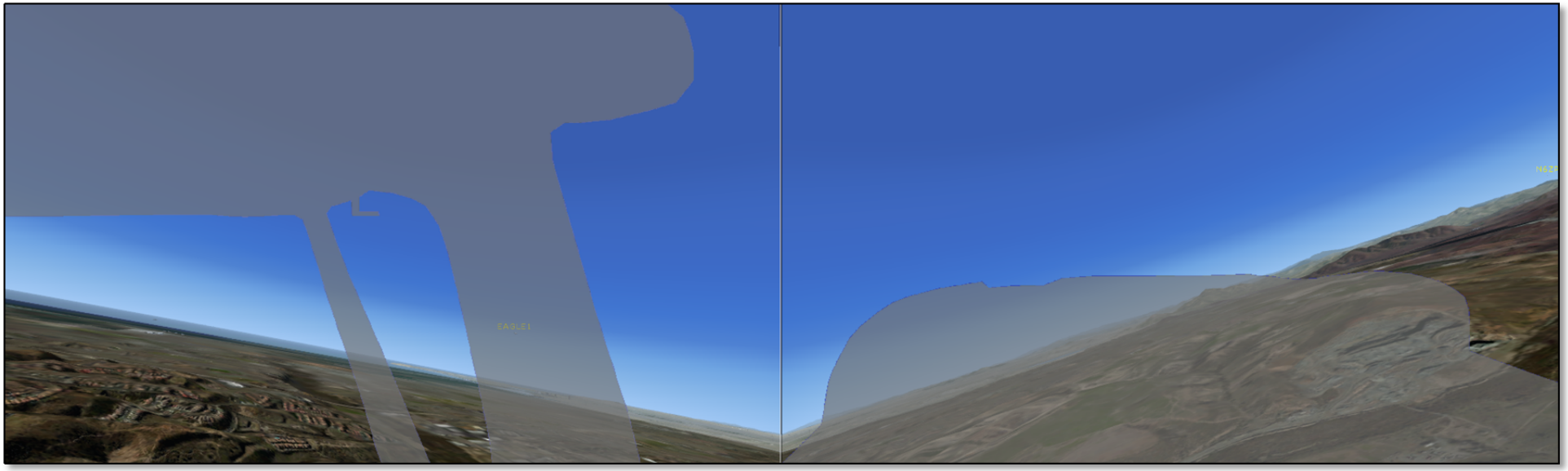

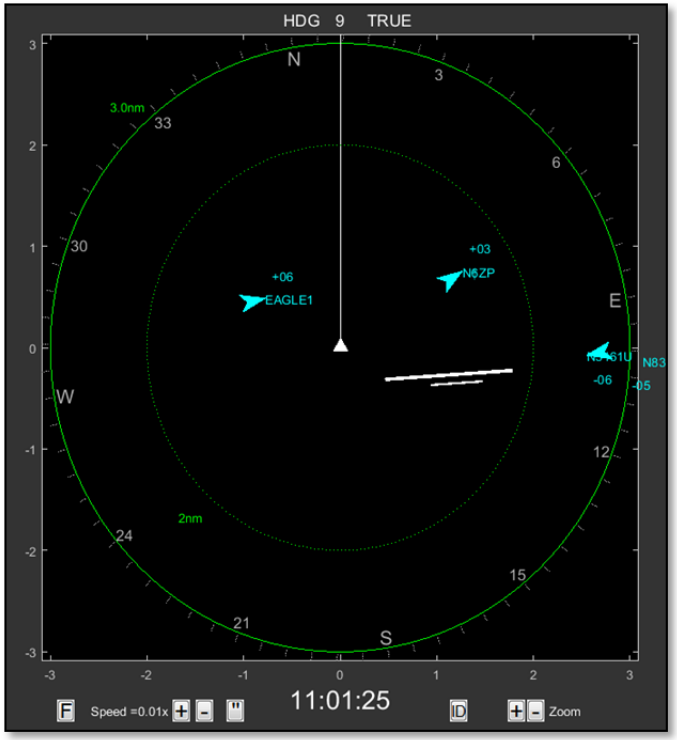

11:01:24.6 PDT
(01:45.6 min:sec before collision)

[HOT-1] I got twelve o'clock on a climb out.

Events in *italics* are ATC communications; others are EAGLE1 CVR events

Figure 26d.

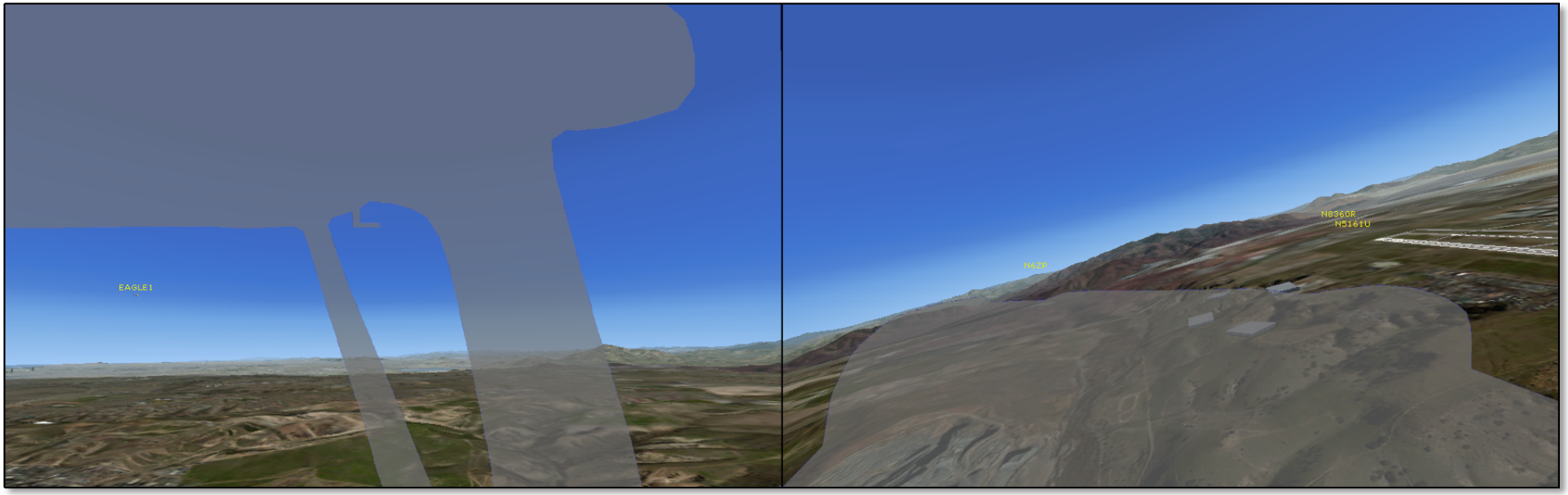

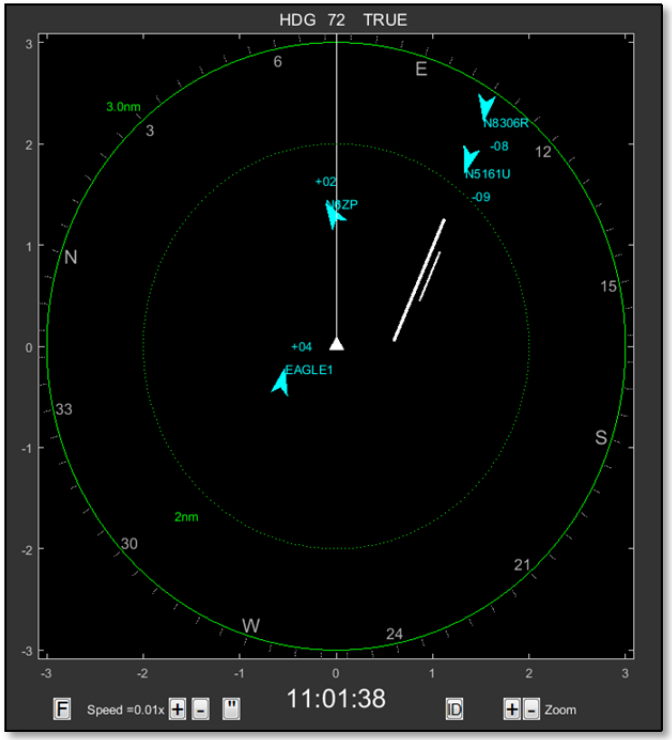

11:01:38 PDT
(01:32.2 min:sec before collision)

[EAGLE1 would have received an ATAS aural alert concerning N1285U, if the airplane had been ATAS equipped; see Figure 25e]

Events in *italics* are ATC communications; others are EAGLE1 CVR events

Figure 26e.

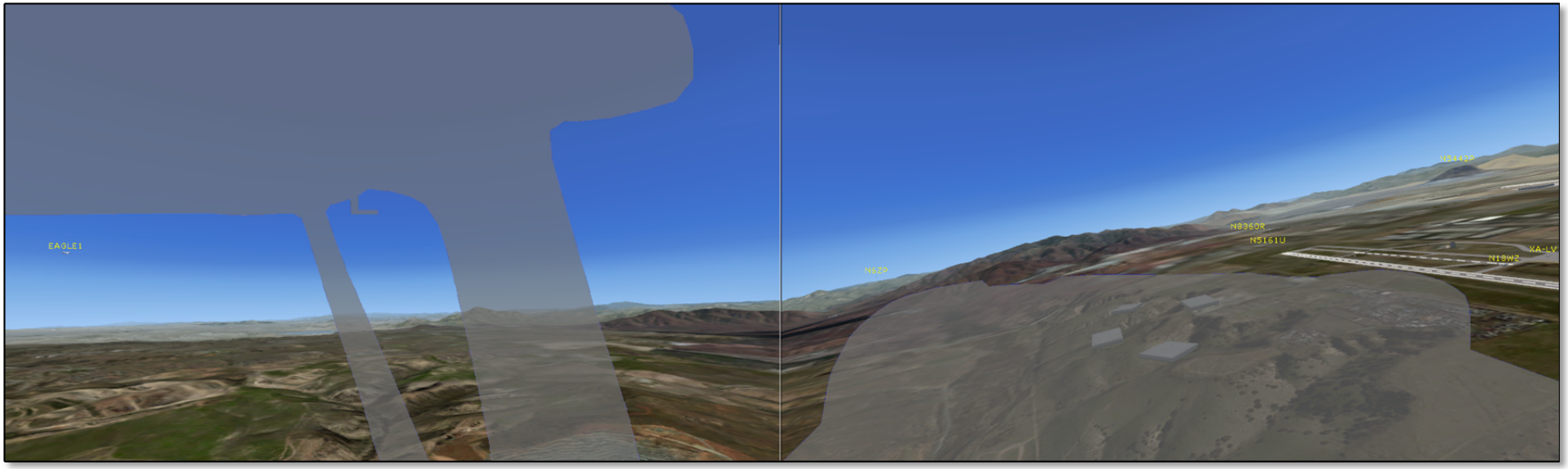

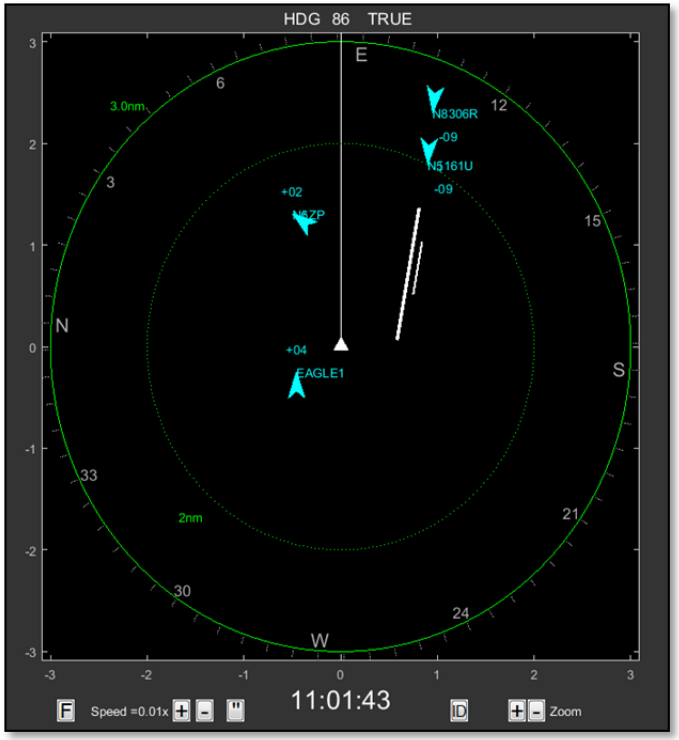

11:01:43.1 PDT
(01:27.1 min:sec before collision)

[HOT-2] (must be) the jump plane.

Events in *italics* are ATC communications; others are EAGLE1 CVR events

Figure 26f.

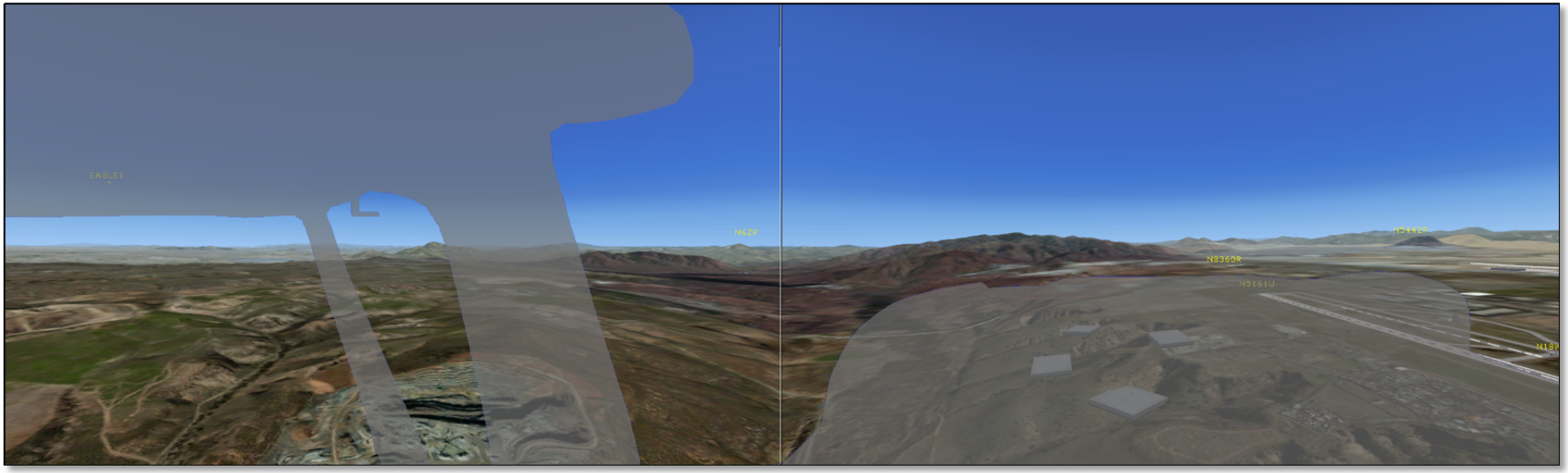

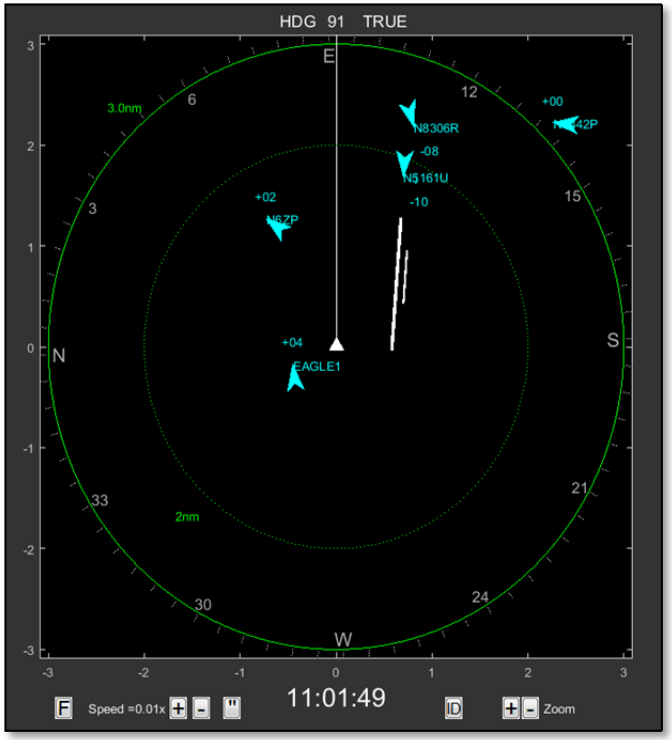

11:01:49 PDT
(01:21.2 min:sec before collision)

[HOT-3] see him right there?

Events in *italics* are ATC communications; others are EAGLE1 CVR events

Figure 26g.

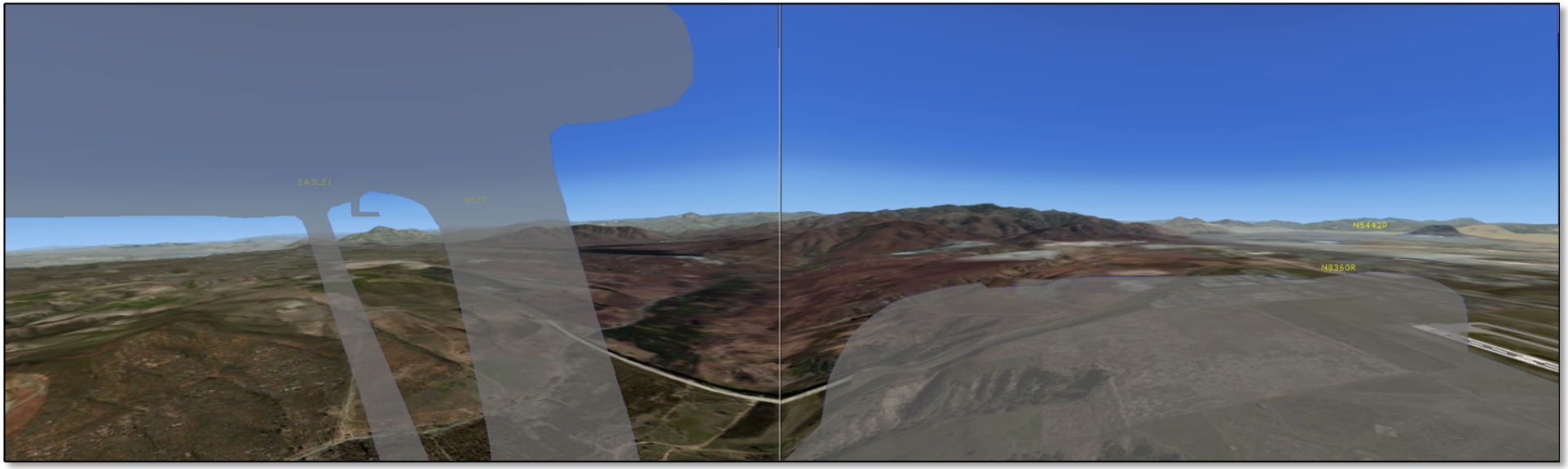

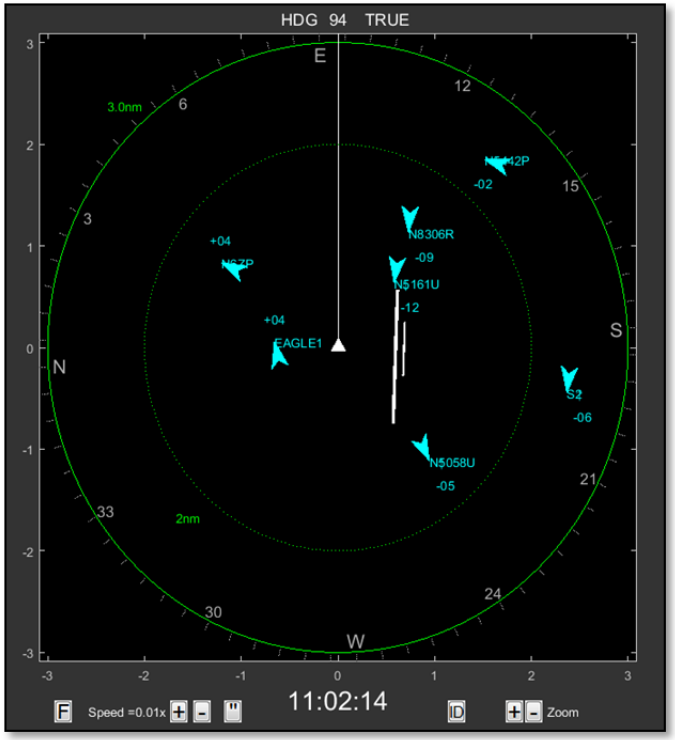

11:02:14 PDT
(00:56.2 min:sec before collision)

[EAGLE1] eagle 1 is right downwind abeam traffic to the left and right in sight

Events in *italics* are ATC communications; others are EAGLE1 CVR events

Figure 26h.

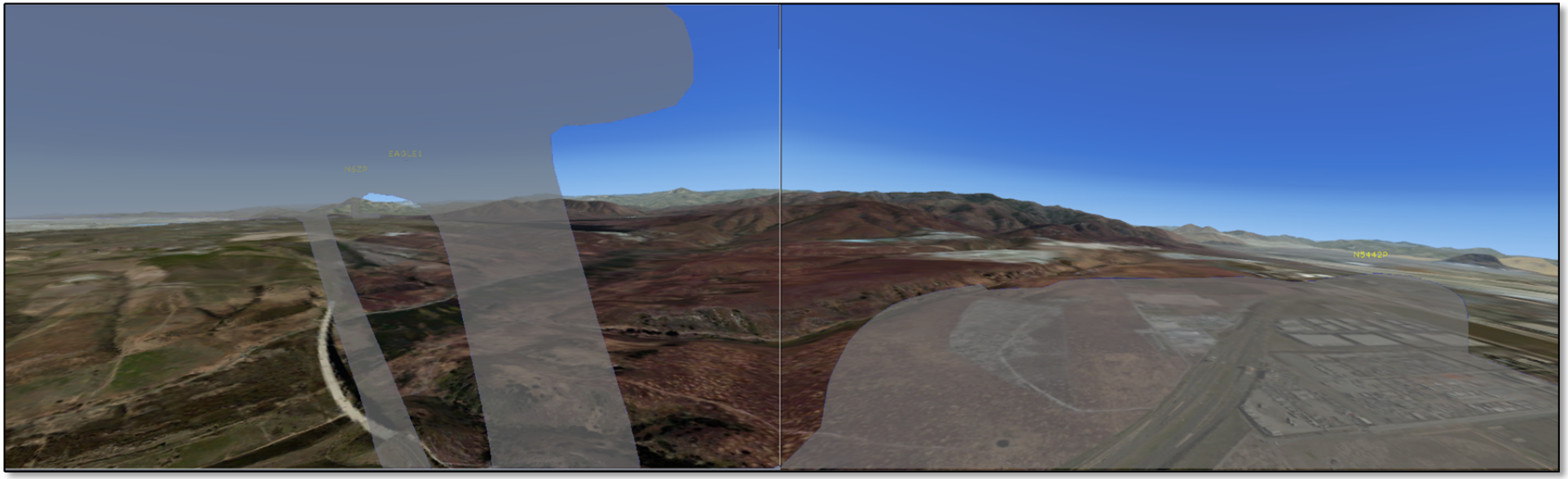

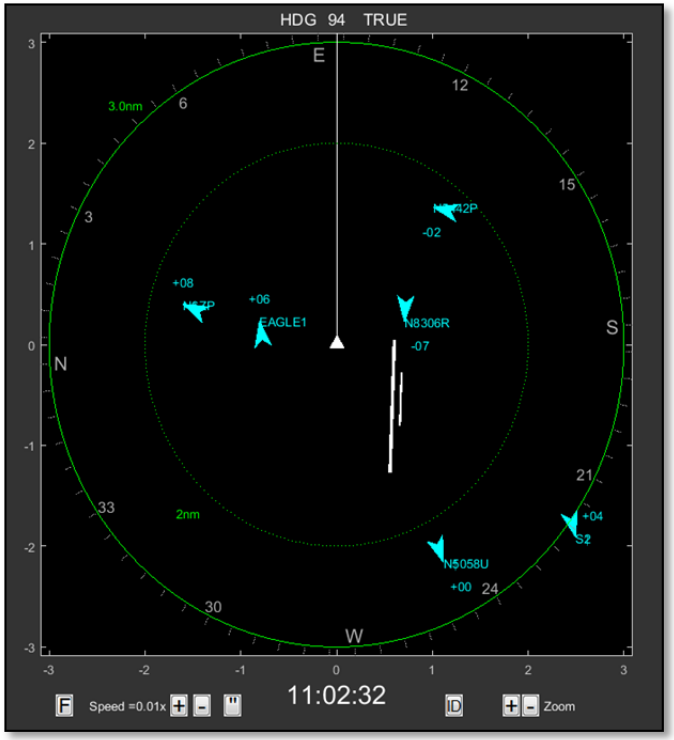

11:02:32.4 PDT
(00:37.8 min:sec before collision)

[TWR (@11:02:32.0)] cessna 6ZP make a right 360 right 360 rejoin the downwind

[HOT-1] you still got the guy on the right side?

Events in *italics* are ATC communications; others are EAGLE1 CVR events

Figure 26i.

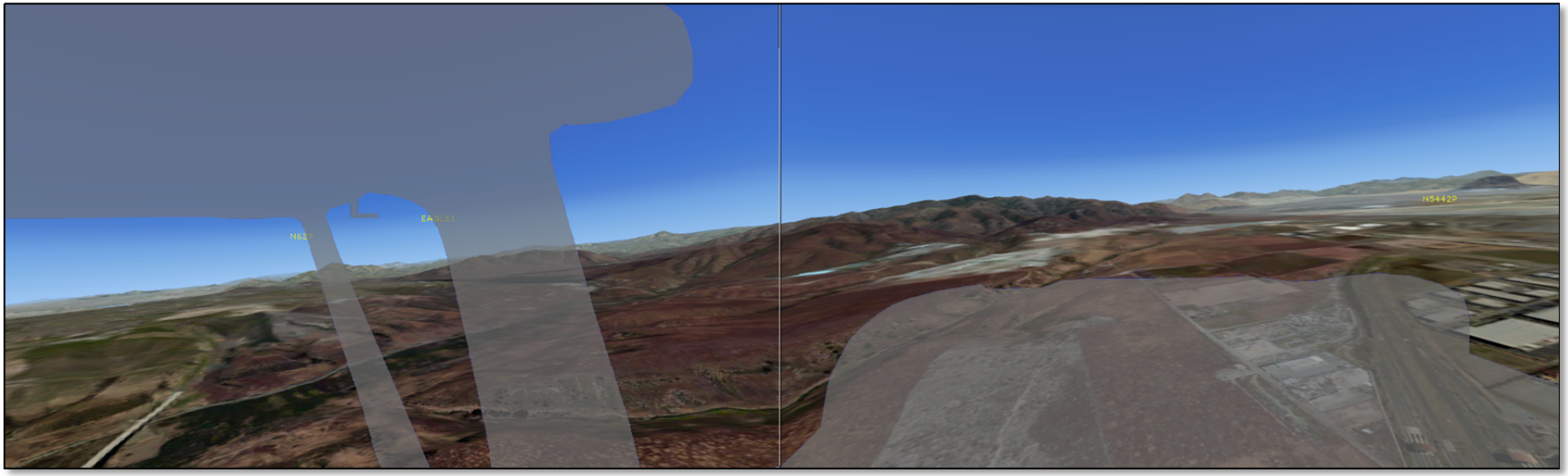

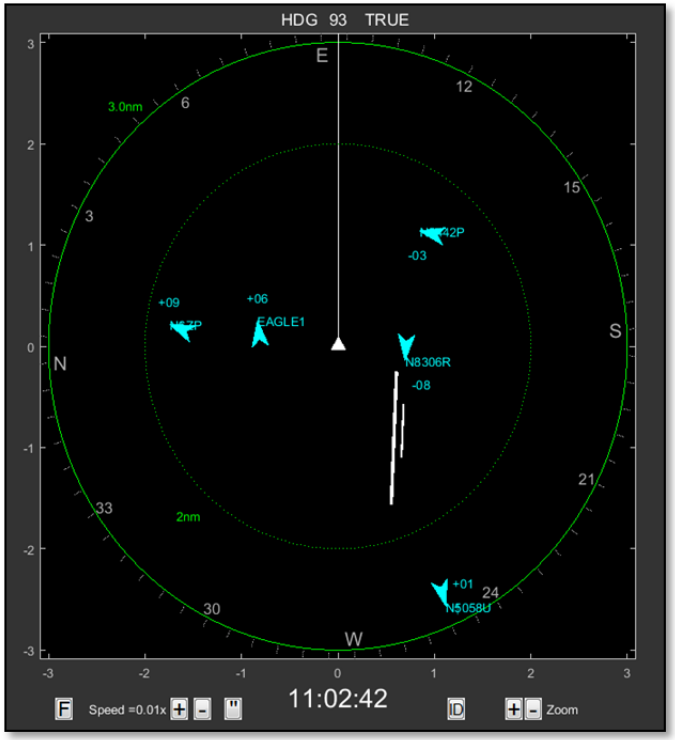

11:02:42 PDT
(00:28.2 min:sec before collision)

[TWR] eagle1 turn base 26R clear to land

Events in *italics* are ATC communications; others are EAGLE1 CVR events

Figure 26j.

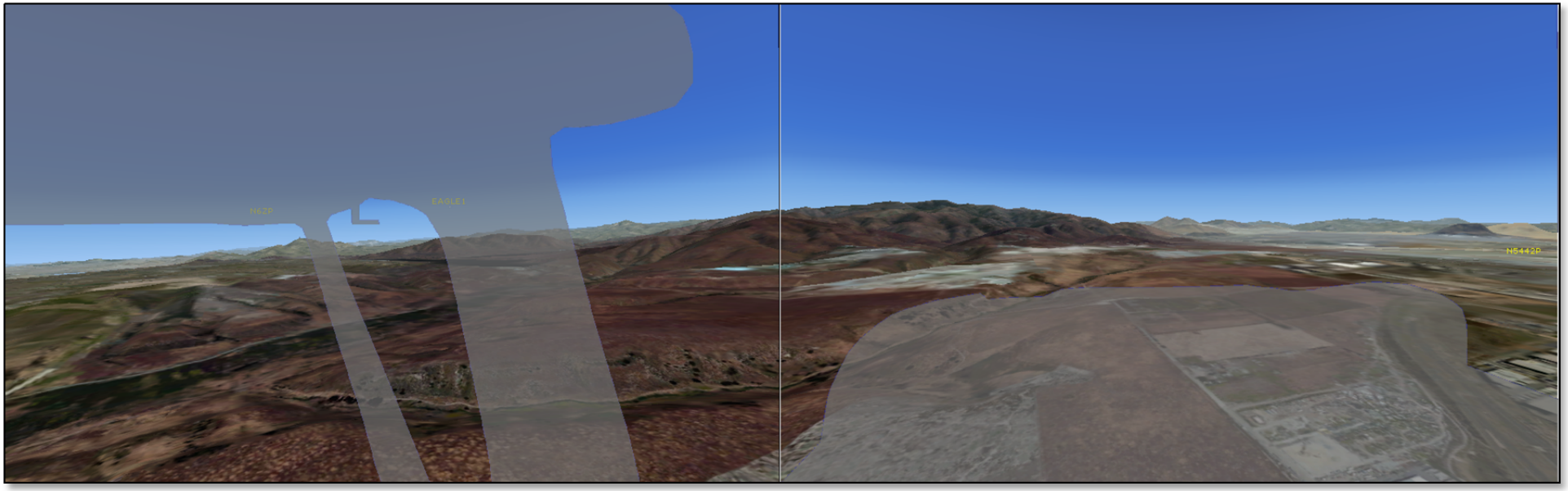

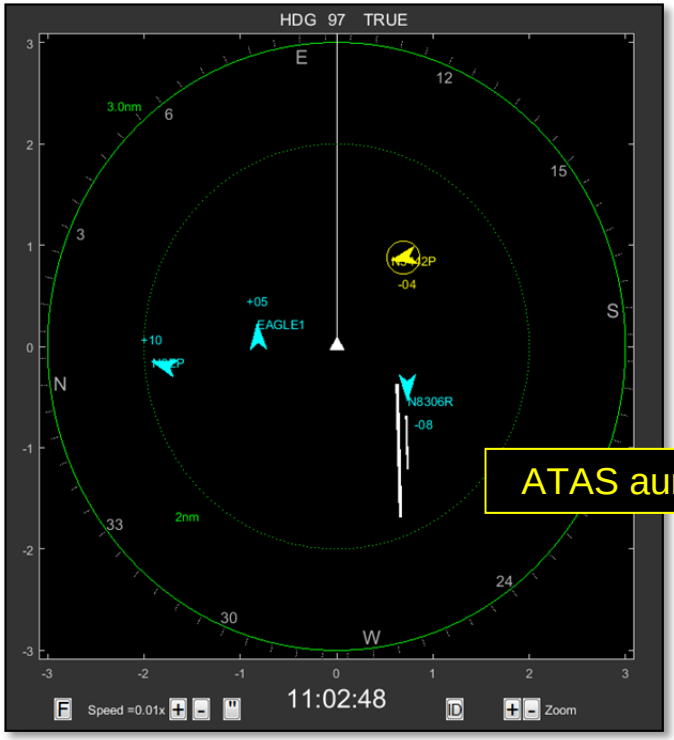

11:02:48 PDT
(00:22.2 min:sec before collision)

ATAS aural alert: "*Traffic, 2 o'clock, low, less than 1 mile.*"

Events in *italics* are ATC communications; others are EAGLE1 CVR events

Figure 26k.

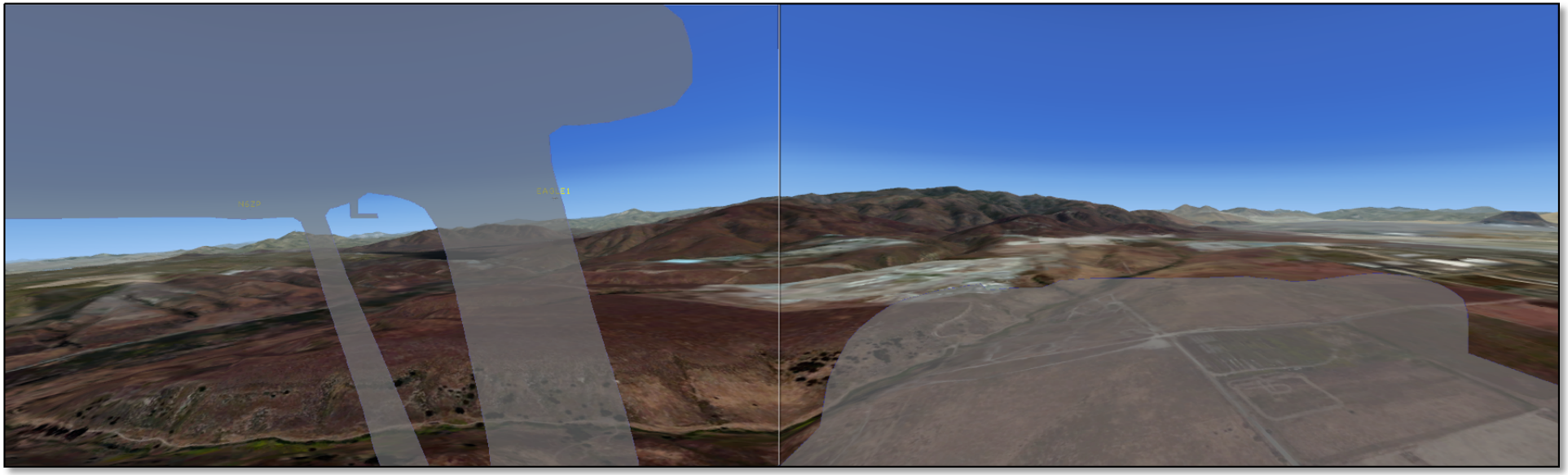

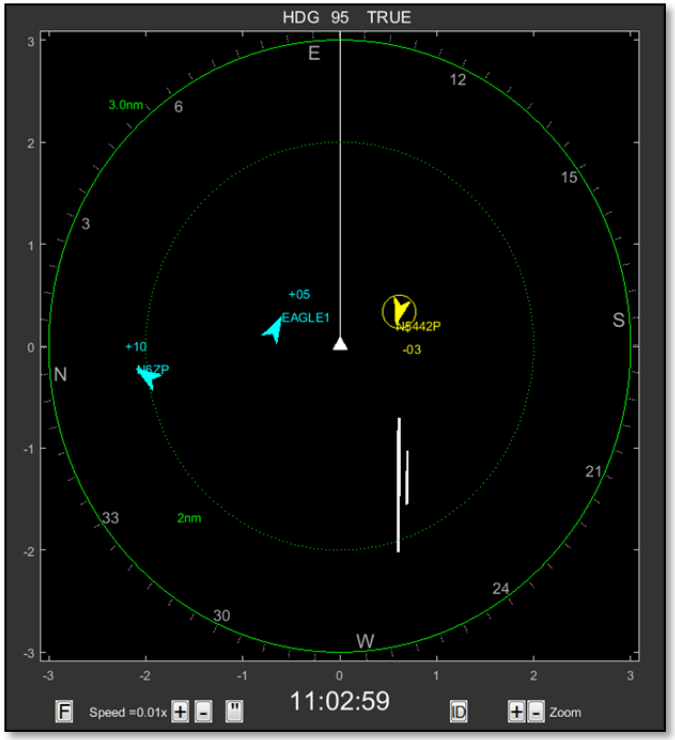

11:02:59.3 PDT
(00:10.9 min:sec before collision)

[HOT-1] I see the shadow but I don't see him.

Events in *italics* are ATC communications; others are EAGLE1 CVR events

Figure 26l.

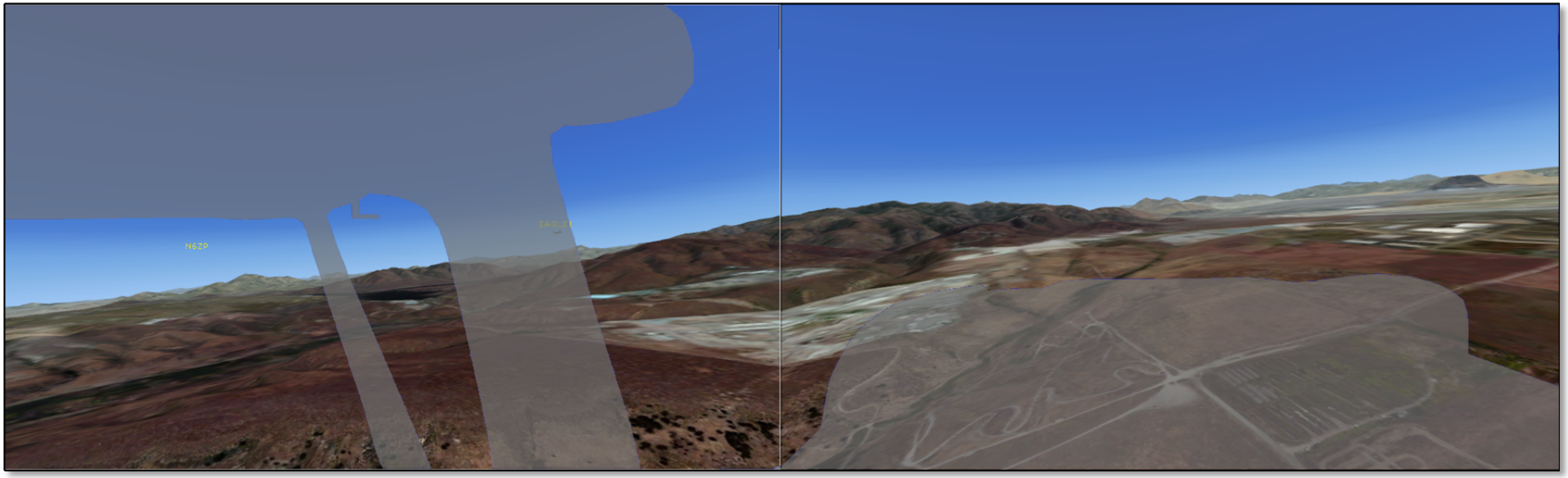

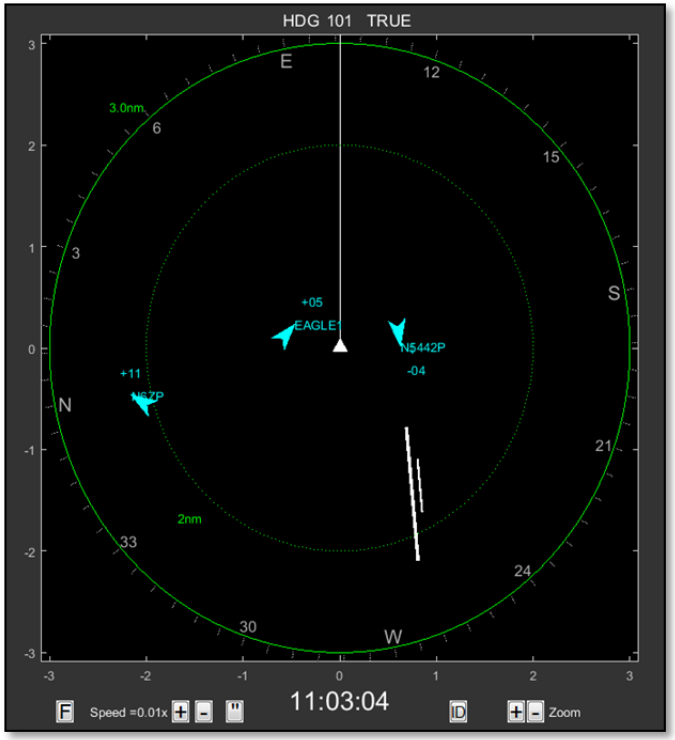

11:03:04 PDT
(00:06.2 min:sec before collision)

[TWR] N85U tower

Events in *italics* are ATC communications; others are EAGLE1 CVR events

Figure 26m.

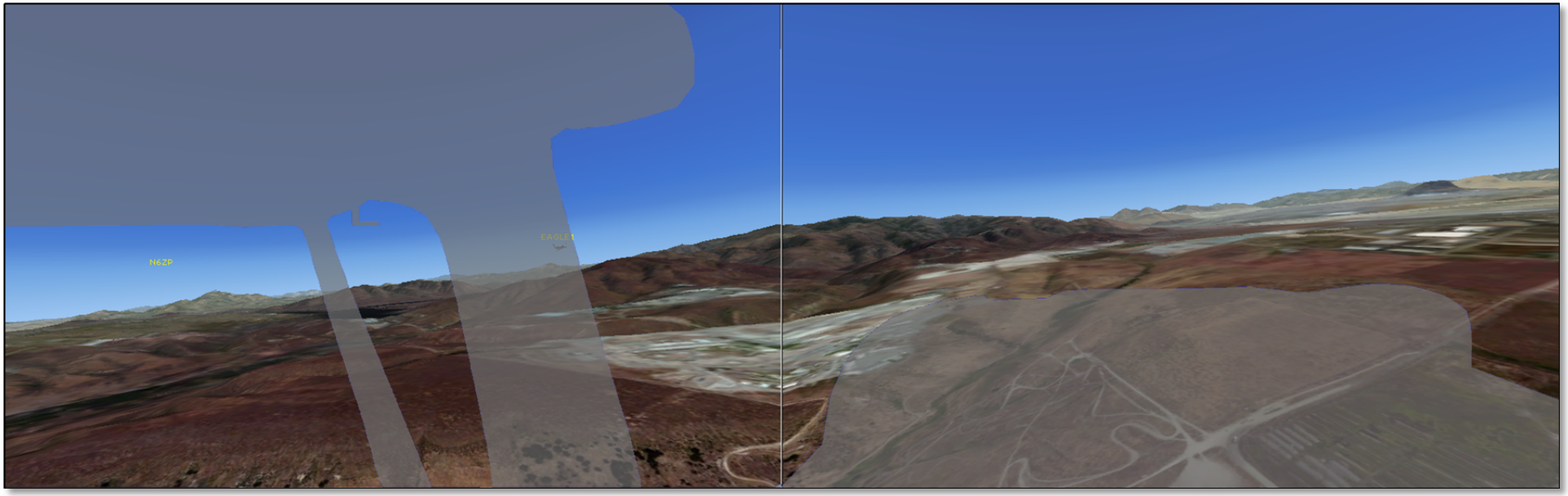

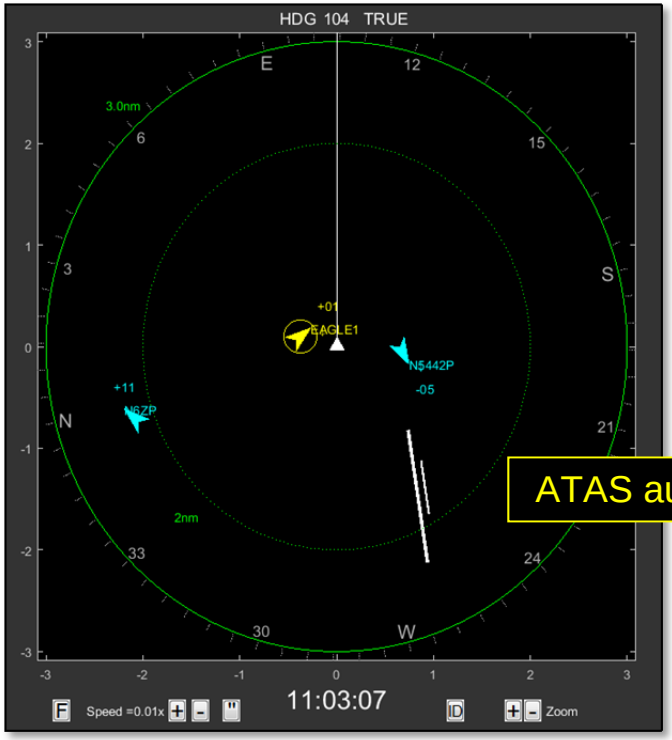

11:03:07 PDT
(00:03.2 min:sec before collision)

ATAS aural alert: "*Traffic, 11 o'clock, same altitude, zero miles, descending*"

Events in *italics* are ATC communications; others are EAGLE1 CVR events

Figure 26n.

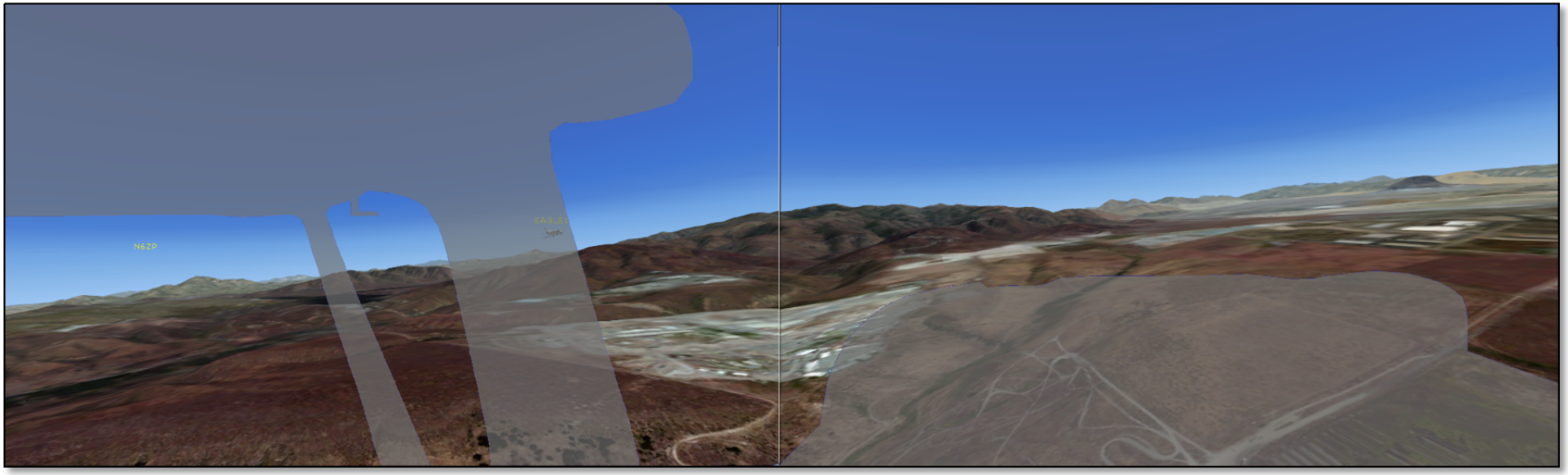

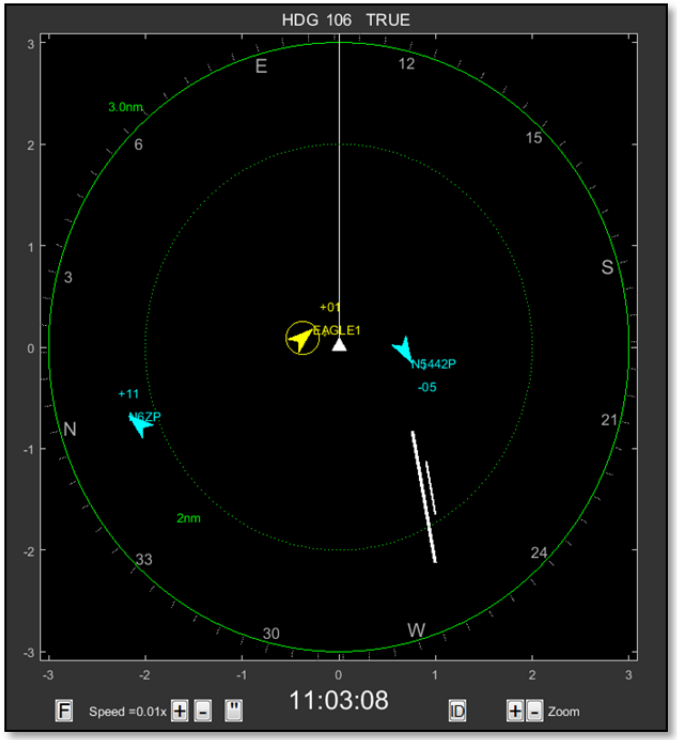

11:03:08 PDT
(00:02.2 min:sec before collision)

[TWR] are you still on downwind sir right downwind

Events in *italics* are ATC communications; others are EAGLE1 CVR events

Figure 26o.

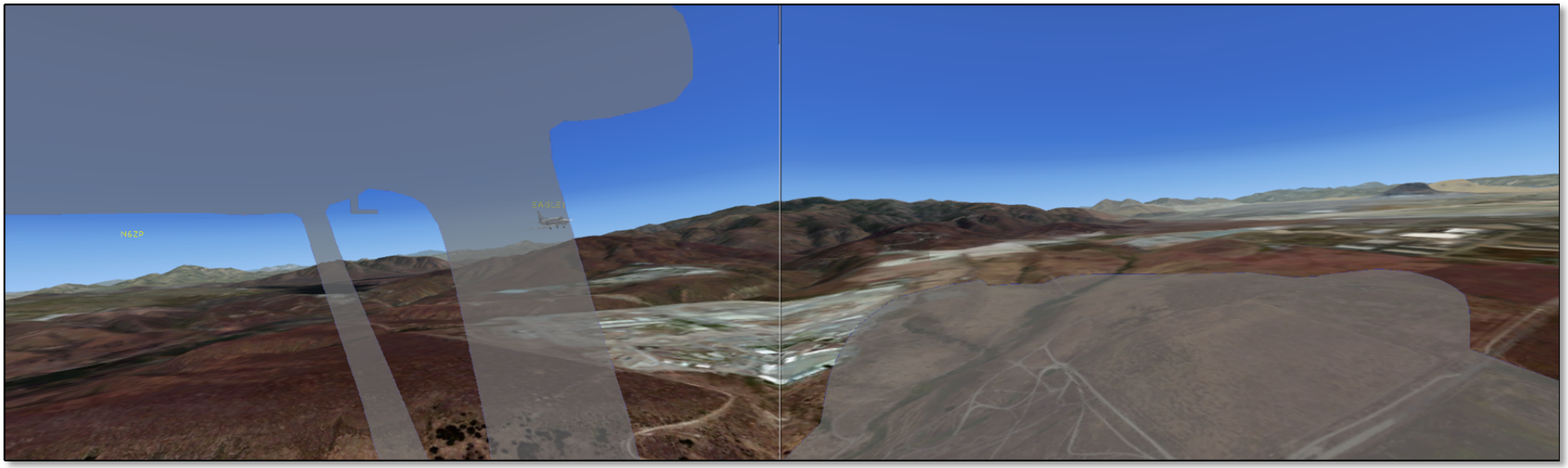

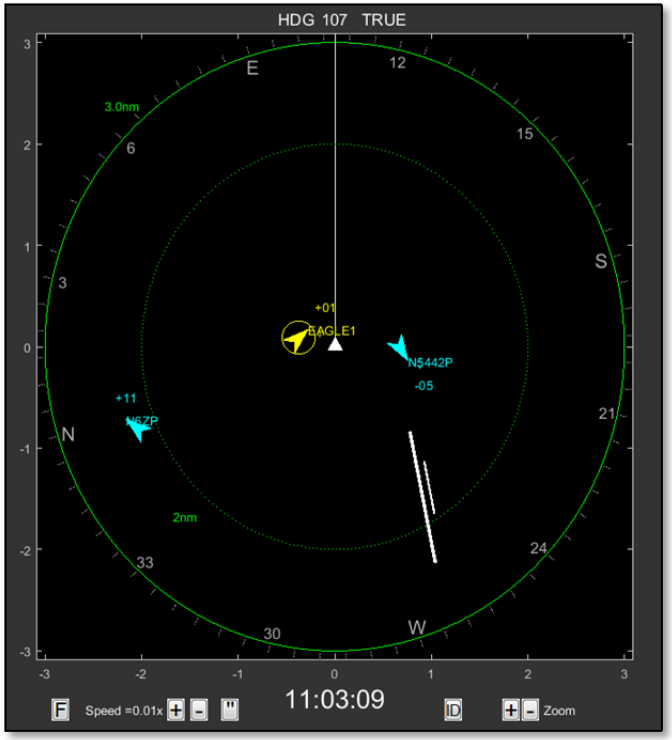

11:03:09 PDT
(00:01.2 min:sec before collision)

Figure 26p.

WPR15FA243AB: Midair collision, Sabreliner EAGLE1 / C172 N1285U, San Diego, CA, 8/16/2015

"Target" airplane size growth vs. time

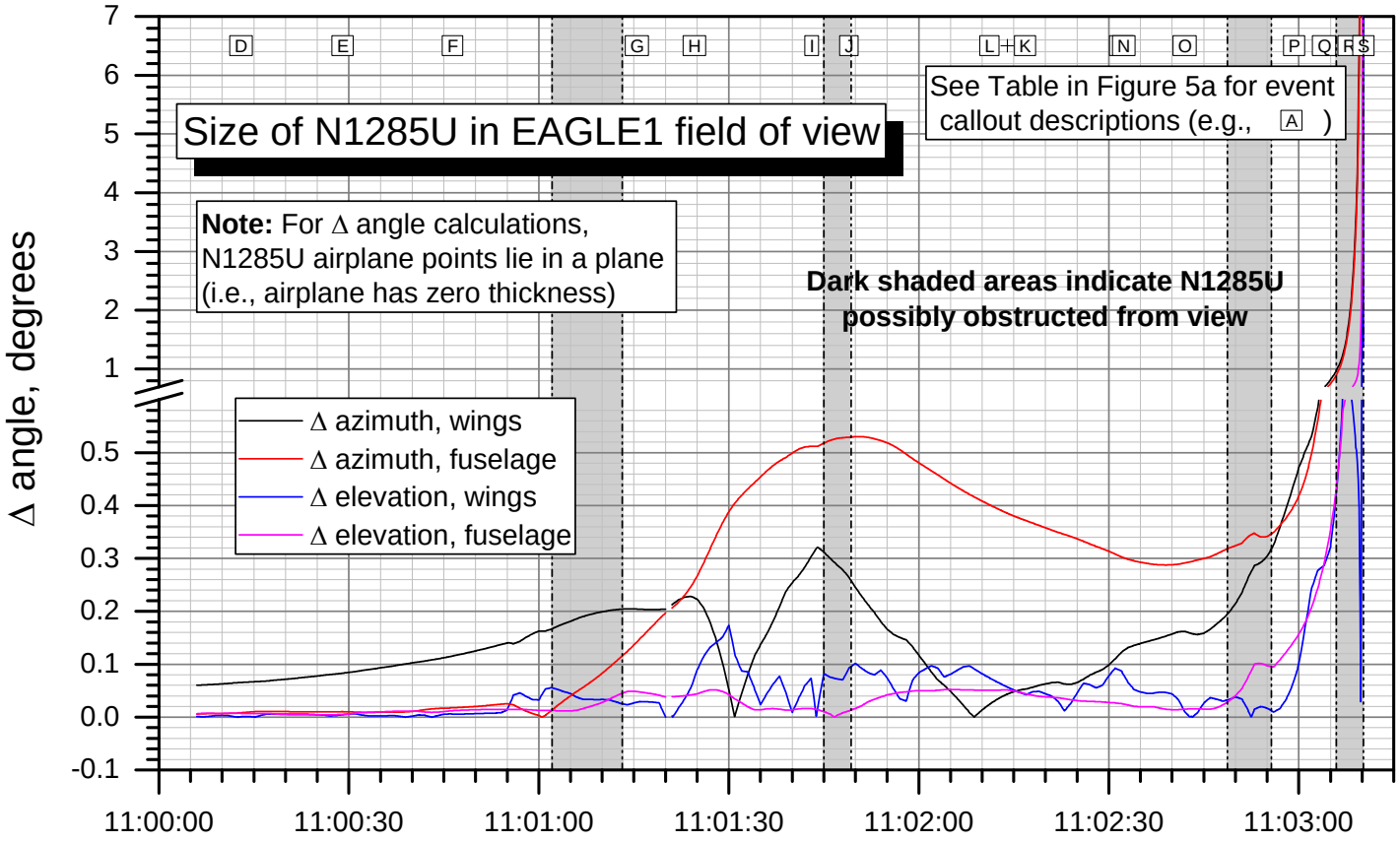

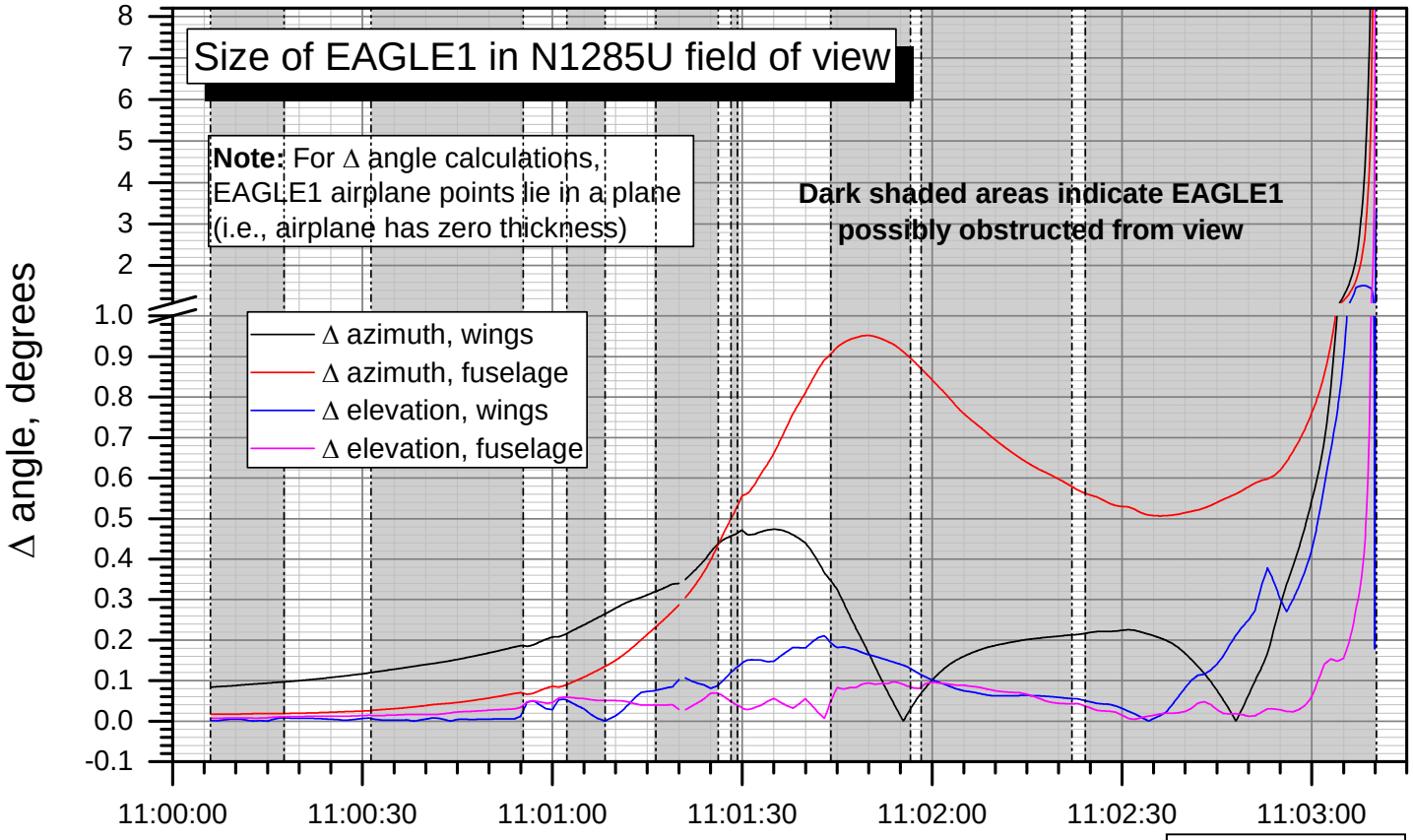

NZY ASR time, HH:MM:SS PDT

Figure 27.

APPENDIX A:

**Computing the Azimuth and Elevation Angles of
Airplane Cockpit Windows and other Structures from Laser Scans**

APPENDIX A: Computing the Azimuth and Elevation Angles of Airplane Cockpit Windows and other Structures from Laser Scans

Azimuth and elevations of "target" aircraft relative to "viewer" aircraft

The "visibility angles" from the "viewer" airplane to the "target" airplane correspond to the angular coordinates of the line of sight between the airplanes, measured in a coordinate system fixed to the viewer airplane (the viewer's "body axis" system), and consist of the azimuth angle and elevation angle (see Figure A1). The azimuth angle is the angle between the x-axis and the projection of the line of sight onto the x-y plane. The elevation angle is the angle between the line of sight itself, and its projection onto the x-y plane. At 0° elevation, 0° azimuth is straight ahead, and positive azimuth angles are to the right. 90° azimuth would be out the right window parallel to the y axis of the airplane. At 0° azimuth, 0° elevation is straight ahead, and positive elevation angles are up. 90° elevation would be straight up parallel to the z axis. The azimuth and elevation angles depend on both the position of the viewer and target airplanes, and the orientation (yaw, pitch, and bank angles) of the viewer.

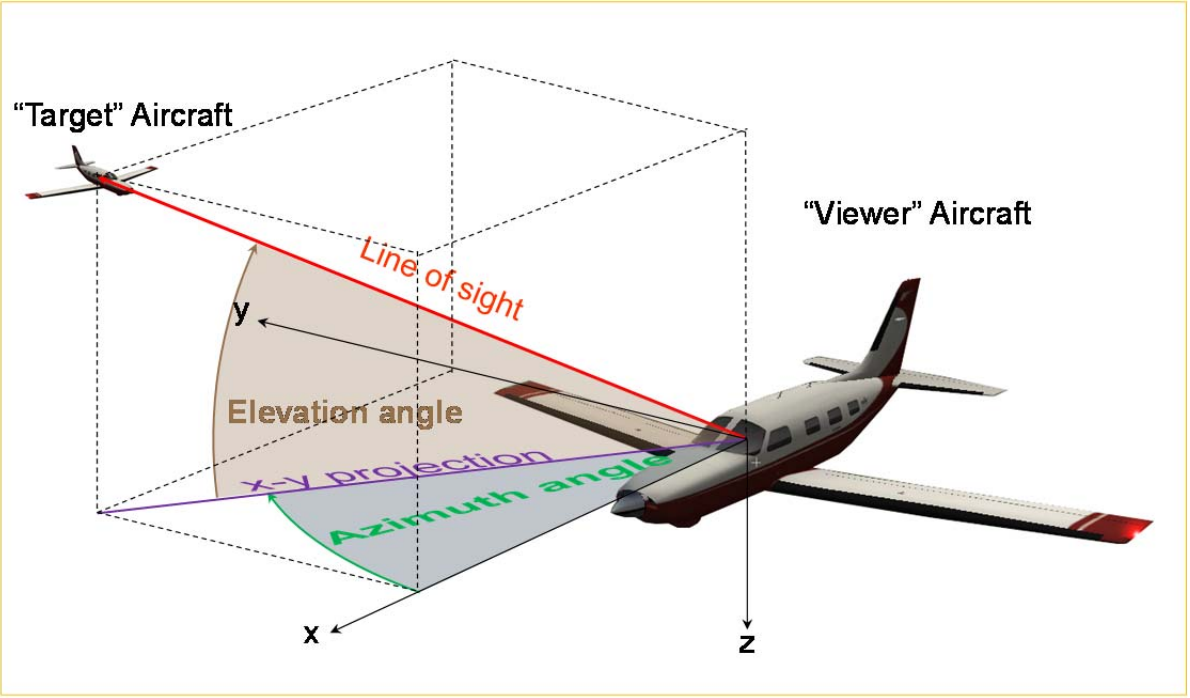

Figure A1. Azimuth and elevation angles from "viewer" airplane to "target" airplane.

The target airplane will be visible from the viewer airplane unless a non-transparent part of the viewer's structure lies in the line of sight between the two airplanes. To determine if this is the case, the azimuth and elevation coordinates of the boundaries of the viewer's transparent structures (windows) must be known, as well as the coordinates of the viewer's structure visible from the cockpit (such as the wings). If the line of sight passes through a non-transparent structure (such as the instrument panel, a window post, or a wing), then the target airplane will be obscured from the viewer.

Azimuth and elevation angles of airplane structures from laser scans

The azimuth and elevation angles of the window boundaries and other structures of the airplane of interest can be determined from the interior and exterior dimensions of the airplane, as measured using a FARO laser scanner.[1] The laser scanner produces a "point cloud" generated by the reflection of laser light off of objects in the laser's path, as the scanner sweeps through 360° of azimuth and approximately 150° of elevation. The 3-dimensional coordinates of each point in the cloud are known, and the coordinates of points from multiple scans (resulting from placing the scanner in different positions) are "merged" by the scanner software[2] into a common coordinate system. By placing the scanner in a sufficient number of locations so that the scanner can "see" every part of the airplane, the complete exterior and interior geometry of the airplane can be defined.

Coordinate transformations: scanner axes to body axes

The scanner software merges the point clouds from multiple scans into a single, "global" coordinate system. By default, this coordinate system is centered at the first scan location, which in general will not be coincident or aligned with the airplane body axis system. Hence, to compute azimuth and elevation angles of the scanned points relative to the pilot's eyes, the following transformations must be accomplished:

1. Translate the scanner global coordinates to the origin of the airplane body axis system.

2. Transform the translated scanner global coordinates into the airplane body axis system using a transformation matrix defined by the three rotations required to align the scanner axis system with the body axis system.

3. Determine the location of the pilot's eyes in the body axis system.

4. Determine the positions of the scanned points relative to the pilot's eyes in the body axis system.

5. Compute the azimuth and elevation angles from the pilot's eyes to the scanned points.

[1] Specifically, the FARO "Focus 3D" scanner; see http://www.faro.com/focus/us.
[2] FARO SCENE software: see http://www.faro.com/focus/us/software.

Note that to accomplish these steps, the following must also be known:

- The scanner global coordinates of the origin of the body axis system
- The three rotation angles between the scanner global coordinates and the body axis system

As will be shown below, these items can be determined from the scanned geometry of the airplane and the following known points:

- The scanner global coordinates at which the body x axis passes through the front and back of the airplane
- The body x coordinates of these points
- The scanner global coordinates of the left and right wingtips
- The body (x,y,z) coordinates of the wingtips

The body coordinates of the points listed above can be determined from technical or scaled drawings of the airplane.

The transformation equations and details of the steps outlined above can be derived starting from the sketch shown in Figure A2, where:

$\vec{R}_{sb}$ = Vector from the origin of the scanner global axis system to the origin of the airplane body axis system

$\vec{R}_{s}$ = Vector from the origin of the scanner global axis system to point *P*

$\vec{R}_{b}$ = Vector from the origin of the airplane body axis system to point *P*

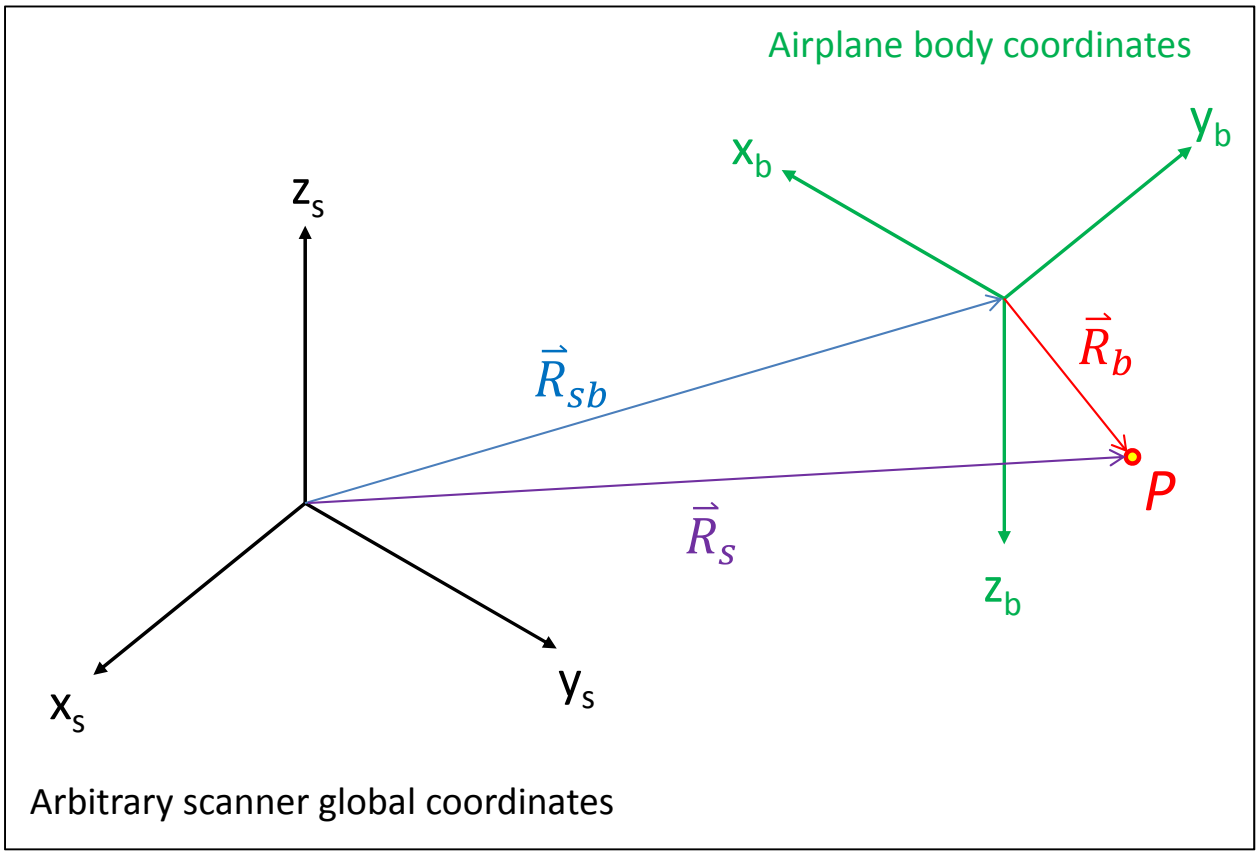

Figure A2. Vectors used to determine coordinates of point P in body axes coordinates.

The vectors $\vec{R}_{sb}$, $\vec{R}_s$, and $\vec{R}_b$ are expressed in the scanner global coordinates. We would like to know the coordinates of point *P* in body axis coordinates; let $\vec{r}_b$ be the vector from the origin of the body axis system to point *P*, expressed in body coordinates. Then, $\vec{r}_b$ is simply $\vec{R}_b$ transformed from scanner global coordinates to body axis coordinates. This transformation can be computed as follows. First, note that:

$\vec{r}_b = \begin{Bmatrix} x \\ y \\ z \end{Bmatrix}_b$ = coordinates of point *P* from body axis origin, in body axes

$\vec{R}_b = \begin{Bmatrix} x \\ y \\ z \end{Bmatrix}_s$ = coordinates of point *P* from body axis origin, in scanner axes

$\vec{R}_s = \begin{Bmatrix} x_s \\ y_s \\ z_s \end{Bmatrix}_s$ = coordinates of point *P* from scanner axis origin, in scanner axes

$\vec{R}_{sb} = \begin{Bmatrix} x_{sb} \\ y_{sb} \\ z_{sb} \end{Bmatrix}_s$ = coordinates of body axis origin from scanner axis origin, in scanner axes

From Figure A2,

$$\vec{R}_b = \vec{R}_s - \vec{R}_{sb} = \begin{Bmatrix} x_s \\ y_s \\ z_s \end{Bmatrix}_s - \begin{Bmatrix} x_{sb} \\ y_{sb} \\ z_{sb} \end{Bmatrix}_s = \begin{Bmatrix} x \\ y \\ z \end{Bmatrix}_s \quad \text{[A1]}$$

Equation [A1] translates the coordinates of point *P* from the origin of the scanner axis system to the origin of the body axis system, which is step 1 in the procedure outlined above. The coordinates are transformed into the body axis system (step 2 in the procedure) using a transformation matrix:

$$\vec{r}_b = [T_{sb}]\vec{R}_b \quad \text{[A2a]}$$

Or, equivalently,

$$\begin{Bmatrix} x \\ y \\ z \end{Bmatrix}_b = [T_{sb}] \begin{Bmatrix} x \\ y \\ z \end{Bmatrix}_s \quad \text{[A2b]}$$

Where $[T_{sb}]$ is the transformation matrix from the scanner axis system to the body axis system. This transformation matrix is defined by a series of three rotations of the scanner axis system, in the following order:

1. A rotation about the z_s axis through the angle ψ, yielding axes $(x_s', y_s', z_s' = z_s)$.
2. A rotation about the y_s' axis through the angle θ, yielding axes $(x_s'', y_s'' = y_s', z_s'')$.
3. A rotation about the x_s'' axis through the angle ϕ, yielding axes $(x_b = x_s'', y_b, z_b)$.

There is a transformation matrix associated with each of these rotations; the elements of the matrices are sines or cosines of the rotation angles involved. Combining these transformations through matrix multiplication yields the final transformation matrix $[T_{sb}]$:

$$[T_{sb}] = \begin{bmatrix} \cos\theta\cos\psi & \cos\theta\sin\psi & -\sin\theta \\ \sin\phi\sin\theta\cos\psi - \cos\phi\sin\psi & \sin\phi\sin\theta\sin\psi + \cos\phi\cos\psi & \sin\phi\cos\theta \\ \cos\phi\sin\theta\cos\psi + \sin\phi\sin\psi & \cos\phi\sin\theta\sin\psi - \sin\phi\cos\psi & \cos\phi\cos\theta \end{bmatrix} \quad \text{[A3]}$$

The details of these operations can be found in textbooks about airplane dynamics (or other subjects associated with rigid body dynamics and coordinate transformations).[3]

[3] See, for example, Roskam, Jan: Airplane Flight Dynamics and Automatic Flight Controls, Part I (Roskam Aviation and Engineering Corporation, 1979), pp. 24-27.

The reverse transformation (from airplane body axes to scanner axes) follows from Equations [2a] and [2b]:

$$\vec{R}_b = [T_{sb}]^{-1}\vec{r}_b = [T_{sb}]^T\vec{r}_b \qquad \text{[A4a]}$$

$$\begin{Bmatrix} x \\ y \\ z \end{Bmatrix}_s = [T_{sb}]^{-1}\begin{Bmatrix} x \\ y \\ z \end{Bmatrix}_b = [T_{sb}]^T\begin{Bmatrix} x \\ y \\ z \end{Bmatrix}_b \qquad \text{[A4b]}$$

Because the transformation matrix $[T_{sb}]$ is orthogonal, its inverse is equal to its transpose.

Note that Equations [A1], [A2b] and [A3] involve the coordinates of the origin of the body axis system in scanner axes $\{x_{sb}, y_{sb}, z_{sb}\}_s$, and the three rotation angles ψ, θ, and ϕ, which are all unknown and must be determined.

The coordinates $\{x_{sb}, y_{sb}, z_{sb}\}_s$ can be determined from the body axis coordinates of the points where the body x axis intersects the front and back of the airplane. It is assumed that these points are known from technical drawings of the airplane. It is also assumed that the location of these points can also be identified in the scanned point cloud by comparing the scan results to the technical drawings of the airplane, and that therefore the scanner coordinates $\{x_s, y_s, z_s\}_s$ of the points, measured from the scanner axis origin, can be determined using the scanner software.

Let $\{x_{sn}, y_{sn}, z_{sn}\}_s$ be the coordinates of the intersection of the body x axis with the front (nose) of the airplane, measured from the scanner axis origin, in scanner axes, as determined from the examination of the scanned point cloud using the scanner software.

Let $\{x_{st}, y_{st}, z_{st}\}_s$ be the coordinates of the intersection of the body x axis with the back (tail) of the airplane, measured from the scanner axis origin, in scanner axes, as determined from the examination of the scanned point cloud using the canner software.

The distance along the body x axis from nose to tail is then

$$l_{nt} = \sqrt{(x_{sn} - x_{st})_s^2 + (y_{sn} - y_{st})_s^2 + (z_{sn} - z_{st})_s^2} \qquad \text{[A5]}$$

Since the ratio of the distance between the body axis origin and the nose (i.e., $(x_n)_b$) to l_{nt} is the same in both the scanner and body axis coordinate systems, the scanner coordinates of the body axis origin, measured from the scanner axis origin, are given by

$$\begin{Bmatrix} x_{sb} \\ y_{sb} \\ z_{sb} \end{Bmatrix}_s = \begin{Bmatrix} x_{sn} \\ y_{sn} \\ z_{sn} \end{Bmatrix}_s + \left[\begin{Bmatrix} x_{st} \\ y_{st} \\ z_{st} \end{Bmatrix}_s - \begin{Bmatrix} x_{sn} \\ y_{sn} \\ z_{sn} \end{Bmatrix}_s \right] \frac{(x_n)_b}{l_{nt}} \quad [A6]$$

There remains to determine the rotation angles ψ, θ, and ϕ. From Equation [4b],

$$\begin{Bmatrix} x_n \\ y_n \\ z_n \end{Bmatrix}_s = \begin{Bmatrix} x_{sn} \\ y_{sn} \\ z_{sn} \end{Bmatrix}_s - \begin{Bmatrix} x_{sb} \\ y_{sb} \\ z_{sb} \end{Bmatrix}_s = [T_{sb}]^T \begin{Bmatrix} x_n \\ y_n \\ z_n \end{Bmatrix}_b \quad [A7]$$

Where $\{x_n, y_n, z_n\}_s$ are the scanner coordinates of the nose measured from the scanner origin, and $\{x_n, y_n, z_n\}_b$ are the body coordinates of the nose measured from the body origin. From Equations [A7] and [A3],

$$\{z_{sn} - z_{sb}\}_s = (-\sin\theta)\{x_n\}_b + (\sin\phi\cos\theta)\{y_n\}_b + (\cos\phi\cos\theta)\{z_n\}_b \quad [A8]$$

Since by definition the "nose" lies on the x body axis, $(y_n)_b = (z_n)_b = 0$, and Equation [A8] gives

$$\theta = \sin^{-1}\left(\frac{-\{x_n\}_b}{\{z_{sn} - z_{sb}\}_s}\right) \quad [A9]$$

Similarly, Equations [A7] and [A3] with $(y_n)_b = (z_n)_b = 0$ give

$$\{x_{sn} - x_{sb}\}_s = (\cos\theta\cos\psi)\{x_n\}_b \quad [A10]$$

$$\{y_{sn} - y_{sb}\}_s = (\cos\theta\sin\psi)\{x_n\}_b \quad [A11]$$

And therefore

$$\psi = \cos^{-1}\left(\frac{\{x_{sn} - x_{sb}\}_s}{\{x_n\}_b\cos\theta}\right) \quad [A12]$$

$$\psi = \sin^{-1}\left(\frac{\{y_{sn} - y_{sb}\}_s}{\{x_n\}_b\cos\theta}\right) \quad [A13]$$

These two equations for ψ allow the proper quadrant for ψ to be determined.

To solve for the remaining rotation angle (ϕ), the coordinates of the wingtips can be used. Let $\{x_{sl}, y_{sl}, z_{sl}\}_s$ be the coordinates of the left wingtip, measured from the scanner axis origin, in scanner axes, as determined from the examination of the scanned point

cloud using the scanner software. Similarly, let $\{x_{sr}, y_{sr}, z_{sr}\}_s$ be the corresponding coordinates for the right wing. The coordinates of the wingtips in body coordinates, measured from the body axis origin, are

$\begin{Bmatrix} x_r \\ y_r \\ z_r \end{Bmatrix}_b = \begin{Bmatrix} x_w \\ y_w \\ z_w \end{Bmatrix}_b$ for the right wing, and

$\begin{Bmatrix} x_l \\ y_l \\ z_l \end{Bmatrix}_b = \begin{Bmatrix} x_w \\ -y_w \\ z_w \end{Bmatrix}_b$ for the left wing.

From Equation [A4b],

$$\begin{Bmatrix} x_r \\ y_r \\ z_r \end{Bmatrix}_s = \begin{Bmatrix} x_{sr} \\ y_{sr} \\ z_{sr} \end{Bmatrix}_s - \begin{Bmatrix} x_{sb} \\ y_{sb} \\ z_{sb} \end{Bmatrix}_s = [T_{sb}]^T \begin{Bmatrix} x_w \\ y_w \\ z_w \end{Bmatrix}_b \quad [A14]$$

$$\begin{Bmatrix} x_l \\ y_l \\ z_l \end{Bmatrix}_s = \begin{Bmatrix} x_{sl} \\ y_{sl} \\ z_{sl} \end{Bmatrix}_s - \begin{Bmatrix} x_{sb} \\ y_{sb} \\ z_{sb} \end{Bmatrix}_s = [T_{sb}]^T \begin{Bmatrix} x_w \\ -y_w \\ z_w \end{Bmatrix}_b \quad [A15]$$

Then, from Equations [A14], [A15], and [A3],

$$\{z_{sr} - z_{sb}\}_s = (-\sin\theta)\{x_w\}_b + (\sin\phi\cos\theta)\{y_w\}_b + (\cos\phi\cos\theta)\{z_w\}_b \quad [A16]$$

$$\{z_{sl} - z_{sb}\}_s = (-\sin\theta)\{x_w\}_b + (\sin\phi\cos\theta)\{-y_w\}_b + (\cos\phi\cos\theta)\{z_w\}_b \quad [A17]$$

Solving Equations [A16] and [A17] for $\cos\phi$ gives

$$\cos\phi = \frac{\{z_{sl}-z_{sb}\}_s+\{z_{sr}-z_{sb}\}_s+2(\sin\theta)\{x_w\}_b}{2(\cos\theta)\{z_w\}_b} \quad [A18]$$

Combining Equations [A16] and [A18] and solving for $\sin\phi$ gives

$$\sin\phi = \frac{\{z_{sr}-z_{sb}\}_s+(\sin\theta)\{x_w\}_b-(\cos\phi\cos\theta)\{z_w\}_b}{(\cos\theta)\{y_w\}_b} \quad [19]$$

$\cos\phi$ and $\sin\phi$ then define the proper quadrant for ϕ, and ϕ itself. Now, Equations [A1], [A2b] and [A3] can be used to compute the body axis coordinates of any scanned point, starting from the scanner coordinates of that point.

Azimuth and elevation angles from body axis coordinates

Once the coordinates of the scanned points are available in the body axis system, the azimuth and elevation angles of these points relative to the pilot's eye position can be computed. In keeping with the previous notation, let $\{x_e, y_e, z_e\}_b$ be the body-axis coordinates of one of the pilot's eyes,[4] and $\{x_P, y_P, z_P\}_b$ be the body-axis coordinates of a point *P*. Then the distance from the eye to point *P* is

$$l_{eP} = \sqrt{(x_P - x_e)_b^2 + (y_P - y_e)_b^2 + (z_P - z_e)_b^2} \quad \text{[A20]}$$

The azimuth angle from the eye to the point *P* is

$$\Psi = \tan^{-1}\left[\frac{(y_P - y_e)}{(x_P - x_e)}\right] \quad \text{[A21]}$$

The elevation angle from the eye to the point *P* is

$$\Theta = -\sin^{-1}\left[\frac{(z_P - z_e)}{l_{eP}}\right] \quad \text{[A22]}$$

[4] Note that the pilot's left and right eyes are in slightly different positions, so these calculations should be made for each eye.

APPENDIX B:

Creating Geometrically Correct Cockpit Window "Masks"
in Microsoft Flight Simulator X (*FSX*)

APPENDIX B: Creating Geometrically Correct Cockpit Window "Masks" in Microsoft Flight Simulator X (*FSX*)

Field of view vs. FSX screen display coordinates

The geometry of an airplane's cockpit windows and other structures can be defined in terms of their azimuth and elevation angles (Ψ and Θ, respectively) from the pilot's eyes. The visual systems of flight simulation programs, such as *FSX*, include a "cockpit view" that similarly displays the cockpit and other airplane structures from the "pilot's point of view." The *FSX "*virtual cockpit,*"* in particular, depicts a 3-dimensional model of the airplane interior from the pilot's seat (or any other point at which a "camera" is placed). The 3D model can be explored by rotating and / or translating the camera from the pilot's eye position.

While many airplane models for *FSX* include "virtual cockpits" that are very convincing and satisfactory for gaming or flight training purposes, the geometrical accuracy of these models is unknown, and so they are not suitable for determining whether outside objects would be visible or obscured in the real airplane in any particular scenario. *FSX* also includes a simple "2D cockpit" view, which presents a forward-looking scene of the outside world, overlaid with an instrument panel that is a compromise between realism, and the desire to have all the necessary flight instruments (and a sufficiently large out-the-window view) visible to the user at the same time, given limited screen real estate. These "2D cockpits" are necessarily less representative of the real airplane than the "virtual cockpits." However, the default 2D cockpit instrument panel can be substituted with a user-created "panel" that correctly represents the pilot's view of the cockpit and airplane structures in the real airplane, as determined from the airplane geometry measured with a laser scanner (see Appendix A). This "geometrically correct" panel can be used to determine whether an object outside the airplane is obstructed from the pilot's view.

The custom panel created by the user is a whole-screen instrument panel that contains transparent and non-tranparent areas. The transparent areas correspond to areas of the windows that offer unobstructed views of the outside world; the non-transparent areas correspond to everything else (cockpit structure, and exterior structure visible from the cockpit that obstructs the outside view). The "panel" is simply a 1024 x 768 bitmap image file, in which transparent areas are defined by assigning pixels a particular color (e.g., black) that *FSX* interprets as "transparent." Hence, the coordinates and color of the pixels in the bitmap file define the shapes of the panel transparent and non-transparent areas.

However, while the scope of the scene of the outside world displayed on the screen is defined in terms of angular and vertical “fields of view,” the screen coordinates of objects “seen” by the camera (including the cockpit windows) are not simply proportional to the angular Ψ and Θ coordinates of those objects from the camera positon. Instead, the screen coordinates of an object correspond to the points where the line of sight from the camera to the object intercepts a flat surface (the screen) placed some distance R between the camera and the object, as shown in Figure B1 (this Figure, and the discussion below, is adapted from Reference B1).

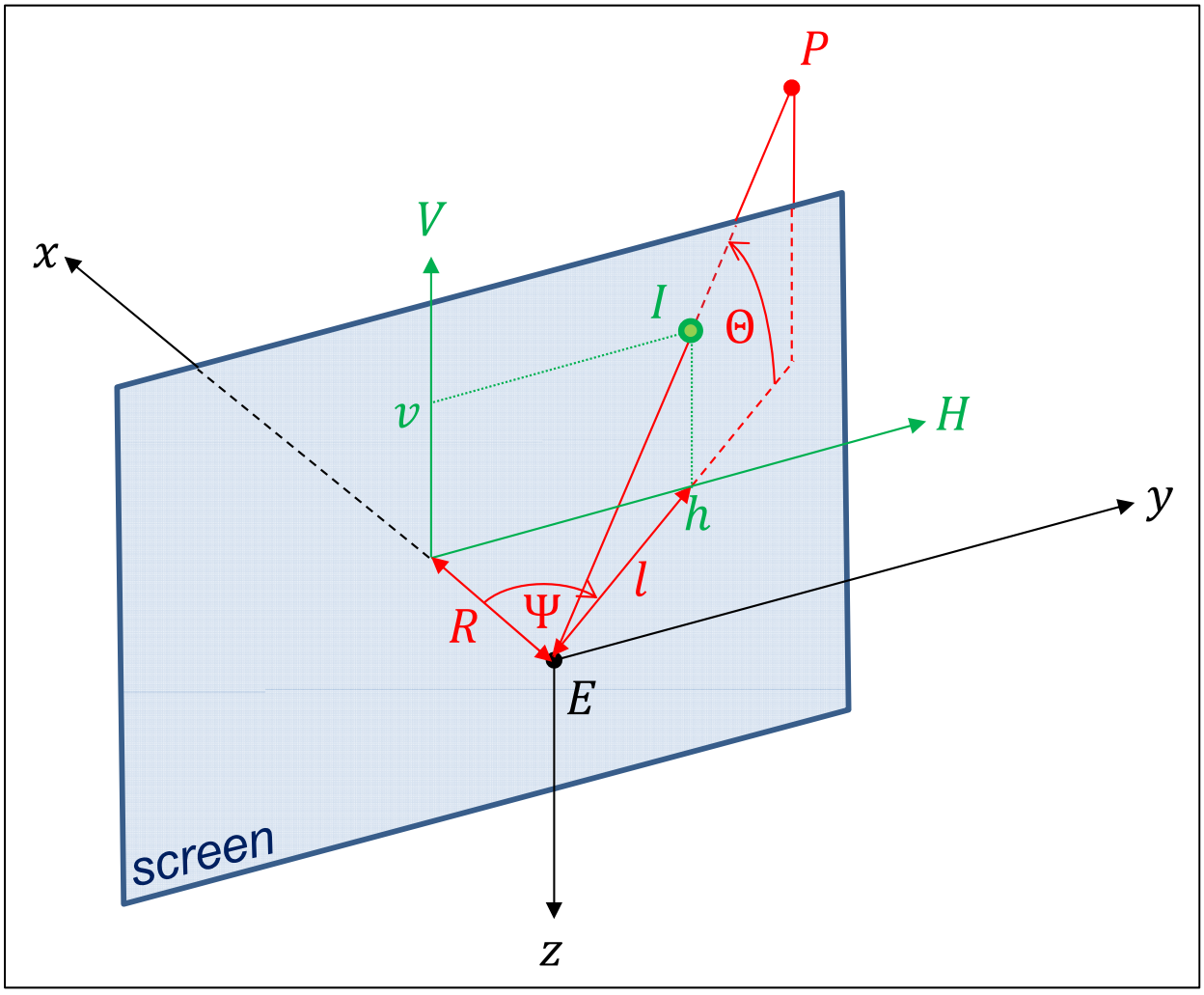

Figure B1. Relationships between the (Ψ, Θ) viewing angles of the line of sight from E to P (EP), and the (h, v) screen coordinates of the point I, where EP intersects the screen.

In Figure B1,

E = location of viewer's eye point (i.e., the camera location in *FSX*);
(x, y, z) = airplane body axis system with origin at E;
P = location of point or object to be drawn on the screen;
EP = line of sight from E to P;
Ψ = azimuth angle of EP;
Θ = elevation angle of EP;
I = point where EP intersects a flat screen placed in the yz plane between E and P;
R = x coordinate of I (i.e., the distance from E to the screen along x axis);
(H, V) = screen horizontal and vertical axis coordinate system, originating where the x body axis intersects the screen;
(h, v) = screen coordinates of I;
l = distance from E to the point defined by screen coordinates $(h, 0)$.

We seek to find the screen coordinates (h, v) at which a point P should be drawn, given the viewing angles (Ψ, Θ) from E to P.

From the geometry of Figure B1,

$$h = R \tan \Psi \qquad \text{[B1]}$$

$$l = \sqrt{R^2 + h^2} = \sqrt{R^2 + R^2 \tan^2 \Psi} = R\sqrt{1 + \tan^2 \Psi} \qquad \text{[B2]}$$

$$v = l \tan \Theta = R \tan \Theta \sqrt{1 + \tan^2 \Psi} \qquad \text{[B3]}$$

Consequently, (h, v) can be computed from (Ψ, Θ) once the distance R is known. R can be determined in *FSX* if the angular range of the horizontal field of view ($HFOV$) and the width of the screen in pixels (w) are known. For example, at the right edge of the screen, $h = w/2$, and $\Psi = HFOV/2$. Then, from Equation [B1],

$$R = \frac{(w/2)}{\tan(HFOV/2)} \qquad \text{[B4]}$$

Unfortunately, determining the exact $HFOV$ in *FSX* is not straightforward. $HFOV$ is modified by the *FSX* "zoom" level (smaller zoom yields greater $HFOV$), but the quantitative relationship between the zoom and $HFOV$ is not specified in any *FSX* documentation. However, both the $HFOV$ and vertical $VFOV$ in *FSX* can be determined by experiment, using a method presented in Reference 2 and described below.

Determining the field of view in FSX

Reference 2 describes how to modify *FSX* .FLT files to customize the geometry (size, shape, and screen location) of *FSX* windows (in which visual scenes are displayed), and to control the cameras used to view the world in each window. Significantly, the camera position, orientation, and zoom level can be defined in the .FLT files.

The field of view of a window of a given shape and zoom level can be determined by creating a second window of similar shape and zoom level adjacent to the first. The camera in the second window is then rotated until the scene at the edge where the two windows meet match. The rotation of the camera required to accomplish this is known. Furthermore, the azimuth angle from the second camera to the common edge is half of the $HFOV$, and since the two windows are the same size, it is also half of the camera rotation angle. Hence, the $HFOV$ is simply the rotation angle of the camera required to match the scene at the window edges (see Figure B2). This method can also be used to determine the $VFOV$.

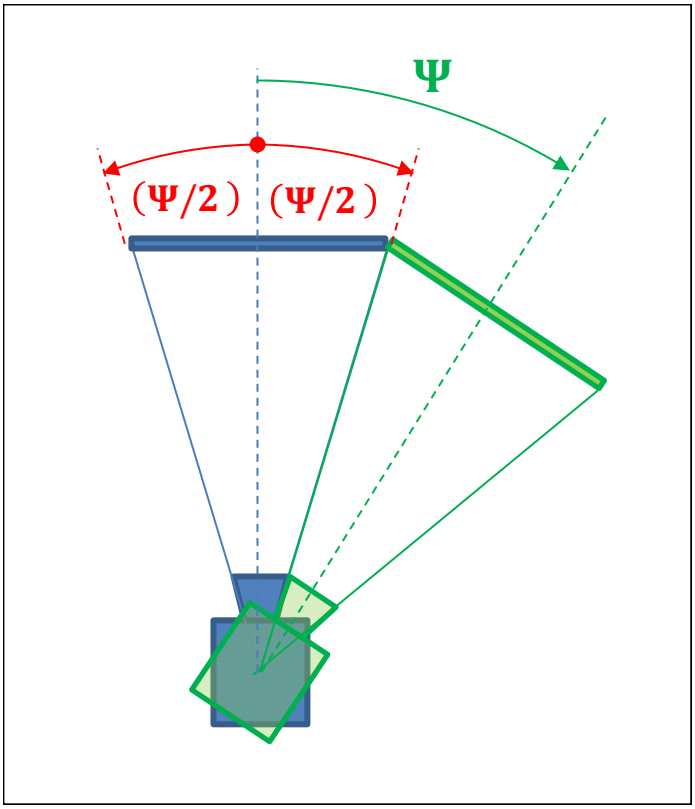

Figure B2. Determining the $HFOV$ by rotating a second (green) camera through angle Ψ to match the scene at the boundary of the view from the first (blue) camera.

Experiments with this method indicate that the $HFOV$ in *FSX* is a function of the window aspect ratio (width / height), as well as the *FSX* zoom level. Results using a window of aspect ratio of 1.6 and a zoom of 0.3 are shown in Figure B3. In this case, the $HFOV$ is 90° and the $VFOV$ is 61.8°. Per Equation [B4], R in this case would be equal to $w/2$.

Creating the FSX *instrument panel "mask" bitmap file*

With the value of R determined as described above, Equations [B1] and [B3] can be used to convert the (Ψ, Θ) viewing angles of the cockpit window structures into the (h, v) screen coordinates at which they should be drawn in order to be consistent with the outside scenery drawn by *FSX*. Once the (h, v) coordinates are in hand, the bitmap file defining the full-screen instrument panel "mask" can be created.

These bitmaps were created for this *Study* as follows.

1. First, the (h, v) coordinates of the windows were plotted into a graph with boundaries set equal to the horizontal and vertical resolution of the computer screen (i.e., the horizontal scale ranged from $-w/2$ to $+w/2$, and the vertical scale ranged from $-h/2$ to $+h/2$, where w is the screen width in pixels and h is the screen height in pixels); see Figure B4.
2. An image of the plot created in step 1 was pasted into Microsoft *PowerPoint*, and the graphical tools in *PowerPoint* were used to create a grey background covering the entire plot area, with black-filled polygons depicting the unobstructed areas of the window transparencies (see Figure B5).
3. The *PowerPoint* image was pasted into the *GIMP2* image-manipulation program, and resized to 1024 x 768, as required by *FSX.*
4. The *FastStone Photo Resizer 3.2* program was used to change the color depth of the bitmap to "4 (2 bit)." This step successfully compresses the bitmap into an "8 bit file," as required by *FSX*.
5. The bitmap is specified in the *FSX panel.cfg* file for the desired airplane model. In addition, the windows that are to use the panel (with camera rotations defined to be consistent with the view created in the bitmap file) are created in the *FSX .FLT* files for the "flight" corresponding to the project. Details concerning configuring the *panel.cfg* and .FLT files can be found in the *FSX* Software Development Kit (SDK) documentation, and in Reference 2.

The instrument panel mask constructed per the steps illustrated in Figures B4 and B5 is shown in its finished form within *FSX* in Figure B6.

Figure B3. Application of the method for determining the $HFOV$ illustrated in Figure B2.

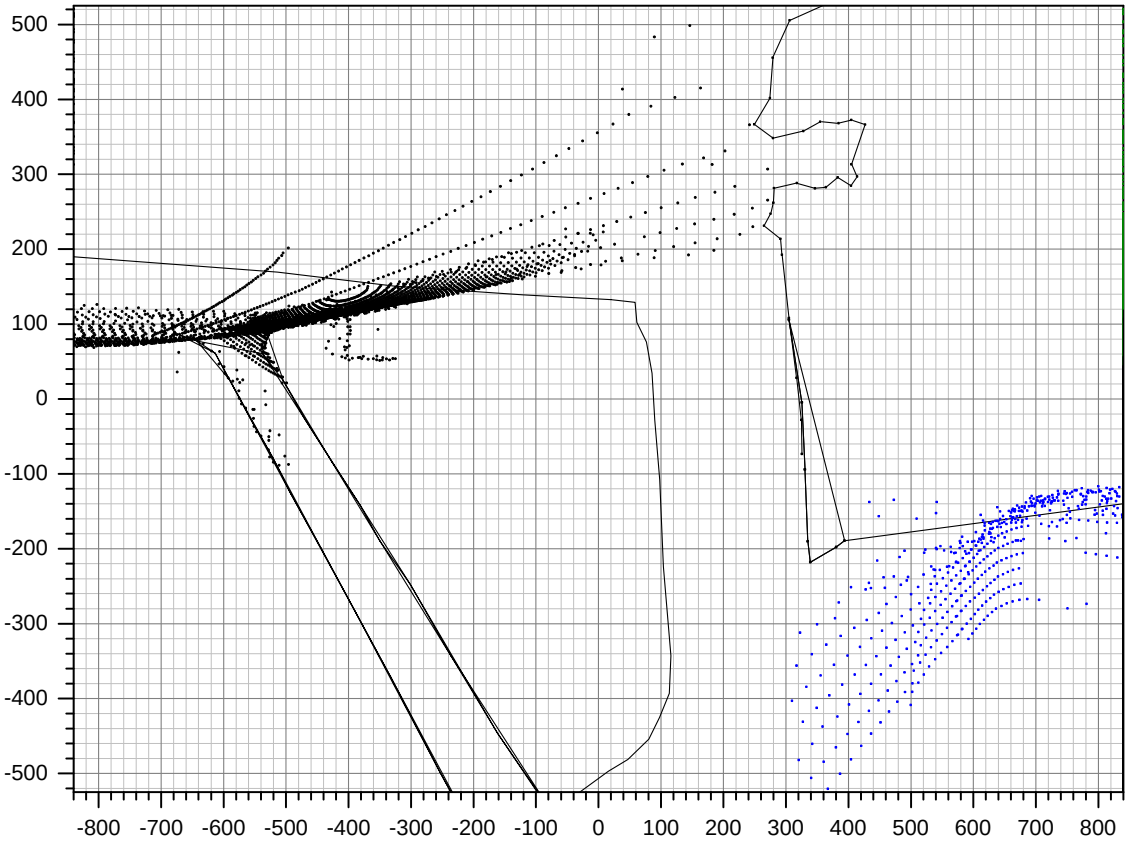

Figure B4. Plot of window v vs. h screen coordinates. The axis scales correspond to screen height and width.

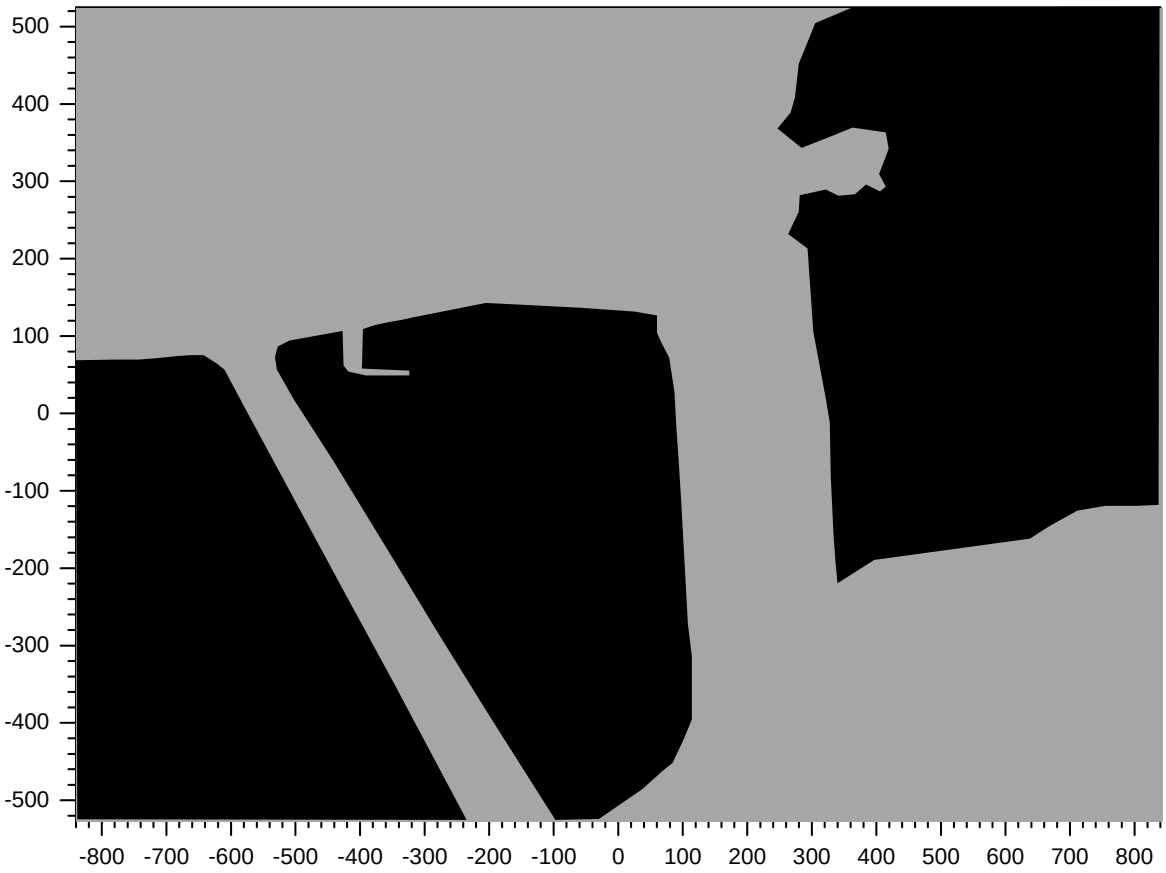

Figure B5. Black color applied to plot of Figure B4 to denote unobstructed window transparencies.

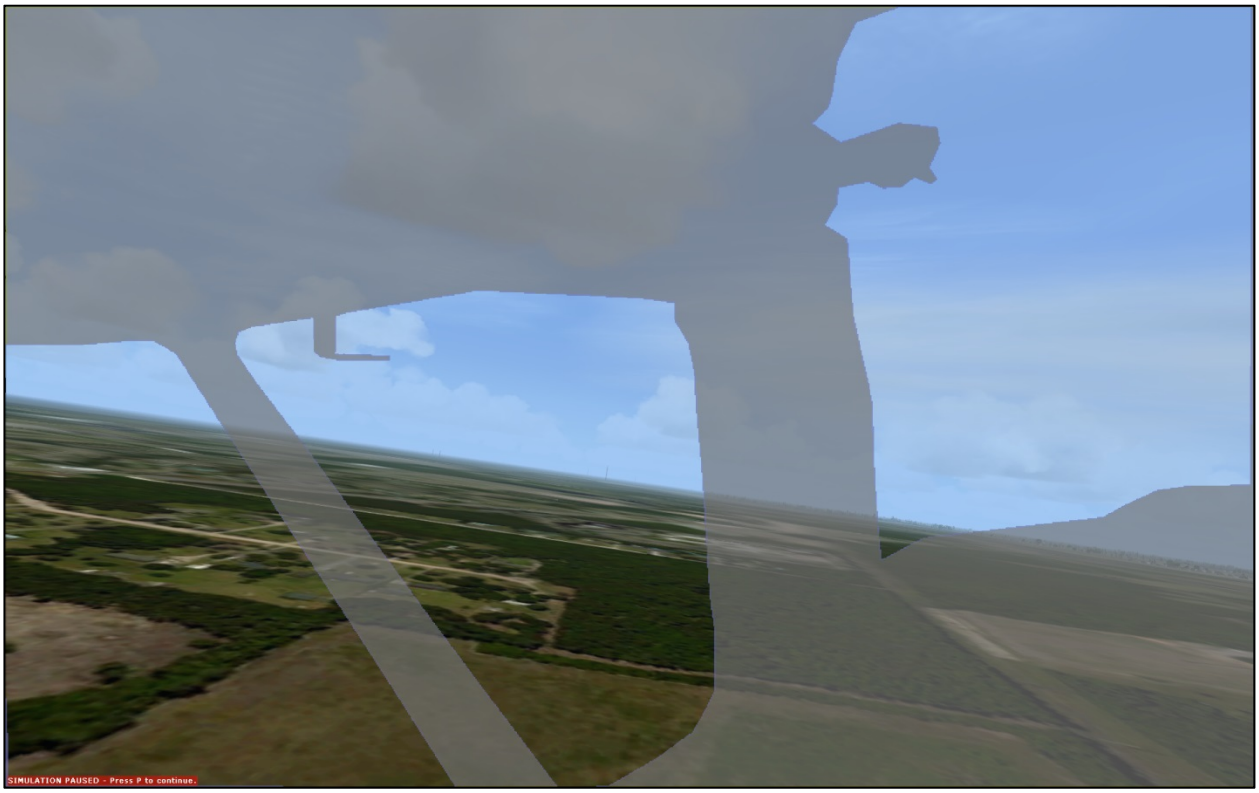

Figure B6. Finished instrument panel mask as it appears in *FSX*, with panel transparency set to 34%.

Joining windows in FSX to create larger field of view

As noted above, the maximum field of view available in a single *FSX* window is 90°, corresponding to the minimum available zoom level of 0.3. In this view, objects beyond an azimuth angle Ψ of ±45° (for a camera pointed straight ahead) will be outside the field of view and not visible.

To see objects beyond ±45° of azimuth while at the same time preserving a field of view of at least ±45° of azimuth about the direction of travel, the view from two co-located cameras can be joined side-by-side, with the second camera pointed in such a way that the boundaries of the fields of view of the cameras coincide at a particular azimuth angle. This method is illustrated in the top two images of Figure B3. In this Figure, the camera in the left image is pointed straight ahead (Ψ = 0°), and the right boundary of its field of view is at Ψ = +45°. The camera in the right image is rotated to Ψ = +90°, and its left boundary is at +90° - 45° = +45° (coinciding with the right boundary of the image on the left). By setting the views from the cameras side-by-side, a continuous field of view from -45° to +135° is obtained.

However, discontinuities (kinks) in straight lines may appear at the boundary of these views when they are viewed side-by-side on a flat surface (such as a computer screen), because the viewer will be viewing both from the same angle, whereas one of the views is intended to be viewed at an angle rotated relative to the other. The discontinuities can be removed if each view is presented on a separate surface (monitor), and then the surfaces are joined at an angle equal to the relative rotation between the cameras (though this may be impractical). The discontinuities are apparent in Figure B3.

To use this method to increase the total field of view, and also use the user-defined instrument panel masks described above, a separate mask must be created for each camera view. In addition, the airplane *model.cfg FSX* file must be modified to comment out the line specifying the airplane interior model, so that this model does not get drawn and the instrument panel masks appear over a scene that only depicts the outside world.

References

1. Diston, Dominic J., *Computational Modeling and Simulation of Aircraft and the Environment, Vol. 1: Platform Kinematics and Synthetic Environment,* p. 58. Copyright © 2009, John Wiley & Sons, Ltd.

2. Hestnes, Ivar, *Visual System Tutorial, Rev. 1.0.* Available at *http://www.google.com/url?sa=t&rct=j&q=&esrc=s&source=web&cd=1&cad=rja&uact=8&ved=0ahUKEwiFkpCX-PDOAhVG7B4KHfVCCtAQFggcMAA&url=http%3A%2F%2Fwww.flightdeck737.be%2Fwp-content%2Fuploads%2F2011%2F03%2FVisual-system-tutorial.pdf&usg=AFQjCNFHJq7T3TRTvT4ylwOAm1PpzJc-Eg*